UNIVERSIDAD AUTÓNOMA DE MADRID

PROGRAMA DE DOCTORADO EN BIOCIENCIAS MOLECULARES

FUNCTIONAL RELEVANCE OF PP2A-B55 PHOSPHATASES IN THE MAMMALIAN CELL CYCLE

TESIS DOCTORAL

María Sanz Flores

Madrid, 2017

DEPARTAMENTO DE BIOLOGÍA MOLECULAR

FACULTAD DE CIENCIAS

UNIVERSIDAD AUTÓNOMA DE MADRID

FUNCTIONAL RELEVANCE OF PP2A-B55 PHOSPHATASES IN THE MAMMALIAN CELL CYCLE

María Sanz Flores

Licenciada en Biología

Director: Marcos Malumbres Martínez

Codirectora: Mónica Álvarez Fernández

Centro Nacional de Investigaciones Oncológicas (CNIO)

Madrid, 2017

Mónica Álvarez Fernández, Investigadora del Grupo de División Celular y Cáncer del Centro Nacional de Investigaciones Oncológicas (CNIO)

y,

Marcos Malumbres Martínez, Jefe del Grupo de División Celular y Cáncer del Centro Nacional de Investigaciones Oncológicas (CNIO)

Certifican: que María Sanz Flores ha realizado bajo su dirección el trabajo de Tesis Doctoral titulado:

FUNCTIONAL RELEVANCE OF PP2A-B55 PHOSPHATASES IN THE MAMMALIAN CELL CYCLE

Revisado el presente trabajo, consideran que reúne todos los méritos necesarios para su presentación y defensa con el fin de optar al grado de Doctor por la Universidad Autónoma de Madrid.

Mónica Álvarez Fernández Marcos Malumbres

RESUMEN/SUMMARY

RESUMEN

La fosforilación reversible de proteínas es un mecanismo esencial en la regulación del ciclo celular. Mientras que el papel llevado a cabo en mitosis por las proteínas quinasa ha sido profundamente caracterizado, la identidad y la función específica de las fosfatasas en la mitosis de mamíferos está aún por determinar. La proteína fosfatasa 2A (PP2A) es una fosfatasa de residuos serina y treonina de gran importancia en células eucarióticas. Existen evidencias de que los complejos formados por PP2A con subunidades reguladoras de la familia B55 juegan un importante papel en la desfosforilación de sustratos de quinasas dependiente de ciclina (CDKs) durante mitosis en diferentes organismos. Este hecho sugiere su posible relevancia también en la mitosis de mamíferos. Con el objetivo de dilucidar la función de estos complejos PP2A-B55 en mitosis en mamíferos, hemos generado modelos de ratón deficientes para los genes *Ppp2r2a* (B55α) y *Ppp2r2d* (B55δ) que codifican dos de las cuatro isoformas de esta familia de subunidades reguladoras; en particular, aquellas consideradas ubicuas y previamente relacionadas con el ciclo celular. El estudio de estos modelos ha revelado que B55α, pero no B55δ, es necesaria durante el desarrollo embrionario y resulta esencial para la supervivencia del animal. Además, a nivel celular, ambas isoformas tienen funciones específicas y redundantes. Las células deficientes para los complejos PP2A-B55 presentan alteraciones en la duración de mitosis y en la segregación cromosómica que ocurre en esta etapa del ciclo celular, dando lugar a defectos de proliferación. El análisis detallado de la progresión del ciclo celular en células deficientes para B55 ha revelado un nuevo papel de estos complejos en la agrupación cromosómica durante mitosis, mediada al menos parcialmente por la proteína pericromosómica Ki-67. El tratamiento con compuestos que afectan la polimerización de microtúbulos, en las células deficientes para B55, provoca dispersión cromosómica durante mitosis, una acumulación de la proteína Ki-67 y, en algunos casos, muerte celular. Estos datos ponen de manifiesto la importancia de estos complejos en la regulación de mitosis en mamíferos y en la respuesta a los fármacos que afectan la polimerización de microtúbulos, los cuales se utilizan frecuentemente en tratamientos contra el cáncer.

SUMMARY

Reversible protein phosphorylation is an essential mechanism of cell cycle regulation. Whereas the role of mitotic kinases has been deeply characterized, the identity and specific functions of mitotic phosphatases in mammalian cells has not been fully resolved yet. Protein phosphatase 2A (PP2A) is a major serine/threonine phosphatase in eukaryotic cells and there is evidence that PP2A complexes containing the B55 family of regulatory subunits play a key role in dephosphorylating CDK substrates during mitosis in different organisms. This fact makes these phosphatase complexes might be important for mitosis in mammals. To address the functional relevance of those PP2A-B55 complexes in mammalian cell cycle, we have generated loss-of-function mouse models for *Ppp2r2a* (B55α) and *Ppp2r2d* (B55δ), which encode the ubiquitous and cell cycle-related isoforms out of the four existing ones in mammals (B55α, β, γ, δ). Using these models we have found that B55α, but not B55δ, is required during late embryonic development and therefore essential for mouse survival. Moreover, at the cellular level, both isoforms have specific and overlapping roles in cell cycle regulation. PP2A-B55-null cells display defects in timing and chromosome segregation during mitosis resulting in impaired proliferation. Interestingly, analysis of cell cycle progression in B55-null cells has also revealed a new role for PP2A/B55 complexes in chromosome clustering during mitosis, which is mediated through the perichromosomal protein Ki-67. Treatment of B55 deficient cells with microtubule depolymerizing drugs leads to massive chromosome scattering in mitosis, excessive Ki67 accumulation and eventually mitotic cell death. These data highlight the importance of these phosphatase complexes in regulating mammalian mitosis and the response to microtubule poisons, a common chemotherapeutic reagent used for cancer treatment.

INDEX

ABBREVIATIONS

A
APC/C: Anaphase- **P**romoting **C**omplex/ **C**yclosome

B
BAC: Bacteria**l A**rtificial **C**hromosome

C
CAF: Chromatin **A**ssembling **F**actor
Cdc20: Cell **D**ivision **C**ycle 20
cDNA: **C**omplementary **DNA**
Cdk: Cycle-**d**ependent **k**inase
CIP2A: Cancerous **I**nhibitor of **P**P**2A**
CMV: Cyto**m**egalo**v**irus promoter
Cre: Cre Recombinase

D
DAPI: 4',6-**di**a**p**heny**l**indole
DMEM: **D**ulbecco's **m**odified **E**agle's **m**edium
DOM: **D**uration **o**f **m**itosis

E
E: Embrionic day
EdU: 5-**e**thynyl-2'-**d**eoxy**u**ridine
ER: **E**strogen **R**eceptor

F
FACS: Fluorescence **A**ctivated **C**ell **S**orting
FBS: Fetal **B**ovine **S**erum

G
G0: Gap phase **0**
G1: **G**ap phase **1**
G2: **G**ap phase 2
GFP: Green **F**luorescence **P**rotein

H
H2B: Histone H2B
H&E: Hematoxylin **and E**osin
HR: Homologous **R**ecombination

I
IF: Inmuno**f**luorescence

K
KO: **K**nock**o**ut

L
LacZ: beta-ga**lac**tosidase

M
Mastl: microtubule-**a**ssociated **s**erine/**t**hreonine kinase-**l**ike
MCC: Mitotic **C**heckpoint **C**omplex
MEFs: **M**ouse **E**mbryonic **F**ibroblasts
MTs: Micro**t**ubules

N
NEB: Nuclear **E**nvelope **B**reak-down
Noc: Nocodazole

P
P: Postnatal day
PBS: **P**hosphate-**B**uffered **S**aline
PCR: Polymerase **C**hain **R**eaction
pH3: phospho-Histone **H3**
PI: Propidium **I**odide
Plk1: Polo-**l**ike **k**inase **1**
PM: Prometaphase
PP1: **P**rotein **P**hosphatase 1
PP2A: **P**rotein **P**hosphatase 2A
pRb: Retinoblastoma complex

Q
qRT-PCR: quantitative **R**everse **T**ranscription **P**olymerase **C**hain **R**eaction

R
RFP: **R**ed **F**luorescence **P**rotein
RT: Room **t**emperature

S
SAC: Spindle **A**ssembly **C**heckpoint
SD: Standard **D**eviation
SDS-PAGE Sodium **D**odecyl **S**ulfate **P**olyacrylamide **G**el **E**lectrophoresis
SEM: Standard **E**rror of the **M**ean
siRNA: small **i**nterference **RNA**

T
Tg: Trans**g**enic mice

W
WB: Western **B**lot
WT: **W**ild **T**ype

INTRODUCTION

1. INTRODUCTION

1.1. Mitosis in the mammalian cell division cycle

When Rudolf Virchow in 1858 postulated "*Omnis cellula e cellula*", an important dogma in cell biology was born establishing that every cell must derive from a pre-existing cell. And, certainly, cell division is the only way for life to be expanded and, unfortunately, when uncontrolled, also a road to cancer. The cell division cycle constitutes a series of events that ensures faithful transmission of the genetic information from one cell generation to the next one. The majority of mammalian adult cells are in a quiescent state called G_0, and, only when they are exposed to specific mitogenic stimuli or signalling, cells enter the cell cycle. In eukaryotic cells, the cell cycle was first described as two distinct phases: interphase and mitosis. Interphase was later on divided into three phases, S-phase standing for synthesis of DNA, surrounded by two Gap-phases G_1 (gap1) and G_2 (gap2). The stage preceding S-phase in which the cell grows and prepares for DNA synthesis is G_1. Next, during S-phase the cell replicates its genetic material, and in G_2 the cell prepares for its division. During mitosis (M phase) the cell segregates its DNA into two daughter cells, which are completely individualized once the cytoplasm is divided between them during the cytokinesis process (Figure 1) (Morgan, 2007).

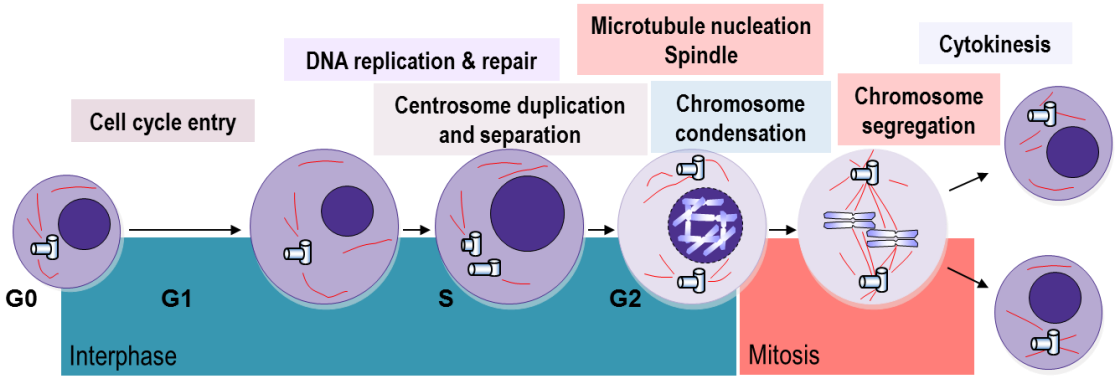

Figure 1. Cell cycle phases. Quiescent cells in G_0 are induced to cycle and enter into G_1 to prepare for DNA replication in S phase. Once the genome is duplicated, cells prepare to divide in G_2. Finally, chromosome segregation takes place in M phase and cell divides by cytokinesis. Adapted from Malumbres, 2011.

1.1.1. Phases of mitosis

Mitosis, described by Walter Flemming 135 years ago, is the nuclear division process in which the previously duplicated genome is reorganized into compact chromosomes,

each made up of two sister chromatids that are equally segregated into two daughter cells. It is the most striking and sophisticated part of the cell cycle. In less than an hour the mother cell organizes complex machinery aiming to have each daughter cell inheriting a complete set of chromosomes, a centrosome (the main microtubule-organizing centre of animal cells), the cytoplasm and all required organelles. Mitosis is divided in five different phases that are mainly defined by the organization and behaviour of the chromosomes: prophase (P), prometaphase (PM), metaphase (M), anaphase (A) and telophase (T) (Figure 2).

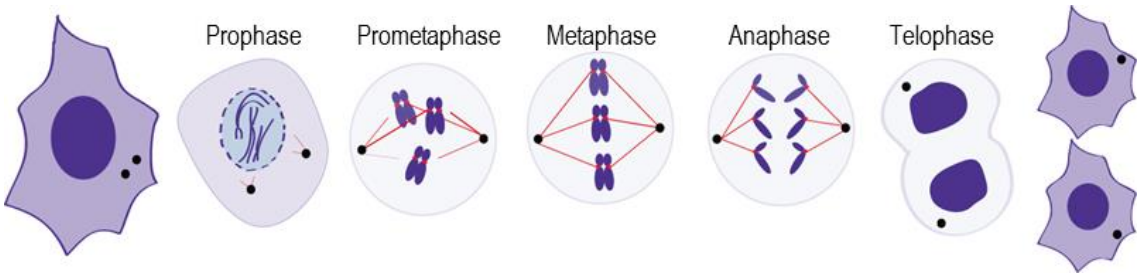

Figure 2. Phases of mitosis. Interphasic chromatin is condensed and kinetochores assemble in prophase. In prometaphase, upon nuclear envelope breakdown, kinetochores bind to microtubules. Chromosomes are bioriented and aligned during metaphase in the spindle midzone, forming a metaphase plate. In anaphase, sister chromatids are pulled apart. At telophase, chromatin decondenses and the nuclear envelope is reformed.

During prophase, interphasic chromosomes start to condense moving to the poles of the cell where the spindle structure will be formed. Nuclear envelope breakdown (NEB) signals the transition between prophase and prometaphase and is an essential step for the mitotic spindle formation. The spindle microtubules rapidly assemble and disassemble searching for attachment sites at chromosome kinetochores, which are complex structures that assemble during prometaphase on one face of each sister chromatid at its centromere. Microtubules from opposite poles interact with chromosomes and make them to become bioriented and congressed. Congression of the last chromosome marks the transition to the next stage of mitosis, metaphase, in which all chromosomes reach the equator of the spindle forming the “metaphase plate”. The progression of cells into anaphase is marked by the abrupt separation of sister chromatids. Early in anaphase, chromosomes lose their cohesion and each chromatid moves apart towards one spindle pole. At late anaphase, the spindle is elongated and separates further the two set of chromatids. Mitosis ends with telophase, the stage at which the chromosomes reach the poles, decondense into their interphase conformation,

and the nuclear envelope is reformed around the two daughter nuclei. Then, the cytoplasm division, also called cytokinesis, and whose regulation is precisely linked to mitosis, occurs. A contractile ring is formed at the cortex of the cell giving rise to the midbody that marks the abscission site. Finally, abscission of the midbody results in the complete physically separation of the two daughter cells which have identical genetic composition (Morgan, 2007).

1.1.2. Molecular mechanisms of mitosis

From the molecular point of view, there are various mechanisms that regulate mitotic progression, being protein degradation and reversible protein phosphorylation the most essential ones. Although for a long time, this phosphoregulation has mostly been attributed to oscillatory kinase activities, it is now appreciated the equal importance of phosphatases for this regulation.

1.1.2.1. Mitotic entry and progression to metaphase

In mammals, activation of the cyclin-dependent protein kinase 1 (Cdk1) triggers entry into mitosis. This requires dephosphorylation of its inhibitory phosphorylation by Cdc25 phosphatases, starting just in this point a very complex and ordered balance between kinases and phosphatases. Surprisingly, Cdk1 itself phosphorylates and inhibits their kinase inhibitors, Wee1 and Myt1; whereas it is also the responsible of activate its own activator, Cdc25. By this way, a positive feedback loop of progressive activation of Cdk1-Cyclin B complexes occurs (Lindqvist et al., 2009) (Figure 3). The activation of Cdk1 results in the phosphorylation of hundreds of substrates, such as laminins, condensins or Golgi elements, among others. In addition to Cdk1, other kinases participates in mitotic entry, such as Polo-like kinase (Plk)1 or the Aurora kinases, A and B. All these kinases participates in diverse processes, such as activation of Cdk1-Cyclin B complexes (Seki et al., 2008, Toyoshima-Morimoto et al., 2001), centrosome maturation and duplication (Barr and Gerlegy, 2007), spindle assembly (Cowley et al., 2009, Brennan et al., 2007, Seong et al., 2002), chromatin condensation (Goto et al., 2002) and proper orientation and stabilization of mitotic chromosomes in the metaphase plate (Adams et al., 2001, Lens et al., 2010, Malumbres, 2011). The activity of all these mitotic kinases is rigorously controlled by protein phosphatases (Bollen et al., 2009, Medema and Lindqvist, 2011). More recently, Mastl (microtubule-associated serine/threonine kinase-like protein), also known as Greatwall, has been identified as a new player in mitosis (Figure 3). When cells enter into mitosis Mastl is auto-

phosphorylated, in part by Cdk1 and increases its kinase activity. Its activity results in the indirect inhibition of Cdk-counteracting PP2A-B55 phosphatase complexes, providing a molecular link between kinase and phosphatase activity at these initial steps of mitosis. MASTL phosphorylates Ensa and ARPP19, two small endosulphine proteins that, when phosphorylated, act as specific inhibitors of PP2A complexes containing the B55 regulatory subunit (Glover, 2012, Lorca and Castro, 2013). Collectively, we can conclude that mitotic entry is the result of the activation of an ordered cascade of mitotic kinases always controlled by their counteracting phosphatases (Álvarez-Fernández and Malumbres, 2014).

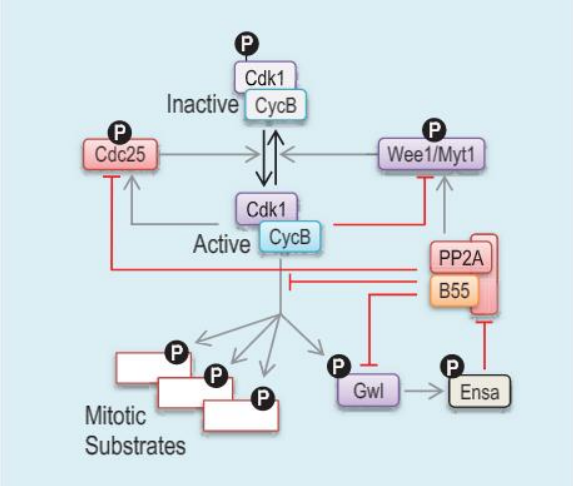

Figure 3. Kinase-phosphatase balance at mitotic entry. Mitotic entry requires Cdk1 activation, which is dependent on reversible phosphorylation of its inhibitor Wee1/Myt1 by Cdc25 phosphatase. Once activated, Cdk1 phosphorylates a wide spectrum of substrates that allow mitotic entry and progression. Among them it is Mastl (Gwl) kinase that is in charge of indirectly inhibition of PP2A-B55 complexes, which are the latest responsible of Cdk1 inactivation, and their phosphorylated substrates. Adapted from Álvarez-Fernández and Malumbres, 2014.

1.1.2.2. Metaphase to anaphase transition and mitotic exit

Once cell enters into mitosis its transition until anaphase, and consequently exit from mitosis, is controlled by the spindle assembly checkpoint (SAC). The SAC is a control mechanism that monitors chromosome biorientation on the mitotic spindle, and, as long as unattached chromosomes remain, it stops cells in mitosis and prevents passage into anaphase (Figure 4). The effector of the SAC, known as the mitotic checkpoint complex (MCC), is specifically located at unattached kinetochores, and is composed by the mitotic arrest deficient 2 protein (Mad2), mitotic checkpoint serine/threonine-protein kinase BUB1 beta (BubR1) and the mitotic checkpoint protein Bub3 (Sudakin et al., 2001). This complex joined to Cdc20 binds to the anaphase promoting complex (APC) preventing its catalytic activity and delaying the anaphase onset. Then, the main function of the SAC is therefore to avoid loss of sister chromatid cohesion (the initiation

of anaphase) and premature chromosome segregation in the presence of unattached or incorrectly attached chromosomes. Similar to other pathways, reversible protein phosphorylation is a crucial regulator of the SAC signalling (Musacchio, 2015). In this step, two different phosphatases, PP2A and PP1, have roles in promoting and maintaining kinetochore-microtubule attachment and SAC silencing (Funabiki and Wynne, 2013). Once all chromosomes are properly attached, SAC is inactivated and Cdc20 binds to APC turning on its activity as ubiquitin-ligase. Once APC is activated, this promotes securin and cyclin B degradation leading to chromatid separation and Cdk1 inactivation, respectively. Both, securin degradation and lower Cdk1 activity activate separase, which release centromeric cohesins. It is now known that PP2A phosphatase is also involved in sister chromatid cohesion by counteracting centromeric cohesin phosphorylation and by timing exactly cohesion degradation (Tang et al., 2006). Therefore, to revert all morphologic changes that a cell suffers at mitotic entry, it is essential the complete inactivation of Cdk1 by Cyclin B degradation. Once Cdk1 is inactivated, phosphatases dephosphorylate and activate Cdh1, the second APC activator. APC/Cdh1 allows completion of mitotic exit through the degradation of other important mitotic regulators.

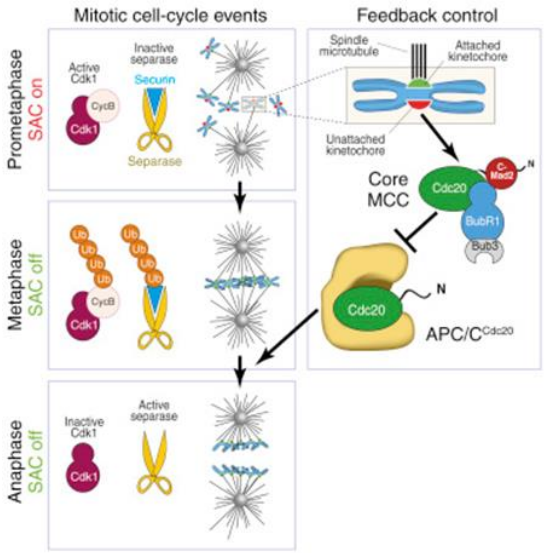

Figure 4. The SAC. During prometaphase the SAC is active, when chromosomes kinetochores start to attach to the spindle microtubules. Properly attached kinetochores (green) 'satisfy' the SAC, which stops signalling, whereas unattached or improperly attached kinetochores (red) prolongs the SAC signal provoking that MCC binds and inhibits APC/C^{Cdc20}, which is required for the metaphase–anaphase transition. Once SAC is satisfied on all kinetochores (at metaphase), activation of APC/C^{Cdc20} promotes Cyclin B and securin ubiquitination and proteolysis. This promotes mitotic exit and sister chromatid separation, the latter through activation of separase. Adapted from Musacchio, 2015.

1.1.2.3. Dephosphorylation as an essential step of mitotic exit

As mentioned above, the progression and entry into mitosis is mostly driven by the kinase activity of Cdk1. Then, to exit from mitosis it is necessary the inactivation of Cdk1 and also the active dephosphorylation of all previously phosphorylated proteins.

This step is mediated by protein phosphatases, for which their importance in mitosis has not been fully recognized until few years ago (Bollen et al., 2009). In *Saccharomyces cerevisiae*, activation of protein phosphatase Cdc14 plays a key role in the direct inactivation of mitotic Cdk1 and also in the dephosphorylation of Cdk substrates (Queralt and Uhlmann, 2008). Although its orthologs in mammals seem to maintain some functional conservation (Vazquez-Novelle et al., 2005), it is not clear its relevance during mammalian mitotic exit (Berdougo et al., 2008, Guillamot et al., 2011). Indeed, other phosphatases assume these functions in other organisms. In *Xenopus laevis*, PP1 has a key role for Cdk substrates dephosphorylation (Wu et al., 2009). In mammals, however, PP2A in complexes with B regulatory subfamily isoforms (B55) has been proposed as the main Cdk-counteracting phosphatase. Its deregulation in mitotic exit impairs several events of mitotic exit, such as reassembly of the nuclear envelope and Golgi apparatus, and chromatin decondensation (Schmitz et al., 2010); and also the dephosphorylation of Cdk phosphosites (Manchado et al., 2010). Nevertheless, the specific B55 isoforms responsible for mitotic exit and the underlying molecular mechanism remains unclear.

1.2. Protein phosphatase 2A (PP2A)

1.2.1. PP2A structure and function

PP2A is the major serine-threonine phosphatase in mammals contributing to almost 1% of the total cellular protein, and plays a crucial role in regulating most cellular functions. In its active form, PP2A is a heterotrimeric complex composed of one catalytic subunit C, one scaffold subunit A, and one of the many regulatory subunits B (Seshacharyulu et al., 2013).

The PP2A C catalytic subunit is the responsible of the phosphatase function targeting phosphatase groups on either serine or threonine. This subunit is encoded by two different and ubiquitously expressed genes, *Ppp2ca* and *Ppp2cb*, resulting in two isoforms, Cα and Cβ. Although both isoforms share almost 100% amino acid sequence, Cα is expressed 10 fold higher than Cβ due to its stronger promoter, which makes it essential and irreplaceable (Eichhorn et al., 2009).

The PP2A A scaffold subunit is in charge of the structural basis. It supports the catalytic subunit promoting the interaction with the regulatory subunit and other substrates to be

a fully active phosphatase. This subunit is also encoded by two different genes, *Ppp2r1a* and *Ppp2r1b*, which also results in two different isoforms, Aα and Aβ. The more abundant isoform is Aα being responsible of almost 90% of PP2A assemblies (Eichhorn et al., 2009)

The PP2A B regulatory subunit is considered as the master regulator of PP2A complexes. These subunits can be expressed in a tissue specific manner and they provide substrate specificity and intracellular localization. The human genome encodes about 15 regulatory subunits that have been classified into four different subfamilies: B55 or PR55, B56 or PR61, B'' or PR72 and B''' or PR93. Each subfamily contains 2 to 5 isoforms and additional splicing variants (Eichhorn et al., 2009) (

Figure 5).

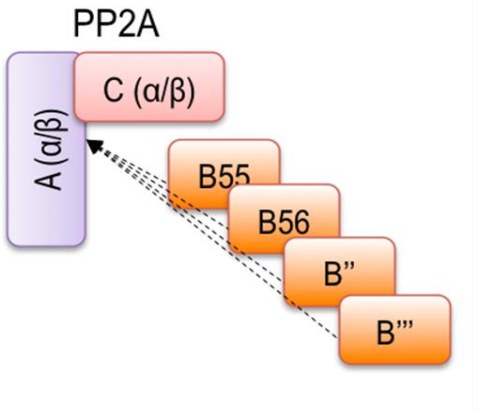

Subunit	Gene	Isoform
Scaffold (A)	*PPP2R1A*	A
	PPP2R1B	B
Catalytic (C)	*PPP2CA*	A
	PPP2CB	B
Regulatory (**B55**)	*PPP2R2A*	A
	PPP2R2B	B
	PPP2R2C	Γ
	PPP2R2D	Δ
Regulatory (B56)	*PPP2R5A*	A
	PPP2R5B	B
	PPP2R5C	γ 1,2,3
	PPP2R5D	Δ
	PPP2R5E	E
Regulatory (B'')	*PPP2R3A*	α 1,2
	PPP2R3B	B
	PPP2R3C	Γ
	PPP2R3D	Δ
Regulatory (B''')	*STRN*	
	STRN3	
	PPP2R4	

Figure 5. Diversity of the PP2A holoenzyme: different genes and subunits (A) Scheme of PP2A core protein: scaffold and catalytic subunits and the four different B regulatory subfamilies. (B). The table shows the three different subunits that allow heterotrimeric active formation of PP2A: scaffold, catalytic and regulatory subunits. Each subunit is encoded by two or more genes resulting in different isoforms. In case of regulatory subunits, there are four different subfamilies: B55, B56, B'' and B''', each one containing more than three isoforms and allowing the formation of a huge number of different PP2A complexes.

The combinatorial assembly of these various A, B and C subunits permits the formation of more than 70 heterotrimeric PP2A complexes, which are distinguished by the B regulatory subunit they contain.

1.2.2. Mouse models of PP2A

The structural complexity of PP2A makes difficult to develop suitable mouse models for the study of its biological function and its tumour suppressor role in cancer. Still, some mouse models have already been generated in an attempt to the study of this phosphatase.

For the PP2A A scaffold subunit, four different mouse models were generated by the same group: an Aα constitutive and an Aα conditional knockout mice, and two knock-in mice expressing human lung and breast cancer-associated Aα point mutants (Ruediger et al., 2011). These four models showed the continuously requirement of Aα in embryonic development and in adult mice, and probed the tumour suppressor activity of PP2A in multiple signalling pathways *in vivo* (Walter and Ruediger, 2012).

Regarding the PP2A C catalytic subunit, knockout mice for both isoforms, Cα and Cβ, were generated (Gotz et al., 1998, Gu et al., 2012), being Cα knockout embryonic lethal whereas Cβ-deficient mice were viable without any obvious phenotype. This fact explains the differential abundance of both isoforms despite being almost identical in protein sequence. Moreover, some tissue specific knockout models for PP2A Cα have recently been studied (Fang et al., 2016, Li et al., 2016, Pan et al., 2015, Lu et al., 2015, Xian et al., 2015), highlighting the wide and important functions of this subunit in the entire organism, participating in the development, proliferation and metabolism of very different tissues through multiple and diverse signalling pathways.

The limitation of mouse models is very noticeable in the study of the PP2A B regulatory subunits, in which the diversity of subfamilies with multiple isoforms is immense. To date, only some knockout and overexpression models for the B56 subunit, one of the four existing subfamilies, have been described. The B56α knockout model is viable, with some cardiac defects (Litter et al., 2015). A B56δ-null mouse model also resulted viable despite its high levels during normal embryogenesis, and, it only developed a tauopathy based on hyperphosphorylation of the protein tau (Louis et al., 2011), or some cardiac aberrancies (Varadkar et al., 2014). In contrast, the B56γ model of overexpression in lung resulted in neonatal death due to its specific expression in a

particular stage of lung development related with the Wnt/β-catenin signalling pathway (Everett et al., 2002). Besides that, no models for any other family of B regulatory subunits have been described. So, the development of new mouse models for the PP2A B regulatory subunits becomes essential to gain more knowledge in the molecular and physiological function of specific PP2A complexes.

1.2.3. PP2A and cancer

Several genetic alterations have to be acquired for normal cells to become malignant. Some studies have linked tumoural formation and Darwin's evolutive theory considering that, in both cases, successive genetic alterations provide a growth advantage (Gillies et al., 2012). In case of tumoural cells, they acquire more proliferative capacity, the capability to avoid cell death signals, a non-limited potential to duplicate its genetic material, and also they develop angiogenic capacities and mechanism to invade adjacent tissues (Hanahan and Weinberg, 2011).

PP2A is a recognized tumor suppressor frequently inactivated in cancer, but also in other non-neoplastic diseases. PP2A complexes are targets of natural toxins like the tumor promoter okadaic acid (Bialojan and Takai, 1988), and of small and medium T antigens which are known viral oncogenes (Pallas et al., 1990). The PP2A scaffold and regulatory subunits were shown to be mutated or aberrantly expressed in many different types of cancer, such as breast, lung, colon, endometrium, ovarian, leukemia, pancreas and melanoma cancer (Seshacharyulu et al., 2013, Ruvolo, 2016, Calin et al., 2000). Reports of different mutations in the *PPP2R5C* (B56γ) have been identified in diverse cell lines derived from solid tumors including, melanoma and lung cancer (Nobumori et al., 2013). Also, some genomic studies have identified 8p21.2 chromosomic deletions, which include the *PPP2R2A* gene encoding for the B55α regulatory subunit, in different tumors. In particular, somatic deletions of *PPP2R2A* have been described in prostate cancer at a frequency of 67.1%, from which 2.1% were homozygous deletions (Mao et al., 2011, Cheng et al., 2011). In breast, *PPP2R2A* deletion and loss of its transcript was associated with estrogen-receptor (ER)–positive breast tumors (Curtis et al., 2012, Beca et al., 2015). Furthermore, *PPP2R2A* is also deleted in primary plasma cell leukemia (Mosca et al., 2013). These data suggest that PPP2R2A (B55α) regulatory subunit could act as a haploinsufficient tumor suppressor in human cancer. Epigenetic inactivation of *PPP2R2B* by methylation has been found in several tumors, such as gliomas, colorectal

tumors and breast cancer, also suggesting a tumor supressor role for this B isoform (Muggerud et al., 2010, Tan et al., 2010, Majchrzak-Celinska et al., 2016).

Moreover, aberrant expression of endogenous PP2A inhibitors such as, Cancerous Inhibitor of PP2A (CIP2A) (Junttila et al., 2007) and Inhibitor 2 of PP2A (SET) (Neviani et al., 2005), promotes malignant transformation of cells in some human cancers, emerging as key players in cancer cell survival and drug resistance. In these cases, restoring PP2A activity has become a therapeutic strategy for cancer treatment (Neviani and Perrotti, 2014, Cristobal et al., 2016).

1.3. PP2A-B55 complexes

In mammals, the B55 family of regulatory subunits includes 4 different isoforms (α, β, γ and δ), each one encoded by a distinct gene (*Ppp2r2a-d*) in a different genomic locus, in some cases with additional splicing variants, giving rise to different isoforms within isoforms (Table 1). This fact increases the complexity of this family of PP2A complexes and the difficulties to understand the specific functions among isoforms of the same regulatory family. Within each of the 4 isoforms, the complexity is even higher in humans, with multiple splicing variants, in comparison to mouse (Table 1).

Table 1. B55 isoforms in mouse and human

B55 isoform	Mouse	Human
B55α	*Ppp2r2a:* one isoform (447 aa)	*PPP2R2A*: Isoform-1 (447 aa) *Isoform-2 (457 aa)*
B55β	*Ppp2r2b:* Isoform-1 (443 aa) Isoform-2 (446 aa) mito.signal *Isoform-3 (425 aa)*	*PPP2R2B*: Isoform-1 (443 aa) Isoform-2 (446 aa) mito.signal Isoform-3 (449 aa) Isoform-4 (501 aa) Isoform-5 (509 aa) Isoform-6 (432 aa) *Isoform-7 (549 aa)*
B55γ	*Ppp2r2c:*one isoform (447 aa)	*PPP2R2C*: Isoform-1 (447 aa) Isoform-2 (447 aa) Isoform-3 (430 aa) *Isoform-4 (440 aa)*
B55δ	*Ppp2r2d:* one isoform (453 aa)	*PPP2R2D:* one isoform (453 aa)

At the protein level, these huge number of isoforms share almost 80% of identity. Regarding their expression pattern, it has been described that both B55α and B55δ isoforms are widely expressed, while B55β and B55γ are highly enriched in brain (Strack et al., 1998, Schmidt et al., 2002, Strack et al., 1999). How three of these four isoforms are regulated during brain development was further studied. Whereas B55α remains present with invariant levels along brain development, B55β and B55γ have opposite expression levels, being B55β highly expressed before birth, then stabilized, and B55γ highly expressed upon birth (Strack et al., 1998).

1.3.1. Function of PP2A-B55 in cell cycle progression

Diverse studies, in different organisms, evidence that B55 has a role in mitosis by targeting PP2A complexes towards substrates phosphorylated at CDKs consensus sequences (S/TP). In *Drosophila* the absence of the only regulatory B55 subunit of PP2A, *twins*, affects mitosis by provoking overcondensed chromosomes and abnormal anaphase figures with bridges or lagging chromosomes (Mayer-Jaekel et al., 1993, Gomes et al., 1993). It was also demonstrated that the absence of this protein led to reduced phosphatase activity towards CDK-substrates (Mayer-Jaekel et al., 1994). Studies in *Xenopus* egg extracts have shown that PP2A-B55δ is suppresed during mitosis but it is essential for dephosphorylation of CDK substrates on mitotic exit. Moreover this isoform also participates in timing mitotic entry (Mochida et al., 2009).

In mammals, a siRNA screening to identify phosphatases implicated in mitotic exit, revealed that only depletion of B55α isoform delays mitotic exit and the postmitotic reassembly of some interphase cell structures, such as nuclear envelope or golgi apparatus, in Hela cells. In the same study, siRNAs against the other existing B55 isoforms (β,γ and δ) were also tested, but no effect was detected for any of those, conluding that B55α was the main isoform involved in mitotic exit in human cells (Schmitz et al., 2010). However, in mouse cells, siRNA depletion of both, B55α together with B55δ, was required for dephosphorylation of CDK targets to allow fully mitotic exit, whereas depletion of B55β was not required for this function probably due to low expression of this isoform in this cell type, individual B55γ was not evaluated in this study (Manchado et al., 2010). Those data, therefore, revealed that PP2A-B55 phosphatases play a role in mitotic exit in mammals, although the specific isoforms responsible for this function are still controversial.

1.2.1. Regulation of PP2A-B55 complexes by the kinase MASTL (Greatwall)

As mentioned above, a key player in the regulation of PP2A-B55 complexesduring mitosis is MASTL (microtubule-associated serine/threonine kinase-like protein) (Glover, 2012). MASTL is the recently found mammalian ortholog of Greatwall (Gwl) and participates in the maintenance of the mitotic state by inhibiting PP2A phosphatases (Voets and Wolthuis, 2010, Burgess, 2010). Gwl was originally identified in *Drosophila* as a protein required for DNA condensation and normal progression through mitosis (Yu et al., 2004). In mammalian cells, MASTL depletion causes multiple mitotic defects characterized by problems in DNA condensation, and also defects on chromosome segregation and cytokinesis (Voets and Wolthuis, 2010; Burgess et al., 2010). Notably, the defects in chromosome condensation could be rescued by concomitant ablation of B55 proteins (Álvarez-Fernández et al., 2013).

PP2A-B55 complexes are indirectly regulated by MASTL through the phosphorylation of two small proteins, Arpp19 and α-endosulfine (Ensa) (Castilho et al., 2009, Gharbi-Ayachi et al., 2010, Mochida et al., 2010, Vigneron et al., 2009). The control of PP2A through the Gwl-dependent phosphorylation of Arpp19/Ensa proteins has also been supported by genetic studies in *Drosophila* (Wang et al., 2011; Rangone et al., 2011).

In mammals, PP2A inhibition prevents the dephosphorylation of CDK1 substrates, whereas the inhibition of MASTL and reactivation of this phosphatase is required for mitotic exit (Alvarez-Fernandez et al, 2013; Burgess et al, 2010; Manchado et al, 2010; Voets & Wolthuis, 2010).

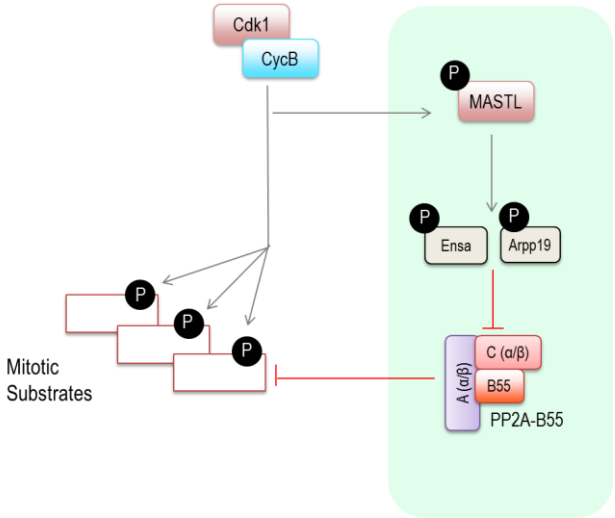

Figure 6. Regulation of PP2A-B55 complexes during mitosis. PP2A-B55 complexes are directly inhibited by the small proteins, Ensa and Arpp19, which are activated through phosphorylation by the kinase, MASTL. At mitotic entry, Cdk1-CycB promotes Mastl phosphorylation, activating the inhibitory pathway of PP2A-B55. Those complexes are the responsible of dephosphorylating Cdk1-mitotic substrates promoting mitotic exit.

1.2.2. Role of PP2A-B55 in other cell cycle phases

Besides its mitotic function, it has been proposed a role for PP2A-B55 complexes in other phases of the cell cycle. The retinoblastoma family of proteins or pocket proteins, (pRb, p107 and p130) in their active –hypophosphorylated- form, negatively regulate cell cycle progression through the G_0/G_1 transition and the G_1/S transition, at least in part by repressing expression of E2F-dependent genes Then, in S and G_2 phases and part of mitosis, Cyclin-Cdk complexes phosphorylate and inactivate these pocket proteins, allowing cell cycle progression. It has been shown that PP2A-B55 complexes, mainly B55α and, to a lesser extent, B55δ isoforms, play an active role in the dephosphorylation of p107 and likely p130, inducing its activation, suggesting its role in the entry or maintenance of the quiescent state (Jayadeva et al., 2010, Kurimchak et al., 2013). Accordingly, depletion of B55α delays mitotic exit in rat chondrocytes upon FGF stimulation (Kurimchak, 2013). Whether PP2A-B55 plays a role in these cell cycle transitions in other cellular contexts remains to be studied. Using small t antigen (st) of SV40 virus to abolish the specific binding of B55α isoforms with PP2A core dimer it was demonstrated not only the disappearance of active –hypophosphorylated- form of these pocket proteins. Nevertheless, the same defect in quiescence cells did not affect phosphorylation of pocket protein meaning this fact depends on Cdk activity (Jayadeva et al., 2010). Although it has not been proved the direct role of PP2A-B55 complexes in proliferation through the reversible phosphorylation of these proteins, it could be conceivable.

1.2.3. Cell cycle independent functions of PP2A-B55

The huge diversity of PP2A complexes allows their participation in multiple and diverse cellular processes, beyond cell cycle regulation.

PP2A-B55 complexes have been found regulating cell proliferation pathways. For example, B55α and B55δ have redundant functions controlling MAPK signaling pathway throught active dephosphorylation of Raf1 protein (Adams et al., 2005). Or, in the same pathway, B55α actively dephosphorylates kinase suppresor of Ras (KSR)-1 protein (Ory et al., 2003). These both activities result in consequential activation of MEK1/2 and ERK1/2 proteins. As well, B55α participates regulating cell proliferation and survival through PI3K pathway in which it regulates Akt phosphorylation status by Thr-308 desphosphorylation (Kuo et al., 2008, Ruvolo et al., 2011). In addition, B55γ is involved in mTOR pathway through dephosphorylation of S6K protein (Fan et al.,

2013). Moreover, these complexes are also involved in the Wnt/β-catenin signaling pathway, which has essential roles in developmental processes. In this pathway, B55α directly interacts with β-catenin regulating its phosphorylation and degradation (Zhang et al., 2009).

Furthermore, it is well-known that PP2A participates in neuronal development through regulation of multiple signaling pathways, and defects in PP2A activity have been reported in several neurodegenerative diseases (Nematullah et al., 2017). As we previously mentioned, all PP2A-B55 complexes are highly expressed in brain and also developmentally regulated, and, as such, it has been extensively proposed their involvement in neurological disorders. In Alzheimer's and Parkinson's disease, PP2A-B55α controls the phosphorylation status of the proteins tau (Sontag et al., 2004) and α-synuclein (Lee et al., 2011), which appear frequently hyperphosphorylated in those diseases, respectively. Further, spinocerebellar ataxia type 12 is a neurodegenerative disease characterized by an expanded CAG repeats mutation found immediately upstream of the B55β gene (Cohen and Margolis, 2016).

As well, this B regulatory subfamily has been found to regulate the function of structural proteins, such as vimentin (Turowski et al., 1999), and to participate in clathrin-coated vesicles transport through phosphorylation of proteins involved in efficient cargo recruitment (Ricotta et al., 2007).

1.3. The mitotic chromosome

The main objective of mitosis is achieving the equal segregation of genetic material from mother to daughter cells. In this process it is essential the chromosome condensation and compaction in the characteristic 'X-shaped' morphology conferred by the two compacted sister chromatids in metaphase. The formation of this characteristic structure starts at prophase when both, resolution of replicated sister chromatids and chromatin compaction, occurs (Nagasaka et al., 2016). The mitotic chromosome was one of the first observations in cell biology studies since 19th century, but nowadays it is still unknown how it precisely acquires its composition and structure.

In the mitotic chromosomes four structural domains are distinguished: centromeres, telomeres, the periphery or perichromosomal layer, and the chromosome arms (Figure 7)

The centromere with its associated kinetochore both comprise a complex structure necessary for spindle microtubules binding during metaphase and consequent chromatid segregation. Telomeres consist on repetitive ribonucleoprotein complexes present at ends of chromosomes that act protecting mitotic chromosome edges. The perichromosomal layer comprises a huge amount of different proteins that supports chromosome external scaffolding and protects chromosome surface (Van Hooser et al., 2005). Finally, the chromosome arms, which contain the highly ordered chromatin around the chromosome scaffold, are mainly composed, in addition to DNA, of non-histone proteins, including condensin, topoisomerase IIα (Topo IIα), and kinesin family member 4 (KIF4). These three proteins are also key determinants in the characteristic shape of mitotic chromosomes (Samejima et al., 2012).

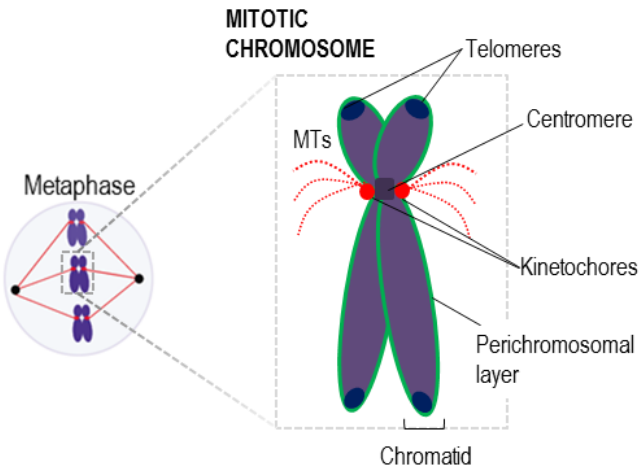

Figure 7. The mitotic chromosome. Scheme of a typical mitotic chromosome at metaphase is shown. It is composed by two sister chromatids joined by the centromere structure, which is flanked by kinetochores, one on each chromatid, which are the responsible of spindle microtubules (MTs) attachment. The chromatids present telomere structures at both ends, and the whole chromosome is surrounded by a structure called perichromosomal layer.
MTs: microtubules.

These four structures comprising several and diverse proteins actively interact with the chromatin, and confer identity to the characteristic mitotic chromosome. But how they are tightly regulated to reach this extremely organized structure is not well known. Recently, a phosphoproteomic study comparing phosphorylation patterns in mitotic chromosome-associated proteins in mitotic cells and asynchronous cells revealed more than 300 mitosis-specific phosphorylation sites (Ohta et al., 2016). Therefore, the coordinated activity of specific kinases and phosphatases during mitosis is also clearly associated to the regulation of mitotic chromosome establishment.

1.3.1. The perichromosomal layer

The perichromosomal layer has probably been the less studied structure of mitotic chromosomes. However, in the last years, its composition and relevance in mitotic chromatin compaction has partially been revealed.

This layer appears on chromosomes from prophase to telophase and it is distributed around most of the chromosome surface and in-between sister chromatids, excluding centromeres (Traut et al., 2002). It is composed by several proteins that play diverse functions in interphase cells, although in their majority belongs to the nucleolar structure (Hernandez-Verdun and Gautier, 1994, Van Hooser et al., 2005). Recent studies revealed that the perichromosomal layer represents 1.4% of the chromosome proteome (Ohta et al., 2010) and comprises more than 40% of the entire chromosome volume (Booth et al., 2016). Despite the knowledge about this layer around mitotic chromosomes since years, the function of this complex structure is not fully understood and until last years it had been overlooked.

1.3.2. Ki67: more than a proliferation marker

Of all components of the perichromosomal layer, Ki-67 is the one most deeply studied. Ki-67 protein is widely used as histological marker for cell proliferation (Whitfield et al., 2006). However, although its localization during the cell cycle is known since years ago (Gerdes et al., 1984), until last year its function remained poorly characterized.

Ki-67 gene contains from the N-terminus to the C-terminus, a phosphopeptide-binding-Forkhead-associated (FHA), a protein phosphatase 1 (PP1)-binding site, 16 repeats of unknown function and a region called LR (leucine-arginine) domain that binds heterochromatin protein HP1(Scholzen et al., 2002, Kametaka et al., 2002) (Figure 8). It encodes a big protein of 350kDa, which is located in the nucleolus in interphase and localized to the mitotic perichromosomal layer from late prophase to telophase (Starborg et al., 1996).

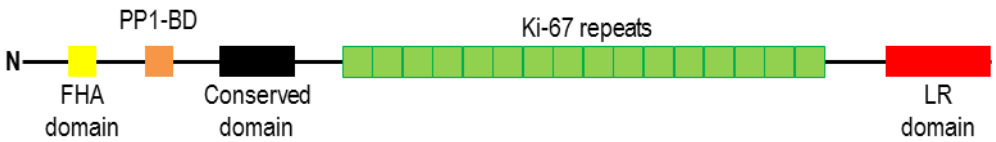

Figure 8. Ki-67 domains. Schematic diagram of Ki-67 human protein. Domains are indicated by boxes, from N-terminus are located: FHA, forkhead-associated domain; PP1-BD, PP1-binding domain; conserved domain among species; 16 Ki-67 repeats; and, LR (leucine-arginin) domain.

Although some studies have unexpectedly shown that Ki-67 is dispensable for cell proliferation (Sobecki et al., 2016), it is clear that it plays a role in chromatin organization. In interphase, it is required for the organization of heterochromatin (Sobecki et al., 2016). And, during mitosis, it is the responsible of the recruitment of other nucleolar proteins in the perichromosomal layer affecting the formation of functional nucleoli in the subsequent interphase (Booth et al., 2014). Furthermore, it acts as a biological surfactant preventing chromosome coalescence into a single chromatin mass upon NEB by its binding to the chromatin surface (Cuylen et al., 2016). Also, it has been proposed a model in which Ki-67 could provide external support to mitotic chromosomes cooperating with the internal support provided by TopoIIα (Takagi et al., 2016).

The specific perichromosomal localization of Ki-67 in mitotic cells must be regulated. It has been described that Ki-67 is hyperphosphorylated in mitosis (Ohta et al., 2016), at least in part by Cdk1 (Takagi et al., 2014). And, it is well known its direct interaction with PP1 through its binding site (Booth et al., 2014, Takagi et al., 2014, Kumar et al., 2016). However, the fact that the mutation of this site does not induce clear defects in progression of mitosis, but only a delay in the timing of dephosphorylation of Ki-67 mutant (Takagi el al., 2014), opens the possibility to be regulated by others phosphatases.

OBJECTIVES

2. OBJECTIVES

The identity and regulation of mitotic phosphatases in mammalian cells is not fully resolved yet. Based on the evidence that PP2A-B55 has a conserved key role in dephosphorylating CDK substrates during mitosis in different organisms, such as *Xenopus* or *Drosophila*, we propose that these phosphatase complexes might also be important for mitosis in mammals. Therefore, the aim of the work presented in this thesis was to characterize the physiological function of PP2A-B55 complexes in mammals. With this purpose the specific following objectives have been proposed:

1. Generate PP2A-B55 loss of function mouse models for B55α and B55δ isoforms.
2. Characterize the relevance of B55α and B55δ phosphatases in cell cycle progression in mammals.
3. Explore a new function of PP2A-B55 in chromosome clustering during mitosis.

MATERIALS & METHODS

3. MATERIALS AND METHODS

3.1. Genetically modified mouse models

3.1.1. Animal housing

All the mice used in this study were housed in the pathogen-free animal facility of the Centro Nacional de Investigaciones Oncológicas (CNIO; Madrid) following the animal care standards of the institution. All mouse procedures carried out in this memory were previously approved by the Bioethics Committee of the Instituto de Salud Carlos III and Comunidad de Madrid. These animals were observed on a daily basis by our specialized technicians, and sick mice were killed humanely in accordance with the Guidelines for Humane End Points for Animals used in biomedical research. All animals were maintained in a mixed 129/Sv(25%) x CD1(25%) x C57BL/6J(50%) background.

3.1.2. Generation of genetically modified mouse models

3.1.2.1. Construction of targeting vectors

The *Ppp2r2d* conditional targeting vector was constructed by Gene Bridges by flanking exon 3 of the murine *Ppp2r2d* locus with loxP sequences (Figure 16). The genomic sequences containing *Ppp2r2d* gene were obtained from two bacterial artificial chromosomes (BACs) named RP23-197B6 and RP23-438L24. A neomycin resistance-gene (neo^r) driven by the phosphoglycerate kinase (PGK) promoter was used for positive selection of clones.

3.1.2.2. Generation of quimeras

To generate the *Ppp2r2d* model, mouse ES cells V6.4 obtained from a hybrid (129 x C57BL/6J) strain were electroporated with 100µg of linearized DNA from the corresponding *Ppp2r2d* targeting vector. Recombinant ES cells and clones were selected in the presence of G418 (neomycin). This step was done at the Transgenic Mice Unit of the CNIO. The identification of the recombinant clones was performed by Southern blot analysis using new restriction sites from the recombinant alleles and external probes to the homology arms. Positive recombinant clones were microinjected into C57BL/6J blastocysts by the Transgenic Mice Unit of the CNIO. The male quimeras obtained were crossed with wild-type females for transmission of the recombinant allele.

For the *Ppp2r2a* gene, ES cell clone EPD0328_1_G08 (KOMP Repository) was directly microinjected into C57BL/6J blastocysts by the Transgenic Mice Unit of the CNIO. The obtained male quimeras were crossed with wild-type females for transmission of the recombinant allele.

3.1.2.3. Generation of *Ppp2r2a* and *Ppp2r2d* alleles

Heterozygous recombinant mice *Ppp2r2a* (+/loxfrt) were first crossed with Tg.pCAG-Flpe transgenic mice that ubiquitously and constitutively express Flp recombinase, to remove the neo selection marker and thus, to generate the conditional *Ppp2r2a* (lox). To generate the null alleles, we crossed *Ppp2r2a* (+/lox) and *Ppp2r2d* (+/loxfrt) mice with Tg.EIIa-Cre transgenic mice that ubiquitously and constitutively express Cre recombinase. In the *Ppp2r2a* (lox) allele, Cre-mediated recombination between the two loxP sites excises exons 5-8; whereas, in the *Ppp2r2d* (loxfrt) allele, Cre-mediated recombination between the two loxP sites excises exon 3, giving rise to *Ppp2r2a* (-) and *Ppp2r2d* (-) null alleles, respectively.

To generate a conditional model for *Ppp2r2a*, homozygous *Ppp2r2a*(lox/lox) mice were crossed with mice harbouring a tamoxifen-inducible Cre recombinase (Cre-ERT2), under the ubiquitous promoter of the RNA polymerase II. In this case, tamoxifen administration is required to induce the deletion of the *Ppp2r2a* gene and to obtain the *Ppp2r2a*(Δ) deleted allele.

3.1.3. Mouse genotyping

The genotyping of the mutant mice was done by PCR. The PCR was performed using tail genomic DNA from 3-4-week old mice and the oligonucleotides shown in (Table 2).

The standard PCR protocol was: 5 minutes at 95°C for denaturalizing the DNA followed by 35 cycles of: DNA denaturalization at 95°C during 30 seconds, primer annealing at 60°C during 30 seconds and polymerase extension at 72°C during 1 minute. The protocol finished with a final elongation step of 10 minutes at 72°C.

Table 2. Oligonucleotides used for *Ppp2r2a* and *Ppp2r2d* locus genotyping

((c)KO: (conditional) knock-out; F:forward, R:reverse primers)

Mouse model	Name	Sequence (5`-3')	Alleles and PCR size
***Ppp2r2a* cKO**	1F	AAGAATCATGCTGTGCTGCCAAGG	*Ppp2r2a*(+): 264bp
	2R	GGTGCTAGAATTAAGAGTGAGCC	*Ppp2r2a*(lox): 449bp
	1F	AAGAATCATGCTGTGCTGCCAAGG	*Ppp2r2a*(null): 518bp
	1R	CATGCTCTTTATACCTGCCTTATGGACC	
***Ppp2r2d* KO**	1F	GCCACCTGGGGTGTTTTG	*Ppp2r2d*(+):771bp
	1R	CATGCTCTTTATACCTTATGGACC	*Ppp2r2d*(null): 445bp

3.1.4. Histological and immunohistochemical analysis

For histological observation, dissected organs or embryos were fixed in 10%-buffered formalin (Sigma) and embedded in paraffin wax. Sections of 3- or 5-µm thickness were stained with haematoxylin and eosin (H&E).

3.2. Generation of PP2A-B55 antibodies

The four members of the B55 family of regulatory subunits display greater than 80% sequence identity at the protein level (Figure 9). Because of that, the development of highly specific reagents is necessary to study their differential expression in cells and tissues. Due to the absence of some B55 isoform-specific commercial antibodies (Table 3), we designed three specific peptides against mouse B55α, B55β/γ and B55δ proteins to immunize rabbits and generate specific antibodies.

The three different antibodies: B55α, B55β/γ and B55δ, were raised in rabbits against synthetic peptides conjugated to keyhole limpet hemocyanin by GenScript (Figure 9 & Table 3). The resulting sera were adsorbed thoroughly with the CNBr-activated sepharose^{TM} 4 Fast Flow or rProtein A GraviTrap^{TM} (GE Healthcare), previously conjugated with the mentioned peptides. After washing the column extensively with PBS, the specific antibodies, which were retained in the column, were eluted with 0.1M glycine (pH 2.5), immediately neutralized with the appropriate amount of 1M Tris (pH 8.8), and dialyzed against PBS.

To test the specificity of these antibodies, the four different human B55 isoforms were overexpressed in 293T cells and whole protein extracts were immunoblotted with all available antibodies against B55, including commercial available ones and the new generated ones (Figure 10 and Table 3). The B55α antibody recognized specifically the overexpression of B55α, but not the other isoforms (Figure 10, middle lower panel).

The B55β/γ antibody recognized specifically B55β but not the others, including B55γ (Figure 10, right lower panel). This can be explained by the completely different N-terminal sequence of human *Ppp2r2c* compared to mouse *Ppp2r2c*. And, unfortunately, the B55δ antibody did not recognized any isoform in spite of the specificity of the peptide sequence we used, so it was discarded.

```
B55α        MAGA------GGGNDIQWCFSQVK-GAVDDDVAEADIISTVEFNHSGELLATGDKGGRVV
B55δ        MAGAGGGGCPAGGNDFQWCFSQVK-GAVDEDVAEADIISTVEFNYSGDLLATGDKGGRVV
B55γ        ---------MGED--TDTRKINHSFLRDHSYVTEADVISTVEFNHTGELLATGDKGGRVV
B55β1       ---------MEED--IDTRKINNSFLRDHSYATEADIISTVEFNHTGELLATGDKGGRVV
B55β2       ------MKCFSRY--LPYIFRPPNTILSSSCHTEADIISTVEFNHTGELLATGDKGGRVV
                                  .     .  :***:*******::*:************
B55α        IFQQEQENKIQSHSRGEYNVYSTFQSHEPEFDYLKSLEIEEKINKIRWLPQKNAAQFLLS
B55δ        IFQREQENKGRAHSRGEYNVYSTFQSHEPEFDYLKSLEIEEKINKIRWLPQQNAAHFLLS
B55γ        IFQREPESKNAPHSQGEYDVYSTFQSHEPEFDYLKSLEIEEKINKIKWLPQQNAAHSLLS
B55β1       IFQREQESKNQVHRRGEYNVYSTFQSHEPEFDYLKSLEIEEKINKIRWLPQQNAAYFLLS
B55β2       IFQREQESKNQVHRRGEYNVYSTFQSHEPEFDYLKSLEIEEKINKIRWLPQQNAAYFLLS
            ***:* *.*   * :***:*****************************:****:***  ***
B55α        TNDKTIKLWKISERDKRPEGYNLKEEDGRYRDPTTVTTLRVPVFRPMDLMVEASPRRIFA
B55δ        TNDKTIKLWKISERDKRAEGYNLKDEDGRLRDPFRITALRVPILKPMDLMVEASPRRIFA
B55γ        TNDKTIKLWKITERDKRPEGYNLKDEEGKLKDLSTVTSLQVPVLKPMDLMVEVSPRRTFA
B55β1       TNDKTVKLWKVSERDKRPEGYNLKDEEGRLRDPATITTLRVPVLRPMDLMVEATPRRVFA
B55β2       TNDKTVKLWKVSERDKRPEGYNLKDEEGRLRDPATITTLRVPVLRPMDLMVEATPRRVFA
            *****:****::***** ******:*:*: :*   :*:*:**:::*******.:*** **
B55α        NAHTYHINSISINSDYETYLSADDLRINLWHLEITDRSFNIVDIKPANMEELTEVITAAE
B55δ        NAHTYHINSISVNSDHETYLSADDLRINLWHLEITDRSFNIVDIKPANMEELTEVITAAE
B55γ        NGHTYHINSISVNSDCETYMSADDLRINLWHLAITDRSFNIVDIKPANMEDLTEVITASE
B55β1       NAHTYHINSISVNSDYETYMSADDLRINLWNFEITNQSFNIVDIKPANMEELTEVITAAE
B55β2       NAHTYHINSISVNSDYETYMSADDLRINLWNFEITNQSFNIVDIKPANMEELTEVITAAE
            *.**********:*** ***:**********:: **::*************:*******:*
B55α        FHPNSCNTFVYSSSKGTIRLCDMRASALCDRHSKLFEEPEDPSNRSFFSEIISSISDVKF
B55δ        FHPHQCNVFVYSSSKGTIRLCDMRSSALCDRHAKFFEEPEDPSSRSFFSEIISSISDVKF
B55γ        FHPHHCNLFVYSSSKGSLRLCDMRAAALCDKHSKLFEEPEDPSNRSFFSEIISSVSDVKF
B55β1       FHPHHCNTFVYSSSKGTIRLCDMRASALCDRHTKFFEEPEDPSNRSFFSEIISSISDVKF
B55β2       FHPHHCNTFVYSSSKGTIRLCDMRASALCDRHTKFFEEPEDPSNRSFFSEIISSISDVKF
            ***: ** ********::******::****:*:*:********.**********:*****
B55α        SHSGRYMMTRDYLSVKIWDLNMENRPVETYQVHEYLRSKLCSLYENDCIFDKFECCWNGS
B55δ        SHSGRYMMTRDYLSVKVWDLNMEGRPVETHQVHEYLRSKLCSLYENDCIFDKFECCWNGS
B55γ        SHSGRYMLTRDYLTVKVWDLNMEARPIETYQVHDYLRSKLCSLYESDCIFDKFECAWNGS
B55β1       SHSGRYIMTRDYLTVKVWDLNMENRPIETYQVHDYLRSKLCSLYENDCIFDKFECVWNGS
B55β2       SHSGRYIMTRDYLTVKVWDLNMENRPIETYQVHDYLRSKLCSLYENDCIFDKFECVWNGS
            ******::*****:**:****** **:**:***:**********.********* ****
B55α        DSVVMTGSYNNFFRMFDRNTKRDITLEASRENNKPRTVLKPRKVCASGKRKKDEISVDSL
B55δ        DSAIMTGSYNNFFRMFDRNTRRDVTLEASRENSKPRASLKPRKVCTGGKRKKDEISVDSL
B55γ        DSVIMTGAYNNFFRMFDRNTKRDVTLEASRESSKPRAVLKPRRVCVGGKRRRDDISVDSL
B55β1       DSVIMTGSYNNFFRMFDRNTKRDVTLEASRENSKPRAILKPRKVCVGGKRRKDEISVDSL
B55β2       DSVIMTGSYNNFFRMFDRNTKRDVTLEASRENSKPRAILKPRKVCVGGKRRKDEISVDSL
            **.:***:************:**:*******..***: ****:**..***::*:******
B55α        DFNKKILHTAWHPKENIIAVATTNNLYIFQDKVN----
B55δ        DFNKKILHTAWHPMESIIAVAATNNLYIFQDKIN----
B55γ        DFTKKILHTAWHPAENIIAIAATNNLYIFQDKVNSDMH
B55β1       DFSKKILHTAWHPSENIIAVAATNNLYIFQDKVN----
B55β2       DFSKKILHTAWHPSENIIAVAATNNLYIFQDKVN----
            **.********** *.***:*:**********:*
```

Figure 9. Alignment of the amino acid sequences of the murine B55 isoforms. Peptide sequences designed for antibody generation are shown; in red for B55α, in orange for B55δ and in dark blue for B55β/γ; note that in light blue are the common amino acids of B55γ for the designed peptide against both B55β/γ isoforms. An ***** (asterisk) indicates positions which have a single, fully conserved residue; a.**:** (colon) indicates conservation between groups of strongly similar properties; and a **.** (period) indicates conservation between groups of weakly similar properties.

Table 3. Primary antibodies against PP2A-B55 used in this work

Antibody	Source (reference)	Species	Antigen	Isoform reactivity	Applications
PP2A-B55-α (2G9)	Santa Cruz (sc-81606)	Mouse monoclonal	Aas 398-411 (rat B55α)	α/δ>β>γ	WB (not for IHQ)
PP2A B subunit (100C1)	Cell Signalling (#2290)	Rabbit monoclonal	Peptide human PP2A B subunit	All isoforms	WB, IHQ
PP2A B	Cell Signalling (#4953)	Rabbit polyclonal	Peptide human PP2A B subunit (N-terminus)	All isoforms	WB
PPP2R2D (N2C3)	Genetex (GTX116609)	Rabbit polyclonal	aas 91-380 (human B55δ)	B55δ (human/mouse)	WB (not for IHQ)
B55α	"Homemade" #8683	Rabbit polyclonal	MAGAGGGNDIQWCFS (aa 1-15 mouse B55α)	B55α (human/mouse)	WB (not for IHQ)
B55β/γ	"Homemade" #8653	Rabbit polyclonal	MEEDIDTRKINSF (aa1-14 mouse B55β-iso1)	hB55β (iso-1, 4, 5, 7) mB55β (iso-1) mB55γ?	WB
B55δ	"Homemade" #8655	Rabbit polyclonal	MAGAGGGGCPAGGND (aa 1-15 mouse B55δ)	-	-

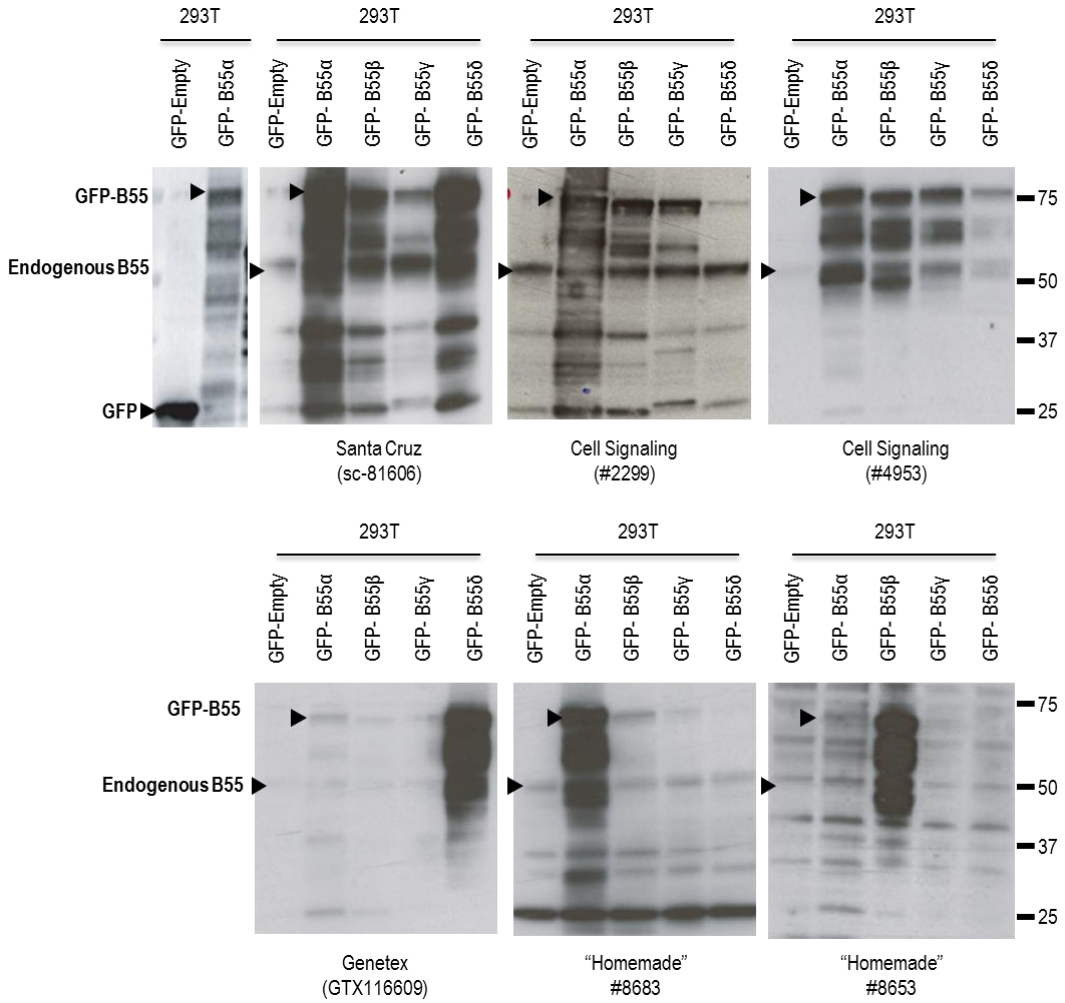

Figure 10. PP2A-B55 antibodies isoform reactivity. All PP2A-B55 primary antibodies were tested in whole cell extracts from HEK293T human cells overexpressing GFP alone or each one of the different isoforms of B55 regulatory subunits N-terminal fused to GFP. Depending on the isoform reactivity of each antibody we can observe a different enrichment of one band or other. The B55-GFP band and the endogenous B55 band are shown. In the upper panel, the antibodies with lower isoform specificity are shown; whereas in the lower panel, antibodies with higher isoform specificity are shown. Note that "Homemade" #8653 cannot recognize human B55γ, but it is expected to recognize mouse B55γ, although we do not have mouse cDNAs to be tested yet. More details regarding PP2A-B55 antibodies are shown in Table 3.

3.3. Cell culture

3.3.1. MEFs extraction and culture

Mouse embryonic fibroblasts (MEFs) were prepared from E13.5 embryos and cultured using standard protocols. E13.5 embryos were extracted from the uterus of pregnant females from heterozygous intercrosses, the placenta was removed, and embryos were isolated from the yolk sac. Embryos, without liver and head, were minced and dispersed

in 0.1% trypsin (5 minutes at 37°C). Cells were grown for two population doublings and then frozen. Once reaching confluence, MEFs were subcultured at a ratio of 1:4. All cultures were maintained in Dulbecco's modified Eagle's medium (DMEM; Lonza) supplemented with 0.1% gentamicin and 10% foetal bovine serum (FBS), and were grown at 37°C in a humidified 5% CO_2 atmosphere.

3.3.2. MEFs immortalization

MEFs at 50-75% confluency were infected with retroviruses expressing Antigen T121 from SV40 virus, in the presence of polybrene (4µg/mL). In order to increase the infection efficiency, two consecutive rounds of infection were performed. Infected MEFs were selected with hygromycin B (150µg/mL) during 2 days and passaged for several weeks to obtained immortalized MEFs (iMEFs).

3.3.3. Viral infections

In order to obtain a *Ppp2r2a*(Δ) allele from a conditional *Ppp2r2a*(lox) allele in vitro, iMEFs infection was performed using adenoviruses expressing CMV-Empty or CMV-Cre (Cre recombinase) obtained from The University of Iowa (Iowa City, IA). Infection was carried out at 250 MOI during 2 days in a cell culture synchronized in G0 by serum deprivation and/or confluence.

For videomicroscopy, iMEFs at 60-70% confluency were infected with lentiviruses containing H2B-RFP in the presence of polybrene (4µg/mL). In order to increase the infection efficiency, two consecutive rounds of infection were performed. Then, RFP-positive cells were sorted in an Influx or FACs Aria sorter, to generate H2B-RFP stable cell lines.

3.3.4. Human and mouse cell lines

HEK293 and U2OS human cells; and, NIH-3T3 mouse cells, were maintained in DMEM medium supplemented with 10% FBS and antibiotics and were grown at 37°C in a humidified 5% CO_2 atmosphere.

3.3.5. Transfection / Nucleofection

Cell lines and MEFs were transfected in subconfluency with Lipofectamine 2000 (Invitrogen) and NEON transfection system (Invitrogen), respectively, in accordance with the manufacturer's instructions.

3.3.6. Flow cytometry

For DNA content analysis, cells were fixed in 70% ethanol at 4ºC at least 1 hour. Then, cells were stained with propidium iodide (PI) (50 µg/mL; Sigma) in presence of RNAseA (0.1 mg/mL; Qiagen) for 30 minutes at 37ºC and keep overnight at 4ºC. The following day the samples were analyzed with a FACS-Canto flow cytometer (BD Bioscience). FlowJo Version 9.6.4 software was used to analyze cell populations (TreeStar).

In order to determine S phase entry, serum starved cells stimulated with FBS 10% were pulsed with EdU (10 µM, Sigma) for 30 minutes and then fixed in 70% ethanol overnigth at 4ºC. The following day, EdU and PI stainings were performed, and the samples were analyzed with a FACS-Canto flow cytometer (BD Bioscience). FlowJo Version 9.6.4 software was used to analyze cell populations (TreeStar).

3.3.7. RNA interference assays

For RNA interference, iMEFs were nucleofected with specific siRNAs against *Mki67* (5'-CGUUGAUAUCAGCAACUUU-3'), gene (Ambion) using Amaxa® Nucleofector® (Lonza) in accordance with the manufacturer's instructions.

3.3.8. Drugs

The following drugs were used in cultured cells at the indicated concentrations: nocodazole (0.8µM, Sigma) and taxol (1µM, Sigma).

3.4. Biochemical and molecular biology procedures

3.4.1. DNA cloning

Human *Ppp2r2a*, *Ppp2r2b*, *Ppp2r2c* and *Ppp2r2d* cDNAs were amplified by PCR from the plasmids #13804 (Addgene), hAF9765, hAF8700 and hAF90289 (Mammalian Gene Collection), respectively,subcloned into pENTR-D-TOPO vector using TOPO technology (Invitrogen), and transferred to a destiny vector as N-terminal-GFP fusions by a LR recombination reaction of the Gateway system (Invitrogen).

GeneArt ™ Strings™ DNA fragments (Invitrogen) were designed to contain the sequence of the eight last Ki67-repeat domains of human *MKI67* in their wild-type form, a phospho-mimetic form and a phospho-mutant form. Each of these sequences, of almost 3Kb, were subcloned as fusions into a lentiviral plasmid (PLVXpuro, Clontech),

in which it was previously subcloned the sequence of the LR domain of *MKI67* gene fused to a reporter fluorescent protein (mNeonGreen).

3.4.2. RNA extraction and Real-time-PCR

To quantify expression of transcripts, total RNA from cells and tissues was isolated using Trizol (Invitrogen). cDNA was synthetized with a M-MLV reverse transcriptase (Promega) and PCR amplification was performed using SYBR Green PCR Master Mix (Applied Biosystems). Amplification of *β-actin* was used for normalization. The oligonucleotides used for amplification of *Ppp2r2a*, *Ppp2r2b*, *Ppp2r2c*, *Ppp2r2d* and *β-actin* are shown in Table 4.

Table 4. Oligonucleotides used for RT-qPCR.

(F: forward, R: reverse primers)

RT-PCR oligos	Species	Target sequence (5`-3')
Ppp2r2a	Mouse	F: CGCTCTGTGACAGGCATTCT R: AACGACCGCTATGGCTGAAT
	Human	F: TGTGGATATCAAGCCTGCCA R: TGCCCTCATGTCACATAGCC
Ppp2r2b	Mouse	F: ACCACAGCTATGCAACCGAA R: CACCCCTACGATGAACCTGG
	Human	F:AAGAGCCGGAAGATCCAAGC R: CTGGTAAGTCTCGATGGGGC
Ppp2r2c	Mouse	F: GAGGTGAGCCCAAGAAGGAC R: TGCCAGAGGTTGATGCGTAG
	Human	F: GGCCACACCTACCACATCAA R: CTGGTAAGTCTCGATGGGGC
Ppp2r2d	Mouse	F: GCGGAAGCCGACATCATC R: CATGACTCTGAAAGGTACTG
	Human	F: TTGAGTGTTGCTGGAACGGT R: GTCTTTCCTCCGCTTACCCC
β-actin	Mouse	F: GACGGCCAGGTCATCACTATTG R: AGGAAGGCTGGAAAAGAGCC
	Human	F: GTCTTCCCCTCCATCGTG R: GGTCATCTTCTCGCGGTTG

3.4.3. Protein extraction and analysis

For immunodetection in protein lysates, cultured cells were harvested and lysed in Laemmli buffer (60 mM Tris pH 6.8; 2% SDS; 10% Glycerol). Proteins were separated on SDS-PAGE, transferred to nitrocellulose membranes (Biorad) and probed using specific primary antibodies (Table 3 &Table 5). HRP-coupled secondary antibodies

(DAKO) were used for immunodetection. Finally, the membranes were developed using the ECL system (PerkinElmer).

3.4.5. Chromosome spreads

Synchronous culture cells were exposed to colcemid (0.5µg/mL; KaryoMax) for 6 hours and hypotonically swollen in KCl (75mM) for 30 minutes at 37ºC. Cells were then spun down and fixed with Carnoy's solution (75% pure methanol, 25% glacial acetic acid). After fixation, cells were dropped from a 5-cm height onto glass slides previously treated with 45% of acetic acid. Slides were mounted with Fluoromount-G® (SouthernBiotech) and 4,6-diamidino-2-phenylindole (DAPI; Invitrogen) or treated for immunofluorescence.

3.5. Microscopy techniques

3.5.1. Videomicroscopy

For videomicroscopy, synchronous, histone H2B-RFP expressing iMEFs were plated on eight-well glass-bottom dishes (Ibidi) and recorded with a DeltaVision RT imaging system (Olympus IX70/71, Applied Precision) equipped with a Plan Apochromatic 20X/1.42 NA objective lens, and maintained at 37ºC in a humidified CO_2 chamber. Images were acquired every 7.5 or 10 minutes, in the absence or presence of drugs, respectively. Images were processed and analysed using ImageJ software.

3.5.2. Immunofluorescence

For immunofluorescence, synchronous cultured cells were grown in coverslips, fixed with 4% paraformaldehyde for 10 minutes at RT and incubated with 0.5% Triton X-100 for 10 minutes at RT for permeabilization. Cells were then blocked with 3% BSA and incubated during 2 hours at RT or ON at 4ºC with the indicated primary antibodies (Table 5), followed by incubation with fluorescent-conjugated secondary antibodies and staining with 4,6-diamidino-2-phenylindole (DAPI; Invitrogen) to visualize DNA, and with Phalloidin-AF647 to visualize the actin pattern. Secondary antibodies, coupled to different Alexa dies (488, 594 or 647), were purchased from Molecular Probes (Invitrogen).

For immunofluorescence over chromosome spreads, previously prepared spreads were rehydrated in PBS for 15 minutes before being swollen in TEEN buffer (1mM triethanolamine-HCl pH8.5, 0.2 mM NaEDTA, 25mM NaCl) for 7 minutes. The

primary and secondary antibodies were diluted (1:100, 1:200) in TEEN plus 0.5% FBS, and washes were performed in TEEN buffer. Final washing was done in KB solution (10mM Tris-HCl pH 7.7, 0.15 M NaCl, 0.5% FBS).

In both cases, image acquisition was performed using either a Leica D3000 microscope or a TCS-SP5 (AOBS) Laser scanning confocal equipped with an oil immersion objective of 40X (HCX-PLAPO 1.2 N.A.). LASAF v2.6. software was used for image acquisition, and analysis was performed with ImageJ or Definiens XD v2.5 softwares, using a customized programmed ruleset.

Table 5. Primary antibodies used in different assays.

(IF: immunofluorescence; WB: Western-blot; IHQ: immunohistochemistry)

Antibody	Source (reference)	Species	Dilution	Applications
ACA (Centromeres)	Antibodies incorporated	Human polyclonal	1:500	IF
C3 Cleaved Caspase-3 (Asp175)	Cell Signaling Technology	Rabbit polyclonal	1:200	IHQ
GFP	Roche	Mouse monoclonal	1:1000	WB
Ki67	Abcam	Rabbit polyclonal	1:500	IF
MPM2	Millipore	Mouse monoclonal	1:500	IF
Phospho-Histone H3 (Ser10)	Millipore	Rabbit polyclonal	1:250	IHQ
α-Tubulin	Sigma	Mouse monoclonal	1:2000	IF
Vinculin	Sigma	Mouse monoclonal	1:5000	WB

3.6. Statistical analysis

Statistical analysis was carried out using Prism 5 (Graphpad Software Inc.). All statistical tests of comparative data were done using two-sided, unpaired Student's t-test or ANOVA for differential comparison between two groups or more groups, respectively. Chi square's test was used for categorical data. Data with $P<0.05$ were considered statistically significant (*, $P<0,05$; **, $P<0.01$; ***, $P<0.001$)

RESULTS

4. RESULTS

4.1. PP2A-B55 expression in mammalian cells

It has been reported that B55α and B55δ isoforms are widely expressed in mammalian cells (including fibroblasts), whereas B55β and B55γ are restricted to the nervous system (Strack et al., 1998, Schmidt et al., 2002). In agreement with that, our data at the RNA level in different mouse (3T3 and *wild-type* MEFs) and human (293 and U2OS) cell lines resulted in high expression of both B55α and B55δ isoforms, but almost no expression of B55β and B55γ isoforms (Figure 11A). Whereas B55α appears to be the most abundant isoform in human cells, both B55δ, and to a lesser extent B55α, are the predominant ones in mouse cells. Furthermore, study of RNA levels in *wild-type* mouse tissues revealed that B55δ appears to be the predominant B55 isoform in mice in all analysed tissues, except for brain, where B55β and specially B55γ are also highly expressed (Figure 11B).

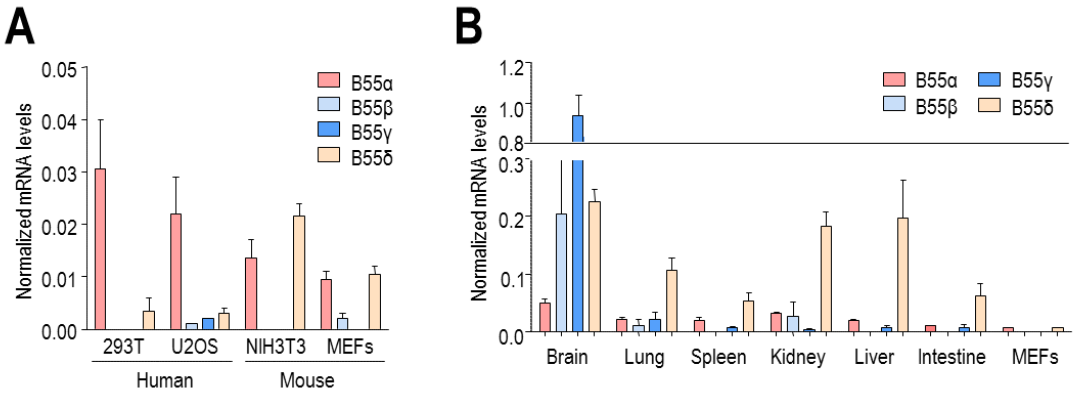

Figure 11. Endogenous B55 mRNA levels. (A) Endogenous mRNA levels for all B55 isoforms (α, β, γ and δ) were analysed in two human cell lines (293T and U2OS) and two mouse cell lines (NIH3T3 and MEFs). (B) Endogenous mRNA levels of all B55 isoforms (α, β, γ and δ) in several *wild-type* mouse tissues. mRNA levels were measured by qRT-PCR and normalized to the mean of β-actin. Error bars show standard error of mean (SEM).

To analyse the expression of these PP2A B regulatory subunits at the protein level we first generated some new antibodies against B55α, B55β/γ and B55 δ isoforms (see Materials and Methods 3.2). Since the one against B55δ did not work, we made use of a commercial antibody (Genetex), which is specific for this isoform (Table 3). Specific B55α and B55δ antibodies identified a single band per isoform in immunoblots, which

corresponds to the expected B55 size. In case of B55β/γ antibody, two bands were detected in mouse brain lysates, which may correspond to B55β (lower band) and B55γ (upper band) (Figure 12B) as previously described (Strack, 1998).

The study of B55α protein expression using our homemade antibody revealed its wide expression in the organism. This isoform was detected in brain, liver, muscle, intestine and lung tissues (Figure 12A) in spite of not being the most abundant at the mRNA level. On the other hand, the analysis of B55β and B55γ protein levels with our other homemade antibody revealed their specific expression in brain tissue. In this case, and according to mRNA data, all B55 isoforms could be detected in protein extracts from brain but not from other *wild-type* tissues (Figure 12B).

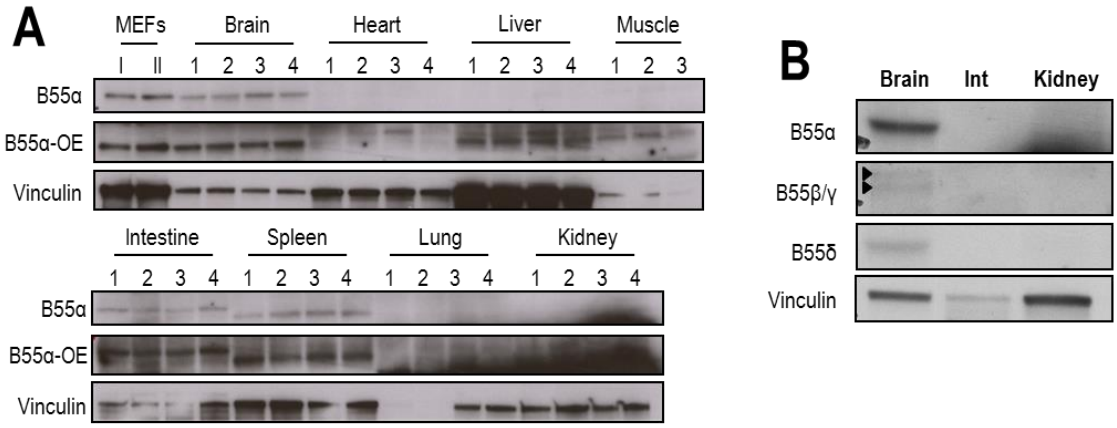

Figure 12. B55 protein levels in *wild-type* mouse tissues. (A) Protein expression levels of B55α in mouse tissues. Two independent MEFs clones (I and II) were used, and tissues from four *wild-type* mice (1, 2, 3 and 4) were analysed. (B) Tissue expression of all B55 isoforms (α, β, γ and δ) in brain lysates. Whole extracts (30µg/lane) of the indicated samples were immunoblotted with the indicated antibodies. Vinculin was used as a loading control. OE: overexposure. Int., intestine.

4.2. Loss of function of PP2A-B55α: *Ppp2r2a* mouse model

4.2.1. Generation of *Ppp2r2a* knock-out mouse models

To generate the *Ppp2r2a* knock-out (KO) model we used ES cell clones positive for a Ppp2r2a targeting vector, obtained by the KOMP repository (EPD0328_1_G08, www.komp.org). The *Ppp2r2a* targeting vector contains exons 5-8 flanked with loxP sequences and a frt-IRES-LacZ (reporter)-loxP-neo^{r} (neomycin-resistant gene)-frt cassette for selection purposes (Figure 13A). The corresponding ES cells were microinjected into wild-type blastocysts to generate *Ppp2r2a*(+/loxfrt) mice. After this

process, we obtained only one chimeric male with 60% of chimerism. The IRES-LacZ and neo^{r} cassette were first removed by crossing with transgenic mice expressing the Flp recombinase resulting in the conditional *Ppp2r2a*(lox) allele. Germline deletion of exons 5-8 was achieved by additional crosses with EIIa-Cre transgenic mice, which express constitutive and ubiquitous Cre recombinase (Cre), to generate the *Ppp2r2a*(-) allele. Genotyping of these alleles was done by PCR using genomic DNA extracted from the tails of these mice and two distinct combinations of primers (1F+2R and 1F+1R, Figure 13A,B)

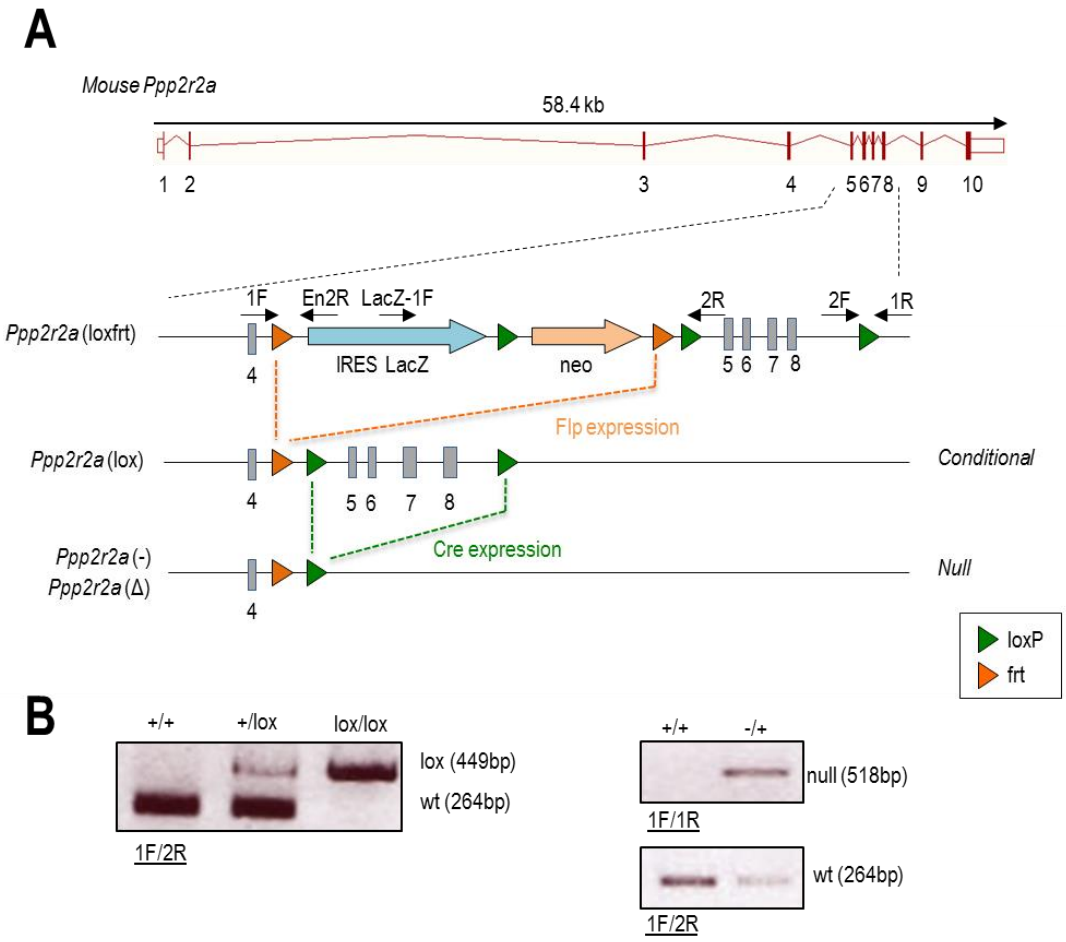

Figure 13. Generation of *Ppp2r2a* conditional and null mutants. (A) Schematic representation of the *Ppp2r2a* genomic structure and targeting vector, with the resulting alleles. The mouse *Ppp2r2a* locus that encodes B55α contains 10 exons (red boxes) harbouring noncoding (open boxes) or protein-coding (filled boxes) sequences. LoxP (green triangles) sites and frt (orange triangles) sites are used to flank B55α exons and the neo-resistance or the neo-resistance and IRES-LacZ in the targeting vector, respectively. The neo cassette (light orange arrow) was used for selection of clones after homologous recombination (HR) in ES cells. The IRES-LacZ and the neo cassette are eliminated *in vivo* by crossing *Ppp2r2a*(+/loxfrt) mice with transgenic mice expressing Flp recombinase. Further excision of exons 5-8

is mediated by expression of Cre recombinase resulting in the *Ppp2r2a*(-) null allele. Primers used for genotyping are also indicated. (B) Representative PCR products confirm the presence of *Ppp2r2a(*wt), *Ppp2r2a*(lox) and *Ppp2r2a*(-) null alleles after amplification from tail genomic DNA using the indicated oligonucleotides.

4.2.2. *Ppp2r2a* is essential for mouse embryonic development

Ppp2r2a(+/-) mice develop normally and are fertile. However, intercrosses of heterozygous *Ppp2r2a*(+/-) mice yielded no live *Ppp2r2a*(-/-) offspring (Figure 14A). No postnatal *Ppp2r2a*(-/-) mice were found among 129 live-born mice from the intercrosses, which suggests that homozygous deficiency in *Ppp2r2a* leads to embryonic lethality, although the timing of embryo demise is not known. Therefore, timed matings were set up between heterozygous animals, and foetuses were collected at E13.5 days of gestational development. A reduced proportion of *Ppp2r2a*(-/-) embryos were obtained (12% vs 25% expected), suggesting that constitutive ablation of *Ppp2r2a* compromise mouse survival during late embryonic development (Figure 14B).

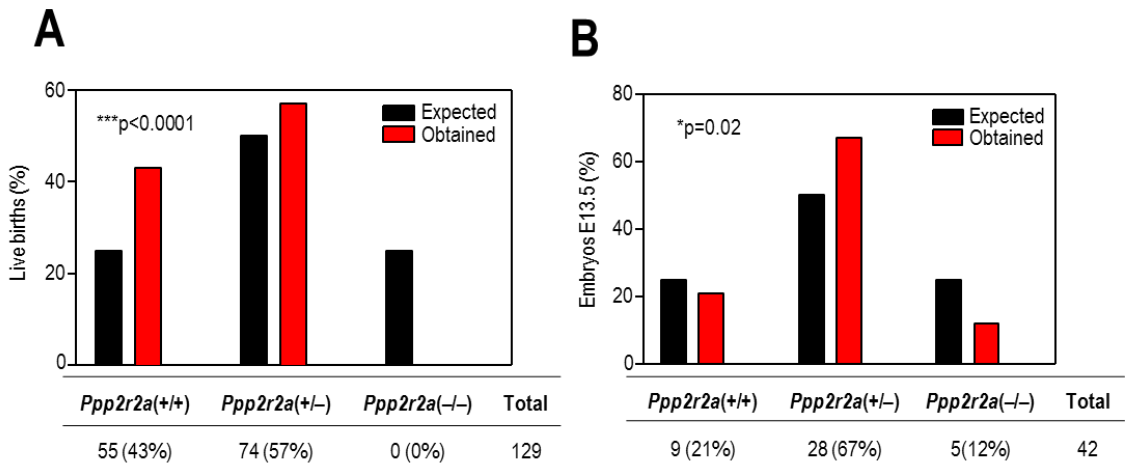

Figure 14. *Ppp2r2a* is essential for late embryonic development. (A) Offspring distribution of crosses between heterozygous *Ppp2r2a*(+/-) mice. Percentage of live-birth mice is shown, demonstrating non-Mendelian inheritance of the knockout allele (red bars: obtained offspring vs. black bars: expected offspring). (B) Distribution of E13.5 embryos (in percentage) obtained from crosses between heterozygous *Ppp2r2a*(+/-) mice. The number (and percentage) of mice or embryos with the indicated genotype is shown below the graphs. **P*<0,05; ****P*<0,001 (Chi-square test).

Inspection of E13.5 embryos by histopathology revealed that *Ppp2r2a*(-/-) embryos that reach this stage are smaller and present a delay in development compared to their wt littermates (Figure 15). Although we could distinguish all organs in the *Ppp2r2a*(-/-) E13.5 embryo , they were generally smaller compared to the wt. Interestingly, a higher

reduction or almost total absence of brain tissues was observed in the null embryos, suggesting that this isoform is essential for brain development during embryonic stages.

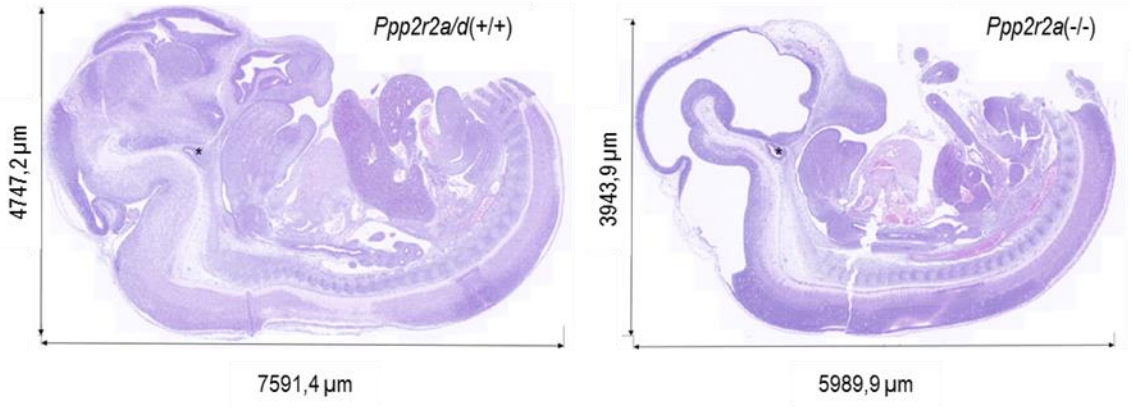

Figure 15 Defective development in *Ppp2r2a*(-/-) mice. Representative H&E images of E13.5 *Ppp2r2a/d*(+/+) and *Ppp2r2a*(-/-) embryos of the same litter. Differences in size and in developmental stage of whole organism are shown. Hypophysis is marked with an asterisk (*) as reference.

4.3. Loss of function of PP2A-B55δ: *Ppp2r2d* mouse model

4.3.1. Generation of *Ppp2r2d* knock-out mouse model

To generate the *Ppp2r2d* knockout model we first constructed a targeting vector in which *Ppp2r2d* exon 3 is flanked with loxP sequences and a frt-neo^r-frt cassette for selection purposes (Figure 16A). At both ends of the constructs we cloned two homology arms to facilitate recombination in ES cells. After homologous recombination, we selected two different clones (ESMS1.137 and ESMS1.129) carrying the recombinant allele *Ppp2r2d*(loxfrt) (Figure 16B) and the corresponding ES cells were microinjected into wild-type blastocysts to generate *Ppp2r2d*(+/loxfrt) mice. After this process, we obtained seven chimeric males with 70-100% of chimerism. Germline deletion of exon 3 was achieved by additional crosses of these chimeras with EIIa-Cre transgenic mice to generate the *Ppp2r2d*(-) allele. Genotyping of these alleles was performed by PCR using genomic DNA from the tails and two combinations of primers (2F+1R+2R and 1F+1R, Figure 16A,C).

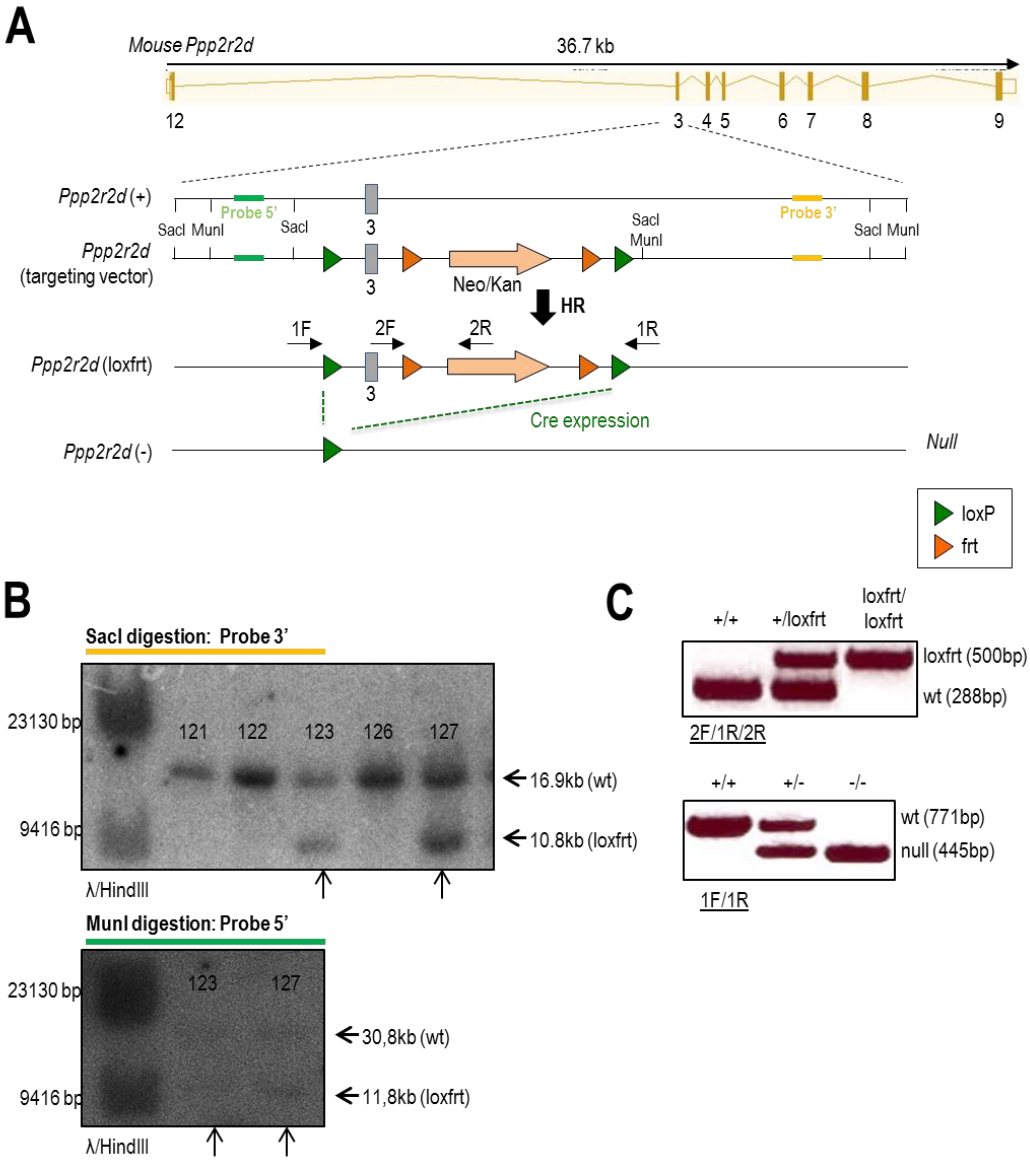

Figure 16. Generation of *Ppp2r2d* null allele. (A) Schematic representation of the *Ppp2r2d* genomic structure, targeting vector and resulting alleles. The mouse *Ppp2r2d* locus encoding B55δ contains 9 exons (orange boxes) harboring noncoding (open boxes) or protein-coding (filled boxes) sequences. LoxP (green triangles) sites and frt (orange triangles) sites are used to flank B55δ exons or the neo-resistance in the targeting vector, respectively. The neo cassette (light orange arrow) is used for selection of clones following homologous recombination (HR) in ES cells. The exon 3 and neo cassette are eliminated *in vivo* by crossing *Ppp2r2d*(+/loxfrt) mice with transgenic mice expressing the EIIa-Cre recombinase. SacI and MunI restriction sites and 5' and 3' probes for Southern blot are indicated; and positions of primers used for genotyping are also shown. (B) Southern blot analysis of recombinant ES cells showing two *Ppp2r2d*(+/loxfrt) clones (marked with arrows) that underwent HR. DNA was firstly digested with SacI and hybridized with the 3' probe. Positive clones were also digested with MunI and hybridized with the 5' probe for confirmation. (C) Representative PCR products showing the presence of the *Ppp2r2d*(loxfrt) allele in chimeras (upper panel), and the *Ppp2r2d*(null) allele after crossing chimeras with transgenic mice EIIa-Cre (lower panel). Amplification was performed with the indicated oligonucleotides.

4.3.2. *Ppp2r2d* loss is dispensable for embryonic development

Ppp2r2d(+/-) mice develop normally and are fertile; and, the result of intercrosses of these heterozygous mice produced *Ppp2r2d*(+/+), *Ppp2r2d*(+/-), and *Ppp2r2d*(-/-) offspring with normal Mendelian ratios (Figure 17), suggesting that loss of *Ppp2r2d* has no major consequences in embryonic development. Moreover, the complete germline deletion of *Ppp2r2d* gene did not cause any impact in the survival or fertility of these mice. In addition, histopathological analysis of representative tissues from *Ppp2r2d(-/-)* young (12 weeks) and aged mice (48 weeks) did not show any specific or severe pathological sign.

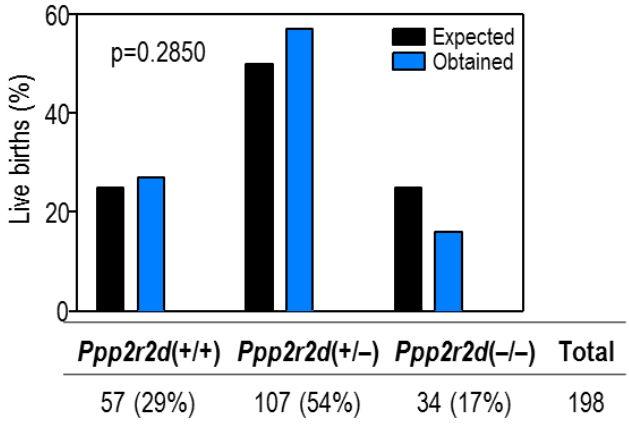

Figure 17. *Ppp2r2d* is dispensable for embryonic development. Offspring distribution of crosses between heterozygous *Ppp2r2d*(+/-) mice. Live-birth mice numbers demonstrate normal Mendelian inheritance of the knockout allele (blue bars: obtained offspring vs. black bars: expected offspring). Number of mice and percentage of each obtained genotype are shown below the graphs. (P>0.05, not significant differences; Chi-square test)

As we mentioned in the introduction, the four members of the B55 family of regulatory subunits display greater than 80% sequence identity at the protein level, so it is important to consider the putative compensation between isoforms. With this purpose, we analysed the expression of the other B55 isoforms in different regions of the brain: cortex, cerebellum and hippocampus, where we can detect all isoforms at protein levels. We analysed expression both at the mRNA and protein level (Figure 18), confirming in both cases how the germline deletion of *Ppp2r2d* gene completely abolished transcription and translation of B55δ, respectively. At the mRNA level we only detected an increase in *Ppp2r2a* expression in hippocampus of *Ppp2r2d*(-/-) mice compare to *Ppp2r2a/d*(+/+) tissue. This was also the case in lung tissue, where there were only detectable mRNA levels of both *Ppp2r2a* and *Ppp2r2d* in *wild-type* tissues but no other B55 isoforms (Figure 18A, left upper panel). However, at the protein level, we could only detect a slight increase of *Ppp2r2a* (B55α) in cortex of *Ppp2r2d*(-/-) mice, but not

in hippocampus, compared to the *Ppp2r2a/d*(+/+) tissue. Interestingly, there was a clear increase in protein expression of the other isoforms, B55β and B55γ, in all brain regions analysed (Figure 18B), although there were not differences in mRNA expression. These data suggest the possibility of other B55 isoforms displaying some compensatory roles in B55δ-null mice.

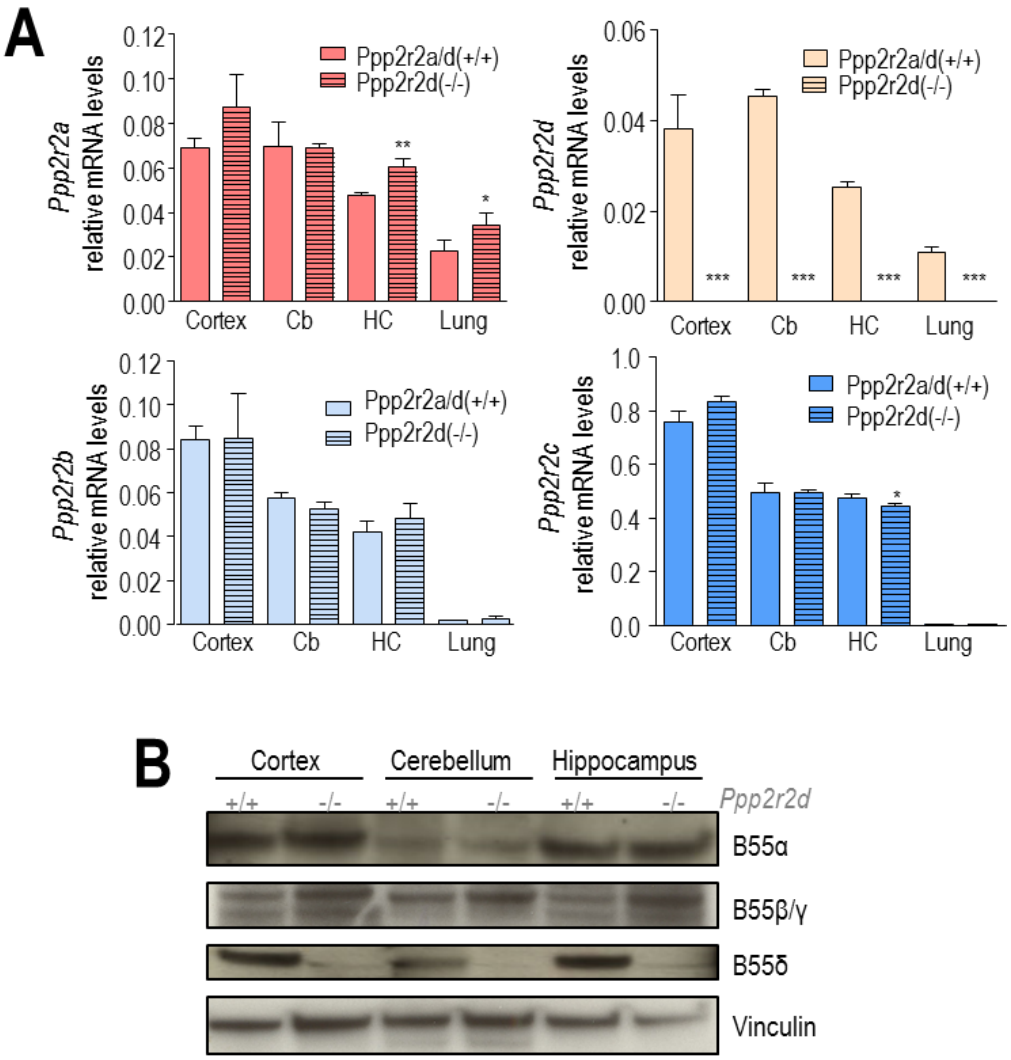

Figure 18. B55 mRNA and protein expression levels in *Ppp2r2d*(-/-) brain tissues. (A) mRNA levels for all B55 isoforms (α, β, γ and δ) were analysed in several *wild-type* (*Ppp2r2a/d*(+/+)) and mutant *Ppp2r2d*(-/-) mouse brain tissues, and lung as a control. mRNA levels were measured by qRT-PCR and normalized to the mean of β-actin. Bars show the average of two mice, and error bars show SEM. Cb, cerebellum; HC, hippocampus. **P*<0.05; ***P*<0.01; ****P*<0.001(Student *t* test). (B) Protein expression of B55 isoforms (α, β, γ and δ) in different *wild-type* and *Ppp2r2d*(-/-) mouse brain regions. Whole protein extracts (30µg/lane) of the indicated tissues were immunoblotted with antibodies against specific B55 isoforms. Vinculin was used as a loading control.

4.4. Function of PP2A-B55 phosphatase in cell cycle progression

To analyse the functional relevance of PP2A-B55 complexes in cell cycle progression we obtained mouse embryonic fibroblast (MEFs) from E13.5 embryos, resulting from heterozygous crosses between previously described different alleles. All MEFs used in these assays were immortalized to work with more stable -not senescence- cell lines and to have enough material for all the performed assays.

4.4.1. Depletion of PP2A-B55 α/δ results in proliferation defects

We first analysed the effect of B55δ ablation on cell proliferation. To do that, we monitored the growth of asynchronous cultures of wild type (wt) *Ppp2r2a/d*(+/+) and *Ppp2r2d*(-/-) MEFs during six days. MEF lines from both genotypes grew at comparable rates and displayed no differences in cell proliferation, indicating that B55δ is not required for cell proliferation at least in MEFs (Figure 19A).

Then, we analysed the consequence of eliminating the α isoform (*Ppp2r2a*) of B55. Since acute ablation of *Ppp2r2a* led to embryonic lethality we made use of MEFs derived from the conditional *Ppp2r2a*_lox model. *Ppp2r2a*(lox/lox) MEFs were infected with adenoviruses expressing Cre recombinase (AdCre) to induce the genetic ablation of B55α generating the null [*Ppp2r2a*(Δ)] allele. As a control, *Ppp2r2a*(lox/lox) cells were infected with an empty adenovirus (AdEmpty). *Ppp2r2a*(Δ/Δ) cells only showed a slight delay in proliferation in comparison with their wt counterparts *Ppp2r2a*(lox/lox) cells, indicating that MEFs are able to proliferate in the absence of B55α (Figure 19B).

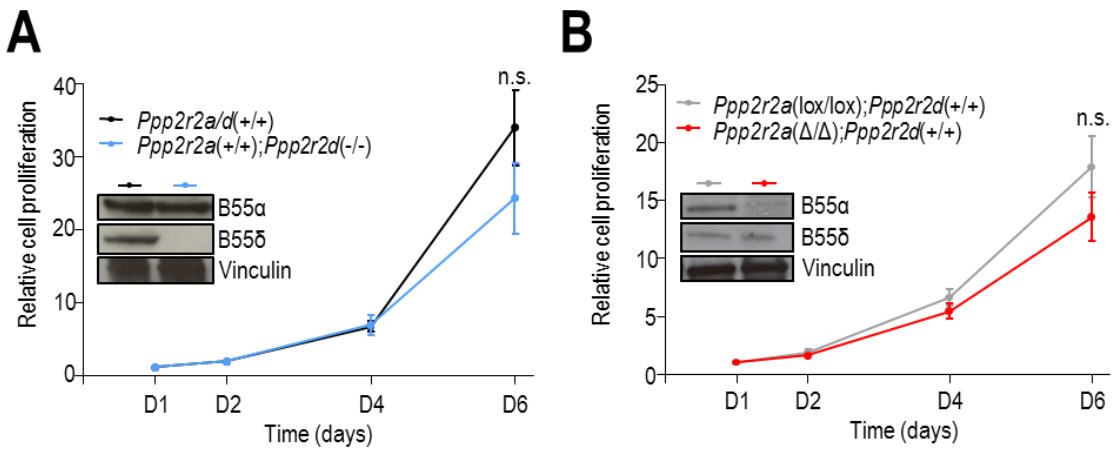

Figure 19. Single deficiency of B55α or B55δ does not cause major proliferation defects. (A) Relative cell proliferation of *Ppp2r2d*(-/-) and *wild-type* MEFs. (B) Relative cell proliferation of *Ppp2r2a*(Δ/Δ)

and *Ppp2r2a*(lox/lox) MEFs. Data are means ±SEM (n=3 independent clones). n.s., not significant differences ($P>0.05$; Student *t* test). Western Blot analysis of B55α and B55δ expression in one representative clone of each genotype is also shown. Vinculin was used as a loading control.

Since there were no major differences in cell proliferation upon B55α- or B55δ depletion, we decided to generate a new mouse model combining both alleles, the conditional allele for B55α, *Ppp2r2a*(lox), and the constitutive null allele for B55δ, *Ppp2r2d*(-), to avoid the potential compensatory effect between both isoform. We generated MEF lines from *Ppp2r2a*(lox/lox);*Ppp2r2d*(-/-) embryos, in which AdCre infection results in genetic deletion of B55α and, therefore, combined depletion of both B55α and δ isoforms (*Ppp2r2a*(Δ/Δ);*Ppp2r2d*(-/-) (Figure 20A). B55α/δ-deficient cells showed a clear reduction in proliferation when compared with single depletion of B55δ (Figure 20A). All together, these data show that whereas the absence of one of these B55 isoforms, either α or δ, does not significantly compromise cell proliferation, combined deletion of both B55 isoforms leads to a severe proliferation defect (Figure 20B).

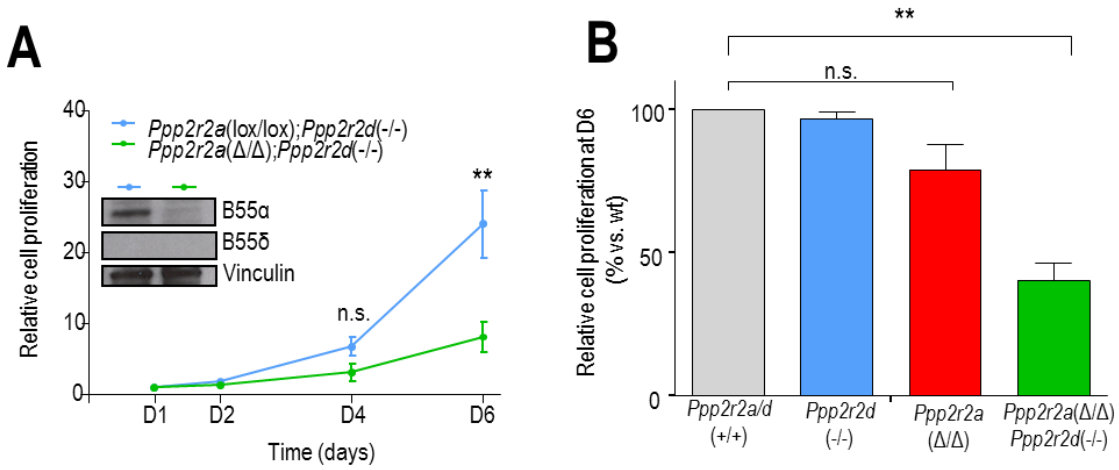

Figure 20. Concurrent depletion of *Ppp2r2a* and *Ppp2r2d* affects MEFs proliferation. (A) Relative cell proliferation of *Ppp2r2a*(Δ/Δ);*Ppp2r2d*(-/-) and *Ppp2r2a*(lox/lox); *Ppp2r2d*(-/-) MEFs. Protein expression of B55α and B55δ in one representative clone of each genotype was analysed by Western Blot. Vinculin was used as a loading control. (B) Relative cell proliferation at D6 of the indicated genotypes, where cell proliferation of their corresponding *wild-type* allele was set as 100%. Data are means ± SEM (n=3 independent clones). n.s., not significant differences; $**P<0.01$ (Student *t* test).

Analysis of cell cycle profiles at different days during the growth curve assay only revealed a slight increase in the over 4n population in the B55α/δ deficient cells at day 6, whereas in the other cells there were not any significantly change (Figure 21). This suggests that decrease in proliferation when both isoforms are depleted could be due to a mitotic defect that increases polyploidy in cells.

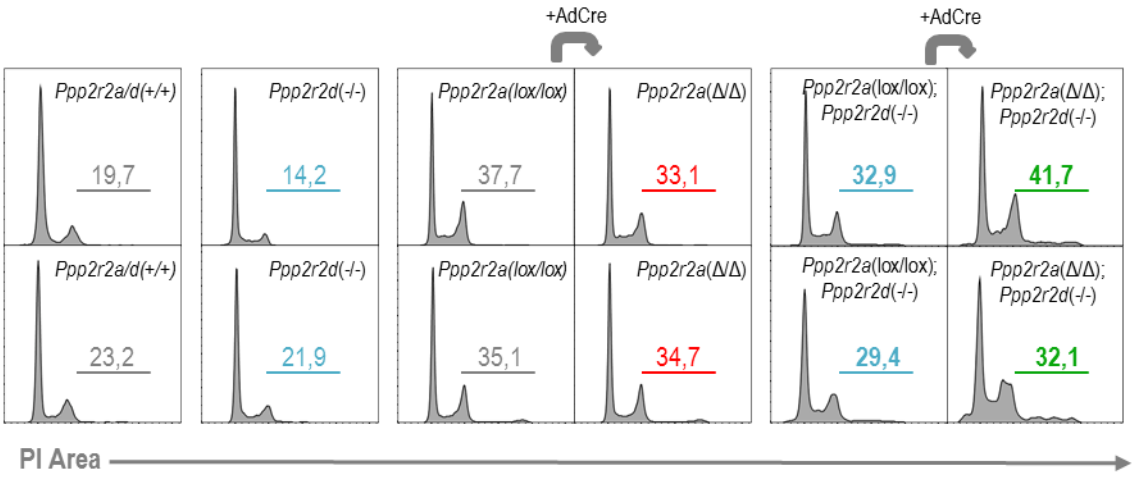

Figure 21. Concurrent depletion of *Ppp2r2a* and *Ppp2r2d* affects G2/M and over 4n populations. Cell cycle profiles of MEFs showing population-based DNA content analysis by flow cytometry (propidium iodide staining), at day 6 of the growth curve. Numbers indicate percentage of the over 4n population.

4.4.2. Elimination of PP2A-B55α/δ does not affect S-phase entry

Besides the role of PP2A/B55 in mitosis, it has been reported that PP2A/B55α counteracts CDK-mediated phosphorylation of retinoblastoma protein (pRB) and the pocket proteins, p130 and 107, and might restrain cell cycle progression at the G_0/G_1 or G_1/S transitions (Jayadeva et al., 2010).

To assess if the proliferation defects of *Ppp2r2a*(Δ/Δ);*Ppp2r2d*(-/-) cells were due to a defect in S phase entry or progression, we monitored S phase entry from quiescence in B55α/δ-deficient cells. To perform this assay, *Ppp2r2a*(lox/lox); *Ppp2r2d*(-/-) MEFs were synchronized in G_0 by serum deprivation and infected with AdCre to generate the double B55α/δ KO, or AdEmpty as a control. Then, cells were collected at different time points after addition of serum: 0h, 12h, 16h, 20h and 24h to follow S phase entry and progression. Before harvesting, cells were incubated in the presence of EdU for 30 min to monitor DNA replication and therefore S-phase. No differences were observed in *Ppp2r2a*(Δ/Δ);*Ppp2r2d*(-/-) cells compared to their controls (Figure 22), indicating that impaired proliferation of B55α/δ -deficient cells is not probably due to a S phase defect.

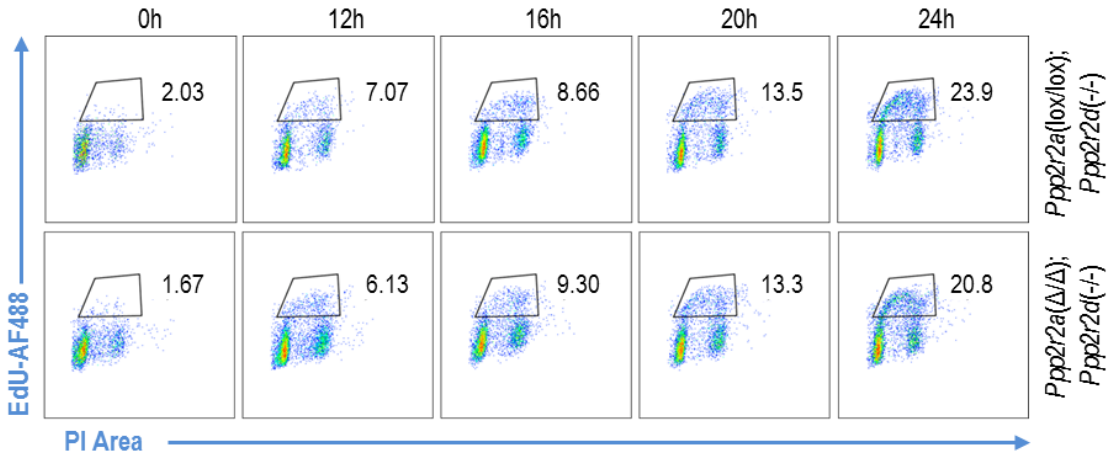

Figure 22. *Ppp2r2a*(Δ/Δ);*Ppp2r2d*(-/-) cells did not show defects in S-phase entry. Analysis of S-phase entry and progression by flow cytometry. The correlation between DNA content (Propidium Iodide staining) and DNA-replicating cells (EdU incorporation) is shown for a representative clone of *Ppp2r2a*(Δ/Δ);*Ppp2r2d*(-/-) (lower panel) and its corresponding *Ppp2r2a*(lox/lox);*Ppp2r2d*(-/-) control (upper panel). Percentages of EdU-positive cells are indicated.

4.4.3. Mitotic defects in PP2A-B55-deficient cells

Although there were not differences in the proliferation of single KO *Ppp2r2d*(-/-) or *Ppp2r2a*(Δ/Δ) cells compared to their controls, we decided to perform an in depth analysis of mitosis in these cells, due to the reported data about their role in mitosis in other organisms (Mayer-Jaekel et al., 1993, Mayer-Jaekel et al., 1994, Mochida et al., 2009).

To study the kinetics of mitotic entry and progression, wt and *Ppp2r2d*(-/-) MEFs, stably expressing histone H2B-mRFP, were arrested in G_0 in the absence of serum, and stimulated with serum to reenter the cell cycle. Twenty hours after the addition of serum, cells were monitored by using time-lapse microscopy during 24h. No differences were observed in the kinetics of mitotic entry (determined by cell rounding and chromosome condensation) in *Ppp2r2d*(-/-) cells compared to wt cells (Figure 23A). Moreover, there were no significant differences in the duration of mitosis in *Ppp2r2d*(-/-) compared with the wt control, *Ppp2r2a/d*(+/+) (55,26±3,92min vs. 61.92±6.86min) (Figure 23B) compared with the wt control, *Ppp2r2a/d*(+/+).Finally, the study of the segregation defects occurring during mitosis did not reveal any major difference in conditions of depletion of B55δ isoform.

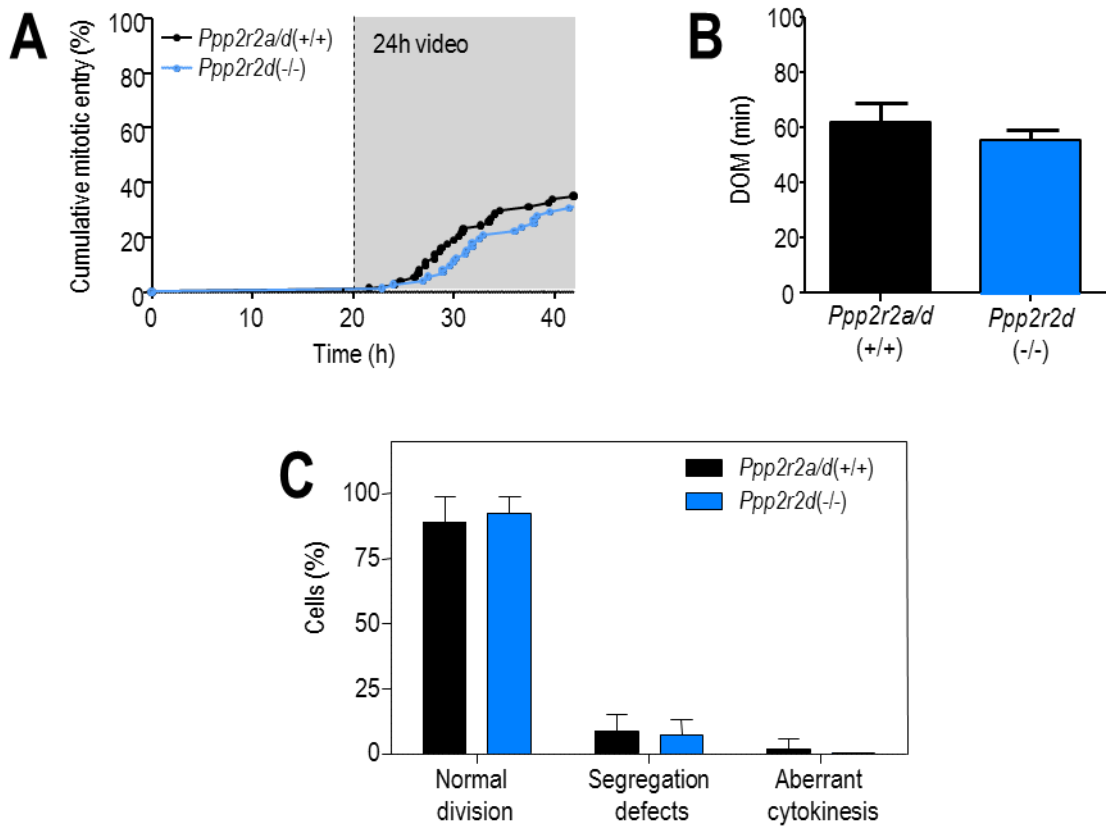

Figure 23 *Ppp2r2d* deletion does not affect mitosis. (A) Quantification of mitotic entry (as scored by cell rounding and chromosome condensation) in *wild-type* (*Ppp2r2a/d*(+/+)) and *Ppp2r2d*(-/-) cells after visual analysis of time-lapse images. (B) Duration of mitosis (from mitotic entry until mitotic exit, based on DNA decondensation and loss of rounded morphology) in *wild-type* (*Ppp2r2a/d*(+/+)) and *Ppp2r2d*(-/-) cells. (C) Quantification of mitotic aberrations in *wild-type* (*Ppp2r2a/d*(+/+)) and *Ppp2r2d*(-/-) cells. Data are means +SEM of n=3 different clones.

Then, to study the kinetics of mitotic entry and progression in the absence of B55α isoform we made use of the conditional MEF lines. *Ppp2r2a*(lox/lox) MEFs, stably expressing histone H2B-mRFP, were arrested in G_0 in the absence of serum, transduced with AdenoEmpty or AdenoCre viruses, and stimulated with serum to reenter the cell cycle. Twenty hours after the addition of serum, cells were monitored by using time-lapse microscopy during 24h. No major differences were observed in the kinetics of mitotic entry in *Ppp2r2a*(Δ/Δ) compared to *Ppp2r2a*(lox/lox) control cells (Figure 24A). Similarly, there were no significant differences in the duration of mitosis in *Ppp2r2a*(Δ/Δ) compared with its corresponding control, *Ppp2r2a*(lox/lox) (71.83±8.77min vs. 63.82±7.16min) (Figure 24B), and a similar percentage and type of segregation defects was observed in Ppp2r2a-deficient cells compared to wt ones

(Figure 24C). In summary, these data indicate that deletion of B55α or B55δ does not lead to major mitotic defects in mouse cells.

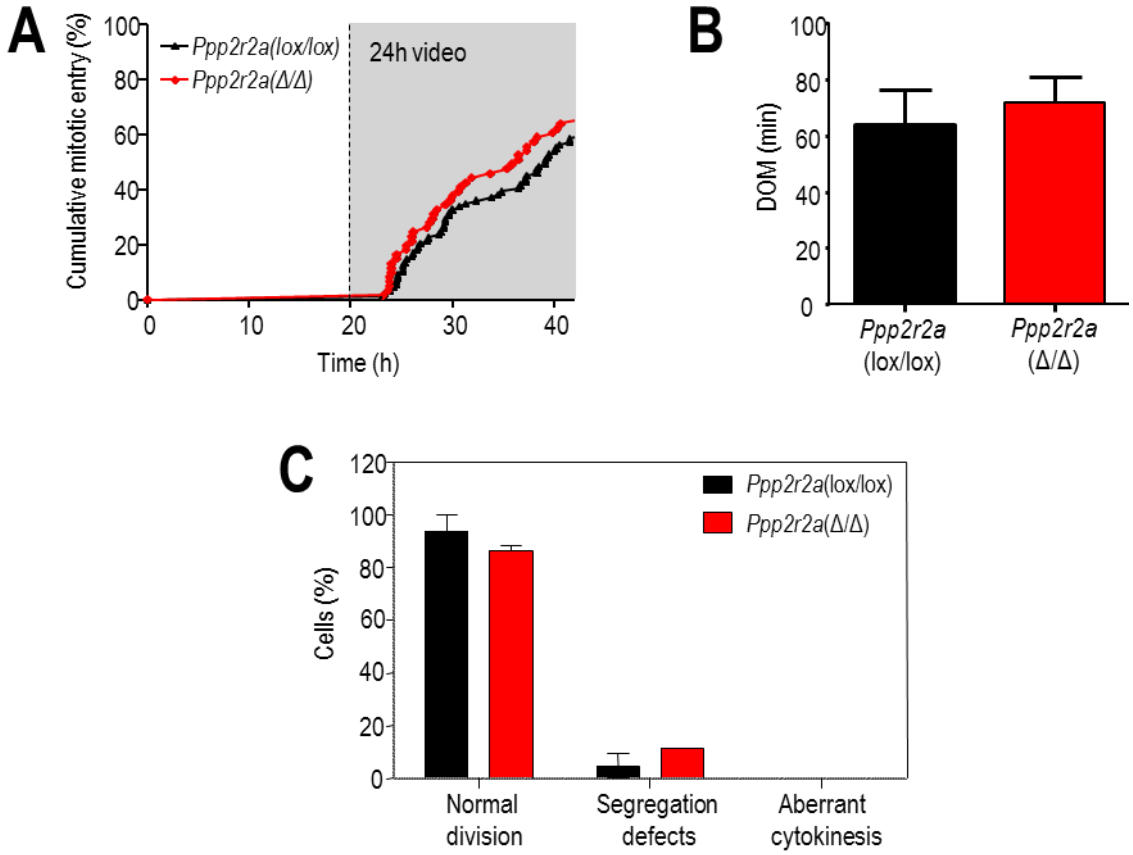

Figure 24. *Ppp2r2a* deletion does not induce mitotic defects. (A) Quantification of mitotic entry (as scored by cell rounding and chromosome condensation) in *Ppp2r2a*(lox/lox)) and *Ppp2r2a*(Δ/Δ) cells after visual analysis of time-lapse images. (B) Duration of mitosis (from mitotic entry until mitotic exit, based on DNA decondensation and loss of rounded morphology) in *Ppp2r2a*(lox/lox) and *Ppp2r2a*(Δ/Δ) cells. (C) Quantification of mitotic aberration in *Ppp2r2a*(lox/lox)) and *Ppp2r2a*(Δ/Δ) cells. Data are means + SEM of n=3 different clones.

Considering the potential redundancy between B55α and B55δ isoforms, we decided to analyze mitotic progression upon combined deletion of both isoforms. Simultaneous depletion of both subunits revealed that *Ppp2r2a*(Δ/Δ); *Ppp2r2d*(-/-) MEFs entered earlier in mitosis than *Ppp2r2a*(lox/lox); *Ppp2r2d*(-/-) MEFs (23.74±13.07h after serum stimulation vs. 27.57±13.04h), when released from quiescence (Figure 25A). Moreover, the lack of both isoforms caused a significant increased in the duration of mitosis (80.97±2.61min compared to 69.65±2.07min in *Ppp2r2a*(lox/lox);*Ppp2r2d*(-/-) MEFs) (Figure 25B,C and Figure 26). A more detailed analysis revealed no differences in

timing between NEB and metaphase; however, timing from anaphase onset till the end of mitosis was on average 10 min longer in *Ppp2r2a(Δ/Δ);Ppp2r2d*(-/-) cells compared to control cells (43.58±6.19min vs. 33.30±3.03min) (Figure 25C). These data suggest that the prolonged duration of mitosis in B55α/δ-deficient cells was more likely due to a defect in mitotic exit.

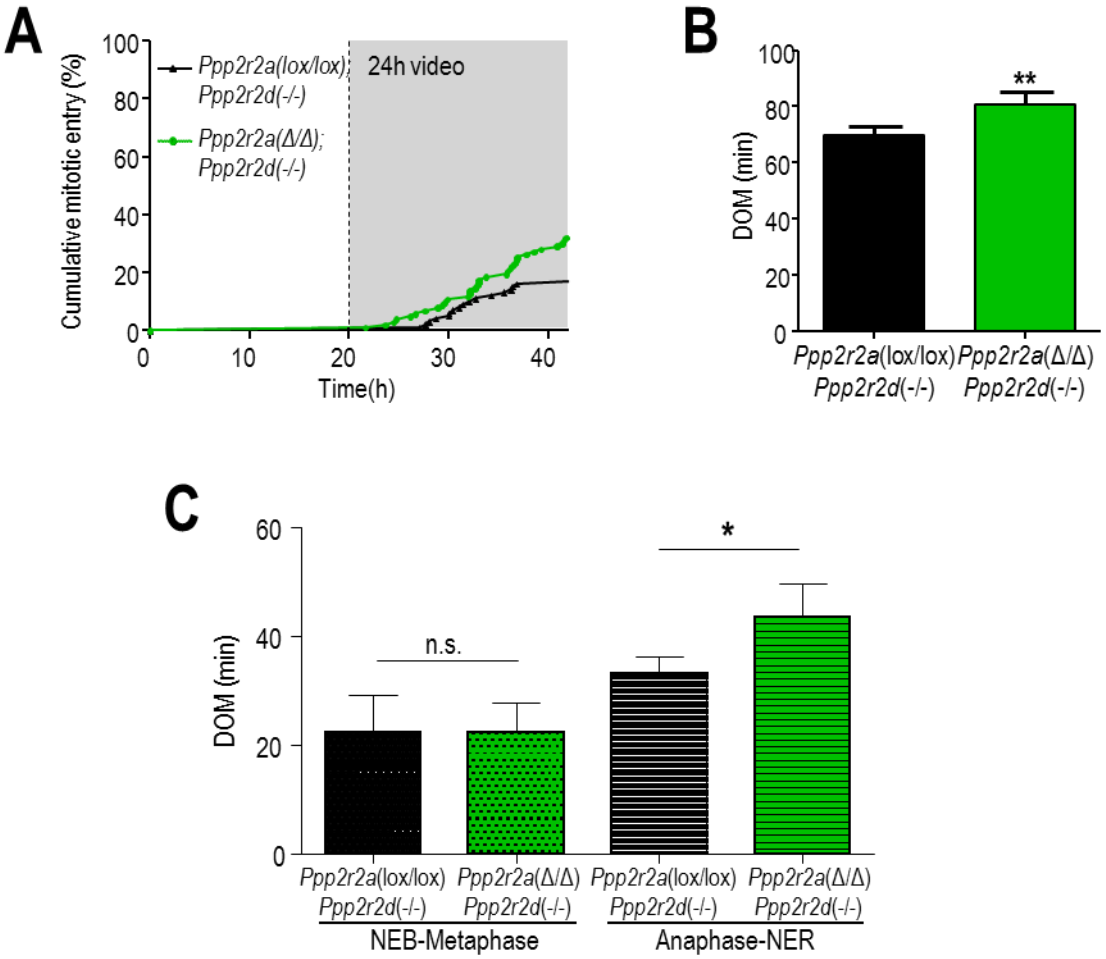

Figure 25. *Ppp2r2a/d* deficiency affects the kinetics of mitotic entry and progression. (A) Quantification of mitotic entry (as scored by cell rounding and chromosome condensation) in *Ppp2r2a*(lox/lox));*Ppp2r2d*(-/-) (black) and *Ppp2r2a*(Δ/Δ);*Ppp2r2d*(-/-) cells (green) after visual analysis of time-lapse images. (B) Duration of mitosis (from mitotic entry until mitotic exit, based on DNA decondensation and loss of rounded morphology) in *Ppp2r2a*(lox/lox));*Ppp2r2d*(-/-) and *Ppp2r2a*(Δ/Δ);*Ppp2r2d*(-/-) cells. (C) Quantification of duration of mitosis from NEB until metaphase; and, from anaphase onset until mitotic exit in *Ppp2r2a*(lox/lox);*Ppp2r2d*(-/-) and *Ppp2r2a*(Δ/Δ);*Ppp2r2d*(-/-) cells. n.s., not significant differences; **P*<0.05; ***P*<0.01 (Student *t* test). Data are means +SEM of n=3 different clones.

This prolonged duration in the last phases of mitosis could be related to the segregation defects that we found in those cells. Although, we did not detect a big increase in the number of cells with segregation defects, we observed a qualitative change in the severity of those defects and, as such, we decided to classify those alterations in two different grades: mild and severe. Mild grade corresponds to the appearance of a single lagging chromosome or chromosome bridge during anaphase (Figure 26C (upper panel)), whereas severe grade corresponds to the occurrence of more than one lagging chromosome or chromosome bridge, and in some cases mix of both defects (Figure 26C (middle and lower panels)). Featuring those two grades, we detected a significant increase in severe segregation defects in *Ppp2r2a*(Δ/Δ);*Ppp2r2d*(-/-) cells compared to their control (Figure 26D). Furthermore, a defect in the kinetics of chromatin decondensation was observed in those cells, in which usually one of the daughter cells maintained the DNA condensed during a longer time than the other daughter cell (Figure 26C (lower panel)). Significant differences (P=0.0138) were observed for this unexpected phenotype that we have termed 'asymmetric decondensation' (Figure 26E).

In summary, simultaneous depletion of B55α and B55δ isoforms showed several mitotic alterations, which were not detected upon single elimination of any of those isoforms, probably due to overlapping functions. These data, therefore, suggest an important role for these PP2A complexes in mitosis, which could explain the proliferation defect of PP2A-B55α/δ-deficient cells.

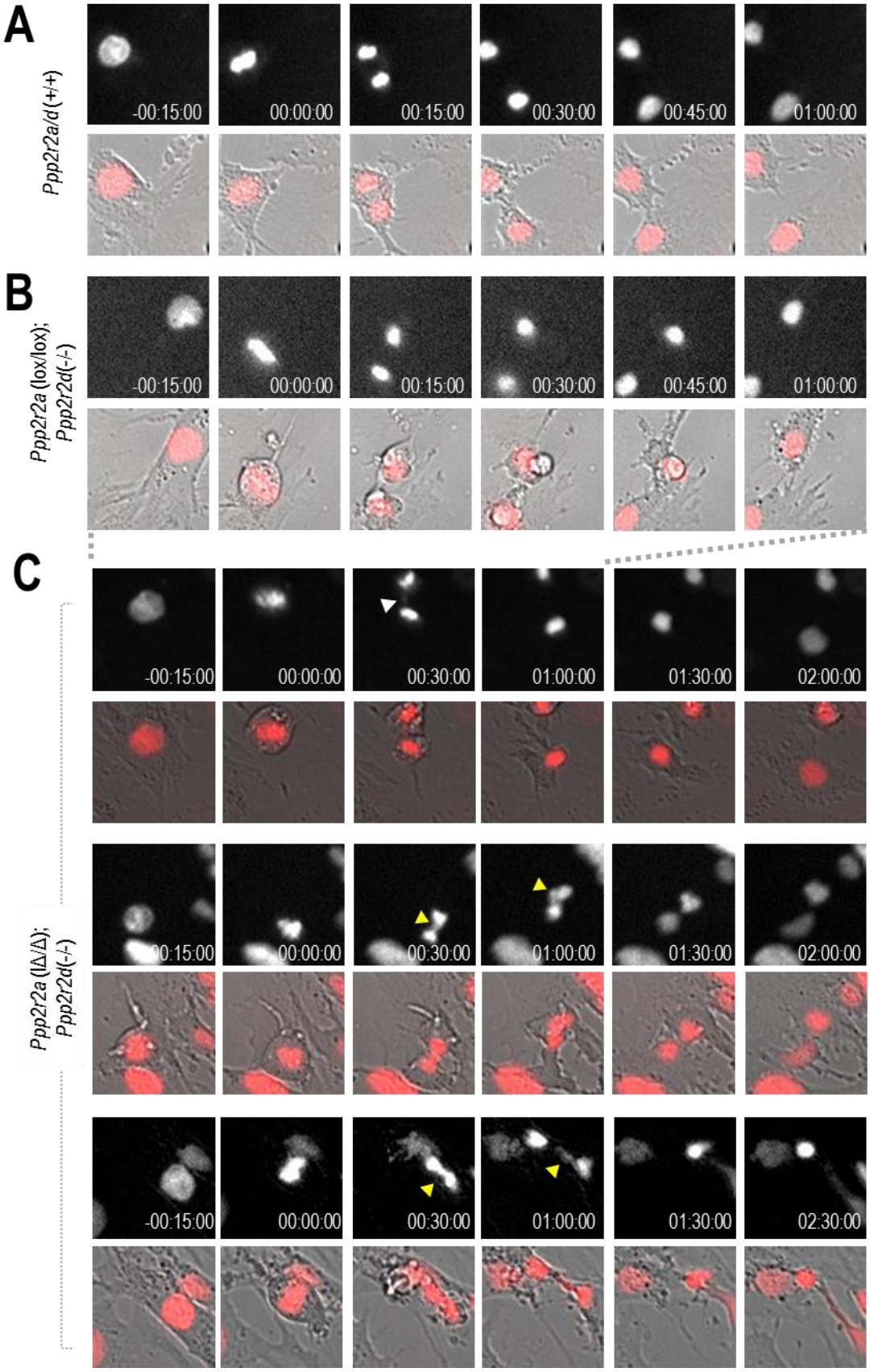
A
Ppp2r2a/d(+/+)
-00:15:00
00:00:00
00:15:00
00:30:00
00:45:00
01:00:00
B
Ppp2r2a (lox/lox); Ppp2r2d(-/-)
-00:15:00
00:00:00
00:15:00
00:30:00
00:45:00
01:00:00
C
Ppp2r2a (lΔ/Δ); Ppp2r2d(-/-)
-00:15:00
00:00:00
00:30:00
01:00:00
01:30:00
02:00:00
00:15:00
00:00:00
00:30:00
01:00:00
01:30:00
02:00:00
-00:15:00
00:00:00
00:30:00
01:00:00
01:30:00
02:30:00

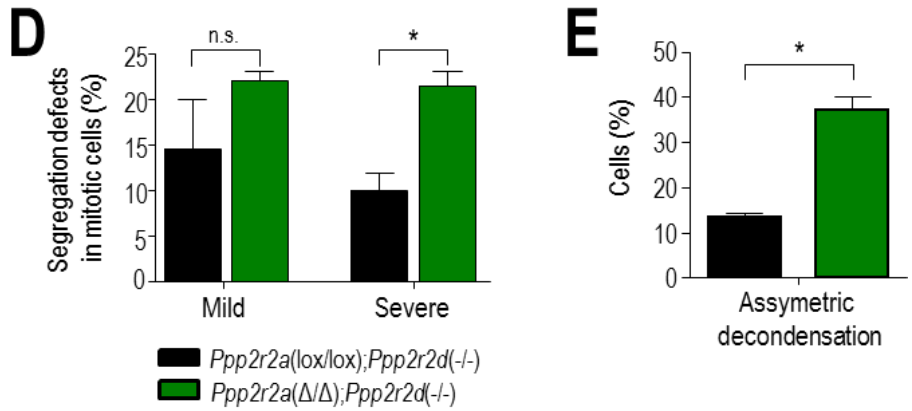

Figure 26. *Ppp2r2a/d* deficiency induces severe segregation defects and assymetric decondensation. Representative time-lapse images of *Ppp2r2a/d*(+/+) (A); *Ppp2r2a*(lox/lox); *Ppp2r2d*(-/-) (B) and *Ppp2r2a*(Δ/Δ);*Ppp2r2d*(-/-) cells(C). H2B-RFP is in red. Mild defect and severe defects are marked by white and yellow arrows, respectively. (D) Quantification and classification of segregation defects in *Ppp2r2a*(lox/lox); *Ppp2r2d*(-/-) (black labelled) and *Ppp2r2a*(Δ/Δ);*Ppp2r2d*(-/-) (green labelled) mitotic cells. (E) Quantification of assymetric decondensation between daugther cells. Data are mean +SEM of n=3 different clones.*P<0.05 (Student t test).

4.5. Role of PP2A-B55 phosphatase in chromosome clustering in mitosis

4.5.1. Response of PP2A-B55 deficient cells to microtubule poisons

Proper chromosome segregation during mitosis is controlled by the spindle assembly **c**heckpoint (SAC), a surveillance mechanism that delays mitosis until all chromosomes are bipolar attached to the spindle microtubules. The phenotype of severe segregation defects that we observed in B55α/δ –deficient cells, could be explained by a deficient SAC that allows cells to continue to anaphase before all chromosomes are bipolar attached.

To evaluate the robustness of the SAC in B55-deficient cells, we performed videomicroscopy analysis in the presence of nocodazole, a microtubule depolimerizing poison that disrupts the formation of the spindle and, as such, leads to the activation of the SAC. In this case, we added the drugs just before imaging, 20 hours after serum addition when cells were reentering into the cell cycle from a G0 arrest. As expected, wt cells were arrested in mitosis for a long time (about 10h) in the presence of nocodazole, and a similar delayed in mitosis was observed in B55-deficient cells, (Figure 27A) suggesting that the SAC is properly activated in the absence of PP2A-B55 complexes.

Mitotic progression in the presence of nocodazole is clearly impaired by improper spindle formation and SAC activation. However, cells in this condition eventually exit from mitosis by mitotic slippage, a process in which progressive degradation of cyclin B1 occurs despite the unsatisfaction of the mitotic checkpoint (Brito and Rieder CL, Current Biology, 2006). Cells that escape from a prometaphase arrest induced by nocodazole can exit as one tetraploid nucleus, or, in some cases, with some multinuclei; or they might die during the arrest state in mitosis. Interestingly, we observed an unexpected and intriguing phenotype in nocodazole-arrested B55 deficient cells. Whereas wt cells stayed in mitosis with condensed chromosomes as a unique chromosome mass (Figure 28 (upper panels)), MEFs lacking either B55α or B55δ or both isoforms together, frequently showed chromosomes scattering from the main chromosome mass (Figure 27B,C). Importantly, this phenotype was already observed upon single elimination of B55δ or B55α, and its incidence increased upon depletion of both isoforms (Figure 27B).

Some cells showing chromosome scattering could exit from mitosis, mostly as multinucleated cells with high number of micronuclei, whereas other cells died during mitosis (Figure 29). In the case of B55δ-null cells, around 50% of cells exhibiting chromosome scattering exited as multinucleated cells, whereas the remaining 50% died in mitosis (Figure 29). A similar phenotype was observed in the depletion of B55α, although with an increase percentage of cells dying in mitosis. However, when both B55α and B55δ isoforms were depleted at the same time, the presence of nocodazole led in the majority of cells to mitotic cell death after a strong chromosome scattering phenotype (Figure 29). Comparing all analysed genotypes we could detect a correlation between the frequency of chromosome scattering (Figure 27B) and the percentage of mitotic cell death, (Figure 27A (red dots) and Figure 29) , suggesting that the observed death in mitosis likely resulted from the lack of chromosome clustering during the arrest. Although there were no significant differences in the duration of the mitotic arrest when comparing cells exiting with cells dying there was a trend to a shorter maintenance of the arrest in cells dying in mitosis (Figure 27A, compare black vs red dots) , which is significant when we co-depleted both B55α/δ isoforms.

In summary, we have identified three major cell fates by videomicroscopy in the presence of nocodazole (Figure 28): i) Exit without DNA segregation, in which the cell

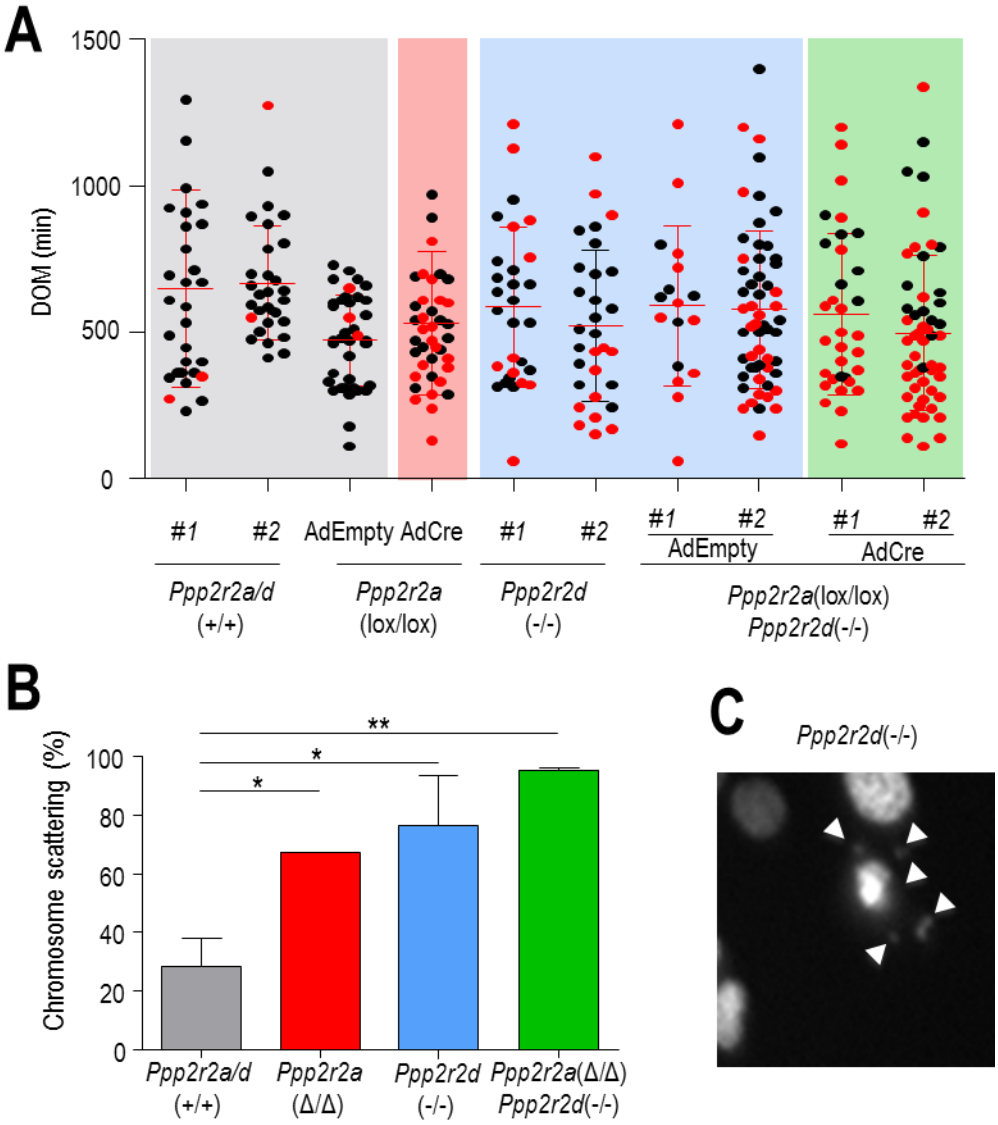

Figure 27. Nocodazole treatment induces chromosome scattering in mitosis in B55-deficient cells. Cells were serum starved and putted in presence of nocodazole, upon 20h of serum stimulation, just before imaging. (A) Percentage of chromosome scattering found in the different genotypes after nocodazole (0.8µM) treatment. Data are means +SEM (n=3 independent clones) **P*<0.05; ***P*<0.01 (Student *t* test). (B). Representative image of chromosome scattering in *Ppp2r2d*(-/-) cells. (C) Duration of mitosis of the indicated genotypes in the presence of nocodazole (0.8µM). Black dots represent cells that exit from mitosis and red dots represent cells that die in mitosis. Mean ±SD is shown.

arrest in prometaphase, showing in some cases a slight chromosome scattering, but, at the end, exiting as a unique daughter cell with one tetraploid nucleus. This was the predominant phenotype in wt cells; ii) Exit as multinucleated cell, in which the cell usually arrest with strong chromosome scattering and, at the end, it exits as a unique daughter cell but with a huge amount of micronuclei; This phenotype was mostly

observed in B55-deficient cells. iii) Death in mitosis, usually after strong chromosome scattering, which was the major fate, almost reaching 80%, in the combined depletion of both B55α and B55δ isoforms (Figure 29). The fact that *Ppp2r2a/d*(+/+) had the same behaviour as the *Ppp2r2a*(lox/lox) treated with AdEmpty viruses, and that *Ppp2r2d*(-/-) cells showed the same phenotype of *Ppp2r2a*(lox/lox);*Ppp2r2d*(-/-) AdEmpty-infected (Figure 29), ensured that the observed phenotype was not due to the viral infection, but, indeed, caused by the depletion of PP2A/B55 phosphatase.

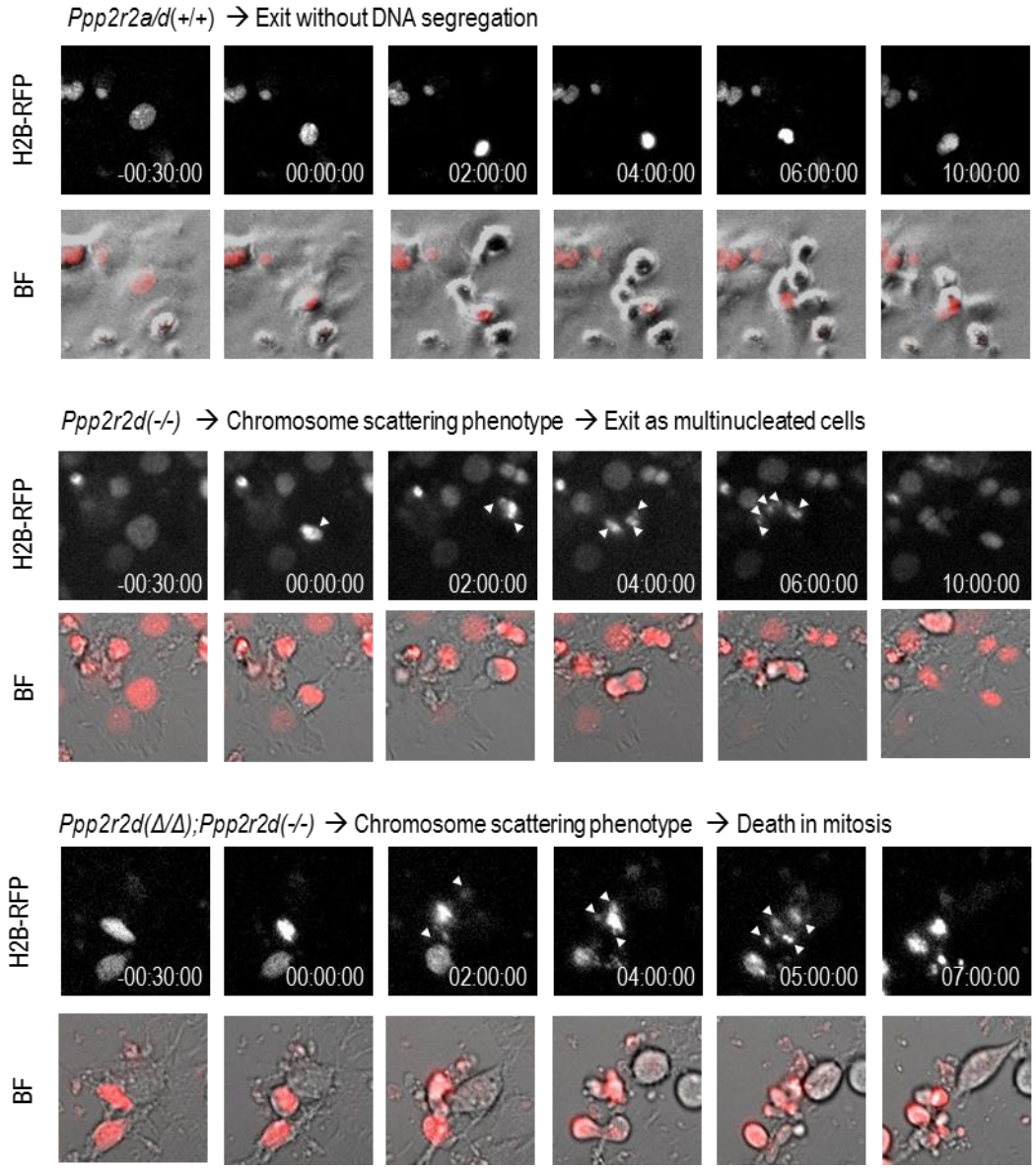

Figure 28. Major phenotypes in nocodazole-treated PP2A-B55-deficient cells. Representative time-lapses images of MEFs treated with nocodazole (0.8µM) showing the major phenotypes observed. White arrows indicate chromosome scattering.

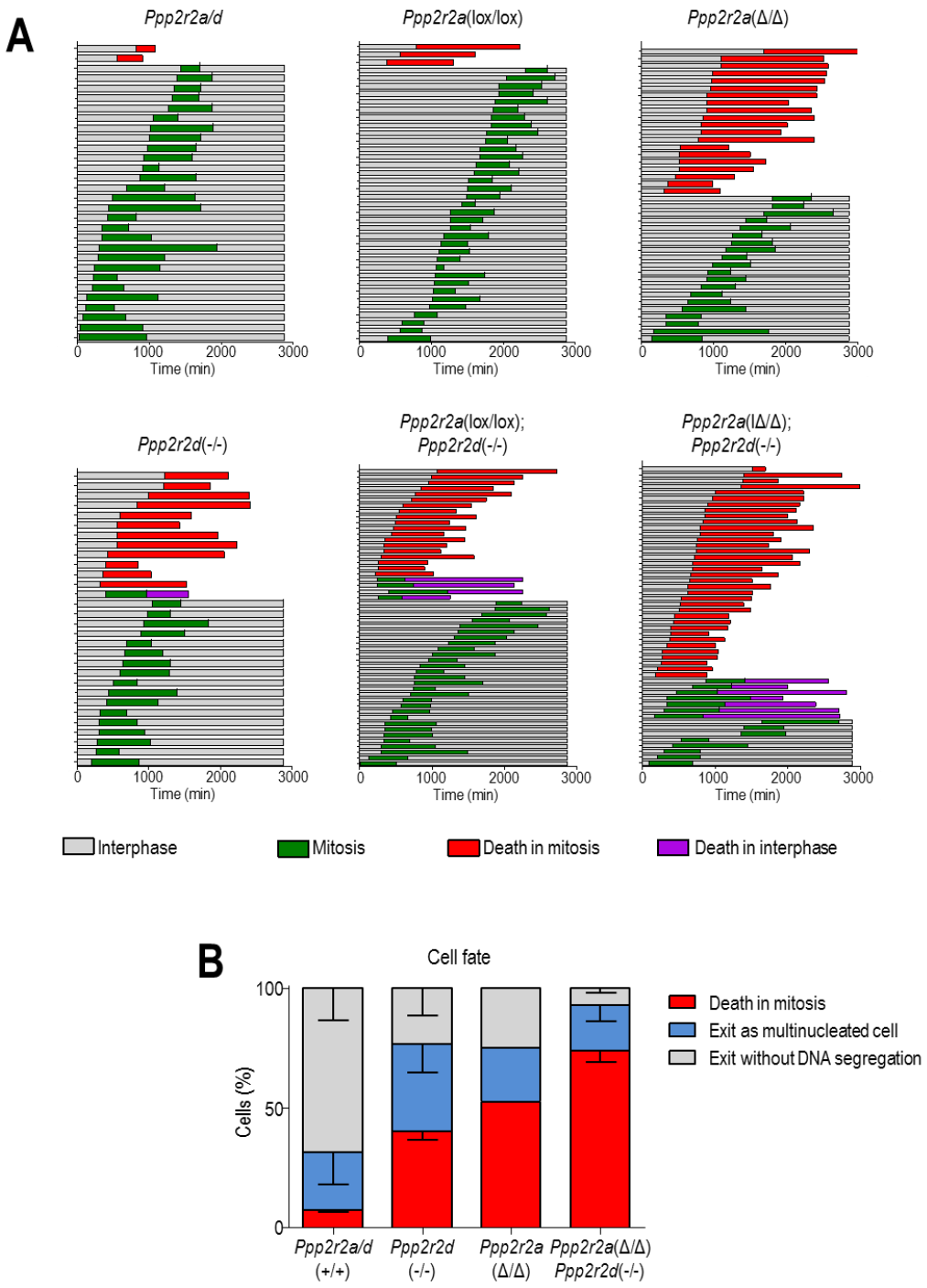

Figure 29. Treatement of PP2A-B55-deficient cells with nocodazole leads to multinucleation and mitotic cell death. (A) Cell fate analysis by videomicroscopy of cells with the indicated genotypes in the presence of nocodazole (0.8µM) . All conditional alleles were analyzed after adenoviral infection with AdEmpty (lox allele) or AdCre (D allele). Only *Ppp2r2a/d*(+/+) and *Ppp2r2d*(-/-) were not infected with adenoviruses. Each row represents the status of an individual cell. (B) Quantification of cell fates in presence of nocodazole of each genotype, as described in Figure 28. Data are means -SEM (n=3 independent clones; n=1 in *Ppp2r2a*(Δ/Δ)) **P*<0.05; ***P*<0.01 (Student *t* test)

As mentioned above, those B55-deficient cells that exit mitosis after chromosome scattering usually exit as multinucleated cells with a huge number of small nuclei. Although wt cells sometimes also exit as multinucleated cells, the number of micronuclei per cell was significantly higher in B55-deficient cells, suggesting that the multinucleation phenotype was also a consequence of the chromosome scattering during the prometaphase arrest (Figure30).

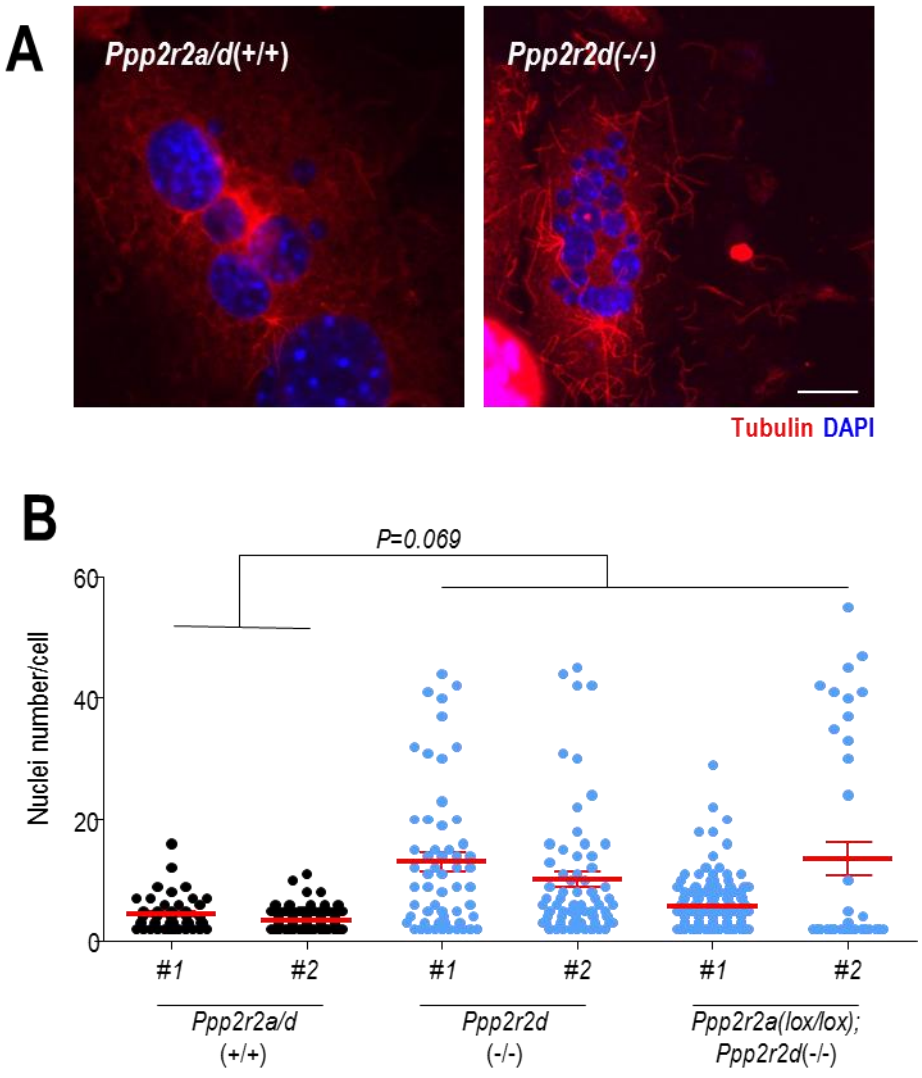

Figure 30. Chromosome scattering during mitotic exit provokes multinucleation in daughter cells. (A) Representative images of multinucleated cells found in *Ppp2r2a/d*(+/+) and *Ppp2r2d*(-/-) cultures after nocodazole (0.8µM) treatment by IF. DAPI was used to dye DNA and tubulin to mark microtubules. Scale bars: 10µm. (B) Quantification of nuclei number per multinucleated cell in *Ppp2r2a/d*(+/+) and *Ppp2r2d*(-/-) cultures after nocodazole (0.8µM) treatment. Mean ± SEM of each clone is shown.

To test if this phenotype was also induced by other microtubules poisons we performed the same analysis using taxol, a microtubule-stabilizing drug. Cells slipping from a taxol-induced mitotic arrest usually exit as multinucleated cells. When compared *Ppp2r2d*(-/-) with wt cells we did not find significant differences in the number of nuclei per cell among these genotypes (Figure 31). This suggests that the defect in chromosome clustering in B55-deficient cells is specifically induced in the absence of microtubules upon nocodazole treatment.

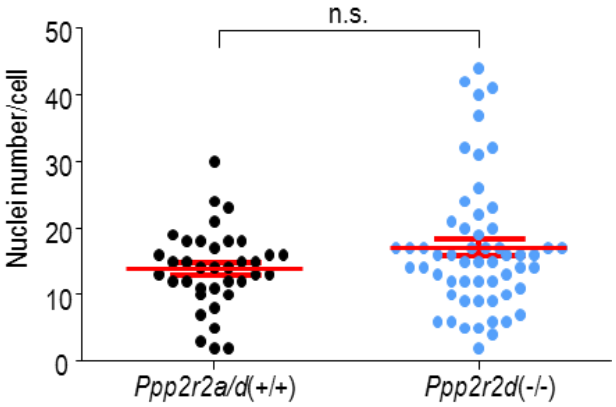

Figure 31. Taxol provokes multinucleation independently of the genotype. Quantification of nuclei number per multinucleated cell in *Ppp2r2a/d*(+/+) and *Ppp2r2d*(-/-) cultures after taxol (1µM) treatment. Mean ± SEM of each clone is shown.

4.5.2. PP2A-B55 regulates chromosome clustering through Ki67

The chromosome scattering phenotype that we have observed in B55-deficient cells could be due to a defect in maintenance chromosome clustering during the mitotic arrest. Interestingly, a recent study looking for molecular factors that contributes to spatial separation of mitotic chromosomes shows that depletion of Ki-67, in presence of nocodazole, favours chromosome clustering (Cuylen *et al*, 2016). This resembles the opposite phenotype to the one we have observed. Indeed, by measuring the chromosomal area (μm^2) of nocodazole arrested prometaphases as a more direct indicator of the level of chromosome clustering, we have detected a clear increase in this value in *Ppp2r2d*(-/-) iMEFs versus *wild-type*, suggesting reduced clustering and chromatin compaction in B55-deficient cells (Figure 32).

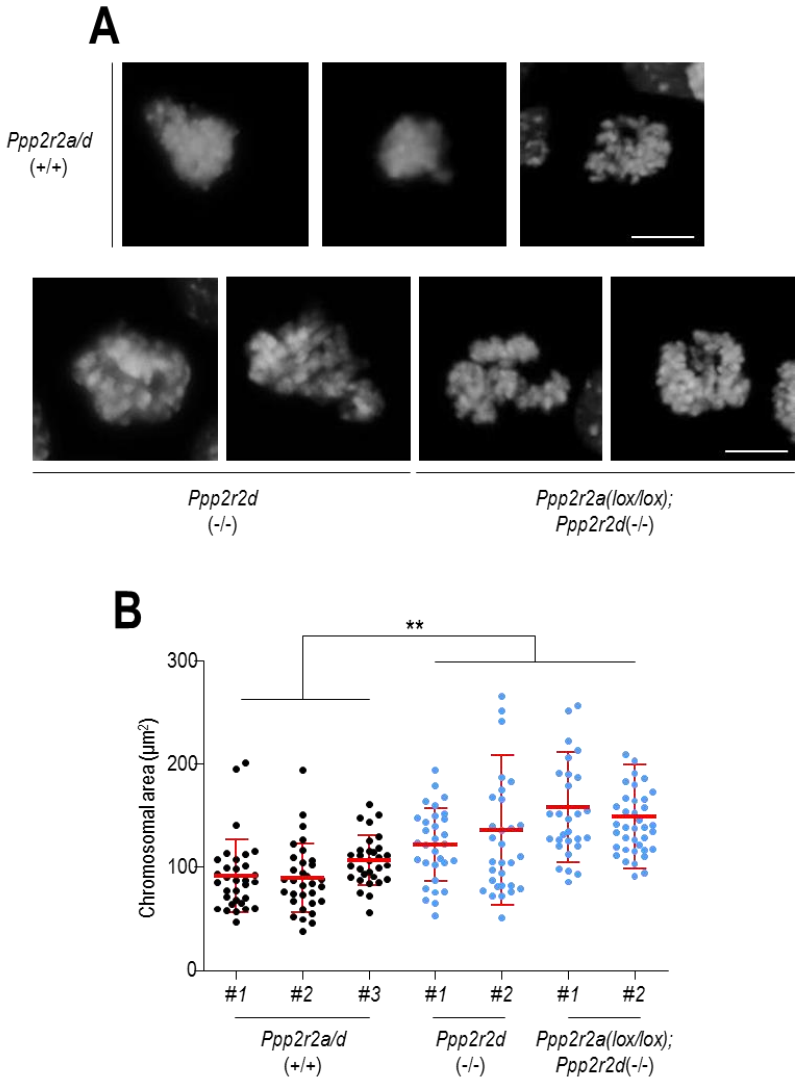

Figure 32. Chromosomal area increases in *Ppp2r2d*(-/-) prometaphase arrested cells. (A) Representative DAPI images of *Ppp2r2a/d*(+/+) (upper panels) and *Ppp2r2d*-deficient nocodazole-arrested cells (lower panels). (B) Quantification of chromosomal area per cell in several *Ppp2r2a/d*(+/+) and *Ppp2r2d*(-/-) clones. All measured cells were arrested in prometaphase by nocodazole treatment and stained positive for the MPM2 mitotic marker. Mean(SD) of each clone is shown. ***P*<0.01 (Student *t* test). Scale bars: 10µm.

In agreement with that, immunofluorescence over metaphase spreads of *Ppp2r2d(-/-)* iMEFs reveals a higher expresion of total Ki-67 levels in comparison with the *wt* (Figure 33), suggesting higher recrutiment of Ki-67 to the perichromosomal layer in the absence of B55. This data together with the recent identification of Ki67 as a putative

PP2A/B55 substrate (Cundell et al., 2016), places Ki-67 as a candidate to mediate the chromosome clustering defect of PP2A/B55 deficient cells.

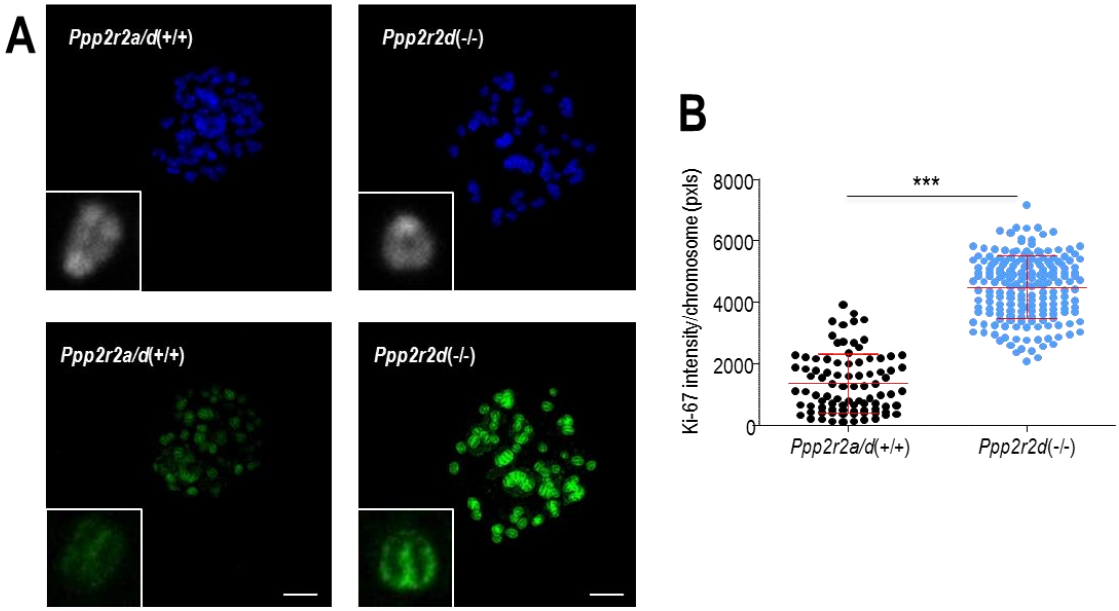

Figure 33. KI-67 levels increase in *Ppp2r2d*(-/-) cells. (A) Images of metaphase spread immunofluorescences of one representative *Ppp2r2a/d*(+/+) clone and one *Ppp2r2d*(-/-) clone. Scale bars: 10µm. (B) Quantification of Ki-67 intensity per chromosome of images showed in panel A. Mean(SD) of each clone is shown. ***P<0.001 (Student t test).***P<0.001 (Student t test).

To prove that, we treated *Ppp2r2d(-/-)* iMEFs with siRNAs against Ki-67 to try to rescue the chromosome clustering defect we observed in B55 deficient cells in the presence of nocodazoleAs we previously showed by immunofluorescence over metaphase spreads, Ki67 levels increased in *Ppp2r2d*(-/-) cells versus wt cells. Importantly, the level of Ki-67 was significantly reduced in cells treated with the specific siRNA against Ki67, both in wt and in B55δ-null cells, validating the specificity of Ki67 signal and confirming the efficiency of Ki67 depletion (Figure 34).

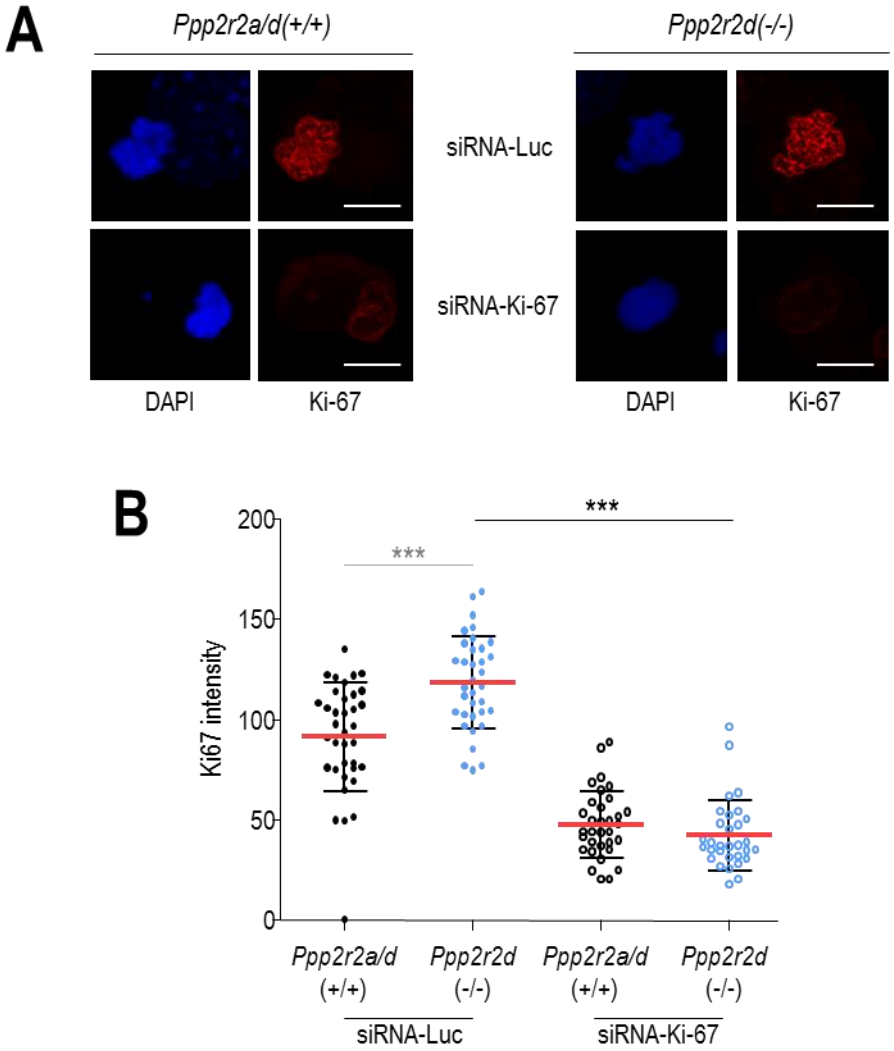

Figure 34. Ki-67 levels in PP2A-B55δ deficient cells. (A) *Ppp2r2a/d*(+/+) and *Ppp2r2d*(-/-) cells were nucleofected with siRNAs against Ki-67, treated with nocodazole after 24h of nucleofection and fixed for IF against Ki67. DAPI was used as DNA marker. Scale bars: 10µm. (A) Representative images of the immunofluorescence using the indicated siRNAs. (B) Quantification of Ki-67 intensity per chromosomal area. siRNA-luciferase was used as control. Mean(SD) of each clone is shown. ***P<0.001 (Student t test).

Interestingly, depletion of Ki-67 siRNAs decreased the chromosomal area of *Ppp2r2d*(-/-) nocodazole-arrested cells to the *wild-type* size (Figure 35A). Importantly, the number of nuclei in *Ppp2r2d*(-/-) multinucleated cells also diminished upon Ki-67 depletion (Figure 35B). These data suggest that the chromosome scattering phenotype accompanied by strong multinucleation in PP2A-B55 deficient cells might indeed be due to a defect in chromosome clustering in mitosis, probably caused by the excessive accumulation of Ki-67 at the chromosome surface.

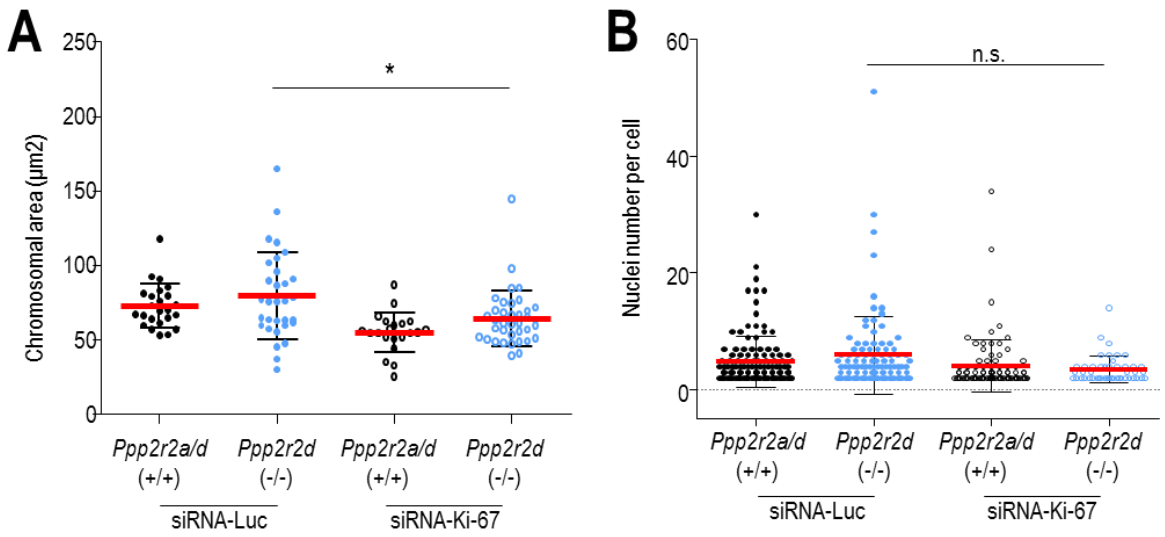

Figure 35. Ki-67 knockdown rescues *Ppp2r2d*(-/-) reduced clustering. (A) Quantification of chromosomal area per cell in *Ppp2r2a/d*(+/+) and *Ppp2r2d*(-/-) clones treated with the indicated siRNAs. All measured cells were arrested in prometaphase by nocodazole treatment and were positive for the MPM2 mitotic marker. (B) Quantification of nuclei number per multinucleated cell in *Ppp2r2a/d*(+/+) and *Ppp2r2d*(-/-) clones treated with the same siRNAs and treated with nocodazole. Mean(SD) of each clone is shown.) n.s., not significant differences; **P*<0.05 (Student *t* test).

Considering the evidences of Ki-67 as a putative PP2A-B55 substrate, our data suggest that PP2A-B55 may play a role in maintaining chromosome clustering in mitosis by regulating the association of Ki67 to the chromosome surface.

DISCUSSION

5. DISCUSSION

Reversible protein phosphorylation is a fundamental regulatory mechanism of many biological processes such as metabolism, transcription, translation, cytoskeleton reorganization, motility, protein stabilization, cell cycle and cell death processes among others. Phosphorylation is a really powerful control mechanism because it is very rapid and does not require new proteins to be synthesized or degraded, and can be easily reverted. This ubiquitous signal transduction mechanism is tightly coordinated by kinases and phosphatases. The fact that in the human genome we find more than 500 kinases whereas it encodes only half number of phosphatases has focused over the years the major scientific interest on kinases (Chen et al., 2017). However, several studies along time have led to the recognition of protein phosphatases as active key players in all these multiple biological processes in which kinases are implicated, including mitotic regulation (Bollen et al., 2009, Medema and Lindqvist, 2011).

5.1. Is PP2A-B55 an essential phosphatase?

Since the beginning of the life of an organism, mitosis is essential. In a very simplistic manner, embryonic development consists of continuous cell cycle rounds since the zygote is formed until the organism is completely developed. Then, some mitotic kinases, such as, Plk1, Cdk1 or Mastl, among others, are essential for embryonic development. And, therefore, germline biallelic disruption of these kinases in loss of function mouse models results in embryonic lethality (Santamaria et al., 2007, Wachowicz et al., 2016, Álvarez-Fernández et al., 2013).

Much less is known about the essentiality of specific phosphatases due to the common existence of multimeric complexes composed by several subunits, which sometimes also contain multiple isoforms in mammals. In the case of PP2A, it is known to date that the scaffold and catalytic subunits of PP2A in their major expressed isoforms, Aα and Cα, respectively, are essential for mouse development (Ruediger et al., 2011, Gotz et al., 1998, Gu et al., 2012). This is not surprising, since it involves the elimination of most PP2A complexes in the cell. The only loss of function mouse models for specific PP2A complexes are knockouts for B56α and B56δ, and both of them are viable (Litter et al., 2015, Louis et al., 2011). In this work, we have generated the first loss of function models in mammals for PP2A-B55 complexes, in particular, B55α and B55δ, which appear to be the ubiquitous isoforms of the family. Our data reflects that in the first

steps of development the absence of B55δ, and probably also the lack of B55α, does not compromise early development. Later on, B55δ is also dispensable but B55α becomes essential to complete mouse embryonic development (Figure 15). This differential requirement could be due to the differential expression of these isoforms during development, or to specific non-redundant functions for the B55α isoform. During mouse development different expression of B55 isoforms have been reported. Between embryonic day (E)7 and E17 the highest expressed isoform, at least at mRNA levels, seems to be B55β (Schmidt et al., 2002). In brain, specifically, from E18 to postnatal day (P)21 and adults, B55β expression, at both mRNA and protein levels, decreases in contraposition to the increase of B55γ expression; while B55α maintains its expression along the time; with no available data for B55δ in these studies (Strack et al., 1998). Recent data published in The e-Mouse Atlas Project (http://www.emouseatlas.org/emap/home.html) complemented this information with in-situ hibridization data of *Ppp2r2b-d* genes, but unfortunately not of *Ppp2r2a*, in E14.5 embryos. These data showed very high levels of B55β mainly in brain, restricted levels of B55γ to the central nervous system, and more ubiquitous but very low expression levels of B55δ, which could partially explain why *Ppp2r2d* gene was dispensable during development and might not be able to compensate the lack of B55α, its more similar isoform. In any case, the embryonic lethality of *Ppp2r2a*(-/-) mice indicates that PP2A-B55α phosphatase complexes play a role during development that cannot be replaced by any other isoforms of the family (B55β-δ).

In adult mice, B55δ is not essential either, suggesting redundancy or compensation among isoforms. This is partially supported by our data in brain tissues showing increase protein levels of B55β and B55γ, and also mRNA levels of B55α, in B55δ-null mice (Figure 18). These data suggest that other B55 isoforms, most likely B55β and γ in brain, and maybe B55α in other tissues, might display some compensatory roles in the absence of B55δ. Whether B55α is also essential in the adult still has to be proved, and the conditional model generated in this work constitutes the ideal tool to answer this question. Finally, the generation of mouse models for the remaining isoforms, B55β and B55γ, and the combinations with the existing ones, will allow knowing definitely whether PP2A-B55 complexes, and/or particular B55 isoforms, are essential for mammalian development and survival.

5.2. Cell cycle functions of PP2A-B55 in mammals

5.2.1. Role of PP2A-B55 in mitotic entry and progression

Before this work the only study in mammals on the role of PP2A-B55 in mitotic entry was performed in Hela cells using siRNAs to deplete single B55 subunits. This study did not reveal any defect in mitotic entry, at least in B55α-depleted cells, which seems to be the predominant isoform in this specific cell line (Schmitz et al., 2010). (Schmitz et al., 2010). In this direction, our data shows that individually elimination of B55α or B55δ does not significantly affect the kinetics of mitotic entry. However, the lack of both isoforms provokes a premature mitotic entry, suggesting putative overlapping roles among these two isoforms. However, this possibility was not considered in the human cell line study, in which combined depletion of isoforms was not tested. Therefore, this role of PP2A-B55α/δ regulating the timing of mitotic entry might also be conserved in human cells. Previously, only depletion studies in *Xenopus* egg extracts have related PP2A-B55 phosphatase complexes with mitotic entry, specifically B55δ, since B55α and B55β could not be detected probably due to their lower levels in these extracts and B55γ was not considered in this work (Mochida et al., 2009). The earlier mitotic entry in the absence of PP2A-B55 activity could be explained by a reduced threshold of Cdk activity required for entering mitosis, as a consequence of the prolonged maintenance of a lower phosphatase state. However, the specific PP2A-B55 substrates responsible for that are not known so far.

To date, no data on PP2A-B55 affecting chromosome segregation in mammals have been reported. In this work, we have shown that co-depletion of both isoforms, B55α and B55δ, in mouse cells, affects mitotic progression through an increase in severe segregation defects. The appearance of this type of defects in anaphase in the absence of PP2A-B55 has only been previously described in two different mutants of Twins, the B55 isoform in *Drosophila* (Gomes et al., 1993; Mayer-Jaekel et al., 1993). The severe segregation defects that we observed in the double B55α/δ knockout during anaphase could be the consequence of a premature mitotic entry in these cells, probably before DNA replication has been properly finished, affecting connections between sister chromatids. On the other hand, these defects could be the result of a direct role of these PP2A-B55 complexes in chromatid segregation that has not previously been demonstrated in mammals. Interestingly, PP2A-B55 phosphatase have been related with maintenance of centrioles assembly and duplication in other organisms, such as *C.*

elegans (Song et al., 2011) and *Drosophila* (Brownlee et al., 2011) through stabilization of Plk4. It is well known that centrosome dynamics alterations during mitosis may also lead to chromosome missegregation (Nam et al., 2015). A putative deregulation in centrosomes by deficiency in PP2A-B55 in mammals has to be demonstrated. Considering the existence of a wide spectrum of Cdk-substrates that participate regulating all these processes, which ensure chromosome segregation fidelity, a significant number of putative substrates of these phosphatase complexes could mediate these functions.

5.2.2. Role of PP2A-B55 in mitotic exit

The implication of PP2A-B55 in mammalian mitotic exit had already been proposed. Depletion of B55α by siRNA in Hela cells, but no other isoforms (β, γ and γ), slightly delays postmitotic reassembly of the nuclear envelope and Golgi apparatus, and chromatin decondensation (Schmitz et al., 2010). Since this phenotype was relatively mild, the authors of this study performed most assays using siRNAs that co-depleted also the scaffold (Aα) and the catalytic (Cα) subunits of PP2A complexes, causing an exacerbation of this phenotype, which suggest other B55 isoforms or other PP2A complexes might cooperate in mitotic exit. On the other hand, in mouse cells, siRNA depletion of both B55α together with B55δ was required for dephosphorylation of CDK targets to allow complete mitotic exit (Manchado et al., 2010). Our data revealed that the depletion of only one isoform, in mouse cells, did not suppose any major change in mitotic exit, whereas co-depletion of B55α/δ complexes significantly prolonged the mitotic exit duration. The apparent controversial data from human and mouse about the specific isoform responsible of mitotic exit in mammals could be due to a specialization in isoform function during evolution, or just a matter of expression levels, since B55α appears to be the most expressed isoform in human cell lines, whereas mouse cell lines present similar expression levels of both B55α and B55δ isoforms, at least at the mRNA level (Figure 11). The prolonged mitotic exit observed in B55α/δ-deficient cells supports the PP2A-B55 role in Cdk-substrates dephosphorylation that occurs during this mitotic time. In agreement with that, how different Cdk-substrates are recognized by PP2A-B55 has been disclosed. All these substrates present consensus sequence determined by a bipartite polybasic motif flanking Cdk1 phosphorylation sites. Interestingly, when more basic are these regions more rapidly are dephosphorylated by PP2A-B55 determining the timing of substrate dephosphorylation (Cundell et al., 2016).

Alternatively, we cannot forget that this prolonged mitotic exit could be also the consequence of the severe segregation defects observed in anaphase caused by defects in earlier mitotic phases, which would force cells to spend more time to solve mitosis.

On the other hand, in late anaphase and telophase, chromosome decondensation is essential to recover its interphase state. This event requires, as all in mitotic exit, inactivation of the kinases and reversion of mitotic phosphorylation by phosphatases. The direct role of PP2A-B55 in this process is unclear although it has been previously described in *Drosophila* mutants for *twins* (Mayer-Jaekel et al., 1993), and also in Hela B55α-depleted cells (Schmitz et al., 2010), that the deficiency of these complexes affects chromosome decondensation. In this work, the depletion of B55α and B55δ isoforms prolonged a condensed state of chromatin once cells supposedly have already exited from mitosis, very curiously in one of the two daughter cells (asymmetric decondensation, Figure 26). In this process, the role of phosphatase PP1 is well-defined, its isoform PP1γ is in charge of dephosphorylate the mitotic histone marks Thr3, Ser10 and Ser28 on histone H3 among others, which are supposed to be reverted to trigger reacetylation of H4 K16 and allow chromatin decondensation (Qian et al., 2011). It is known that the Repo-Man protein is responsible for PP1γ recruitment to anaphase chromosomes, although depletion of Repo-Man but does not impair chromatin decondensation, but nuclear envelope formation (Vagnarelli et al., 2011). Interestingly, Ki67 presents a PP1-binding domain that can also be responsible for PP1γ recruitment to allow chromosome decondensation (Booth et al., 2014). Considering that in our work Ki-67 recruitment to chromosomes is increased in the absence of PP2A-B55 isoforms, and it's a candidate PP2A-B55 substrate (Cundell et al., 2016), it is plausible that PP2A-B55 regulates indirectly PP1g through Ki67 and, as such, also regulates chromosome condensation. The precise molecular mechanism underlying this potential role of PP2A-B55 in chromosome decondensation, and why its depletion leads to an asymmetric decondensation is not known.

In any case, the fact that cells expend more time in mitosis but, at the end, they exit, suggests that other phosphatases are also implicated in mitotic exit. We cannot discard the putative participation of the others isoforms from this family, B55β and B55γ, although they have not been previously related with this function possibly by their lower or lack of expression in the majority of the tissues, except brain. But also, we should consider the other multiple PP2A complexes with other B regulatory subunits,

for which their specific function have not been revealed yet. In addition, we cannot forget that PP1 is responsible together with PP2A of more than 90% of phosphatase activity in eukaryotic cells, and that it has also been reported its participation in mitotic exit (Wurzenberger and Gerlich, 2011, Samuel Rogers, 2015).

It is clear that whereas in budding yeast, only one phosphatase, Cdc14, is essential for regulating all mitotic exit events, in mammals it is more plausible a cooperative mechanism between a set of phosphatases. This occurs in fission yeast, where the ordered phosphatase activity of the orthologues of mammalian PP1, PP2A-B55 and PP2A-B56 are required for completing mitotic exit (Grallert et al., 2015). This type of mechanism would explain why in mammals depletion of only PP2A-B55α/δ isoforms does not completely prevent mitotic exit.

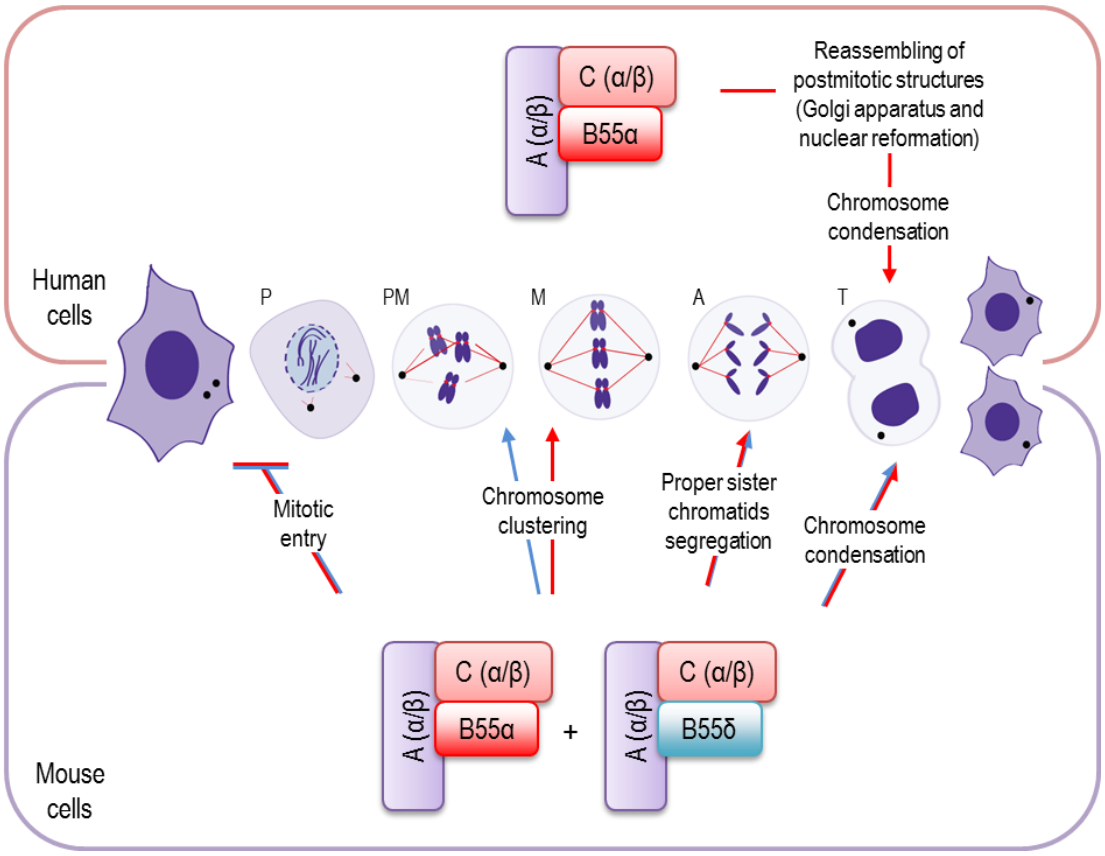

Figure 36. PP2A-B55 cell cycle functions in mammals. The upper panel shows PP2A-B55 functions previously described in human cells (Schmitz et al., 2010). The lower panel shows PP2A-B55 functions described in this work in mouse cells. Separate arrows mean specific functions, mixed arrows mean overlapping function between isoforms. B55α functions are indicated in red. B55δ functions are indicated in blue.

5.3 PP2A-B55 as a new player in chromosome clustering in mitosis

The mitotic chromosome rod-shape structure formation is essential for proper DNA equal segregation during mitosis. Although the initial DNA compaction is principally the result of condensins action, the structure that surrounds the chromosome periphery could also in some manner be involved in this process. Besides chromatin condensation, other mechanisms, such as chromosome individualization and clustering may also contribute to the global chromatin compaction status required for mitosis. In this sense, it has recently been reported that proteins from the perichromosomal layer, such as Ki-67, could bind chromatin and affect the individualization of mitotic chromosomes. This fact was due to the 'surfactant' properties that this big molecule has, which is determined by its amphiphilic structure. How size or charge truncation of this molecule decreases the spatial separation of mitotic chromosomes underlies the importance of overall electric charge for Ki-67 function (Cuylen et al., 2016). It is known that Ki-67 binds to HP1 through its LR domain (Kametaka et al., 2002); and, a very recent work has also reported that p150, the major isoform of Chromatin Assembling Factor (CAF)-1, binds Ki-67 regulating nuclear architecture across the cell cycle (Matheson and Kaufman, 2017).

In this work we show that the absence of PP2A-B55 affects chromosome mitotic clustering (Figure 32), probably due to high levels of Ki-67 in the perichromosomal layer (Figure 33; 34). It is well known that Ki-67 has to be hyperphosphorylated to locate around the chromosome during mitosis (Ohta et al., 2016) leaving its interphase nucleolar location. It is also known that this phosphorylation is in part result of CDK1 activity over a region considered the core of Ki-67-repeat domain (CKRD), which is present in each Ki-67 repeats containing a threonine-proline (TP) consensus phosphorylation site for mitotic kinases such as CDK. The highest phosphorylation levels of these sites occurred in metaphase, which slightly start at prometaphase ending at anaphase onset (Takagi et al., 2014). However, how this activation mechanism is regulated it was unknown. Our data suggest that Ki-67 is kept at the perichromosomal layer localization in a hyperphosphorylated state, due to the deregulation of PP2A-B55 complexes (Figure 33). Then, they might be the responsible of Ki-67 dephosphorylation at the end of mitosis. This fits with the fact that this perichromosomal protein is in part active by CDK1 as we have just mentioned (Takagi et al., 2014) and with the reported

evidence of PP2A-B55 complexes as the responsible of CDK-substrates dephosphorylation, including Ki-67 (Cundell et al., 2016). The data showing that depletion of Ki-67 rescues the clustering defect of PP2A-B55 deficient cells suggest that the Ki-67 role in chromosome clustering could be directly dependent on PP2A-B55 phosphatase (Figure 35).

Based on this data and the previously described Ki-67 role in mitotic chromosomes, we propose a model in which Ki-67 and PP2A-B55 levels need to be balanced or in some manner regulated in order to allow proper chromosome clustering during mitosis (Figure 37).

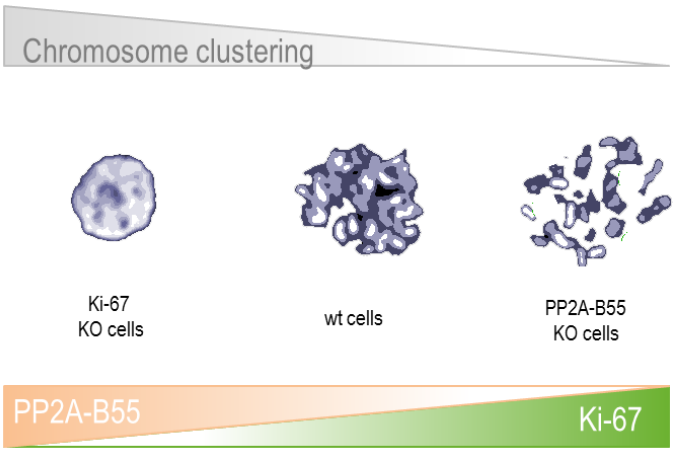

Figure 37. Model of chromosome clustering regulation during mitosis. In mitotic-arrested cells, B55-deficient cells show chromosome scattering in contrast to high clustering in Ki-67-null cells. The higher level of Ki-67 in B55-deficient cells suggests that Ki67 might be mediating the role of PP2A-B55 in chromosome clustering.

5.4. Function of PP2A-B55 in cell cycle progression: Therapeutic implications in cancer

PP2A is considered a tumour suppressor gene, which appears frequently inactivated in different tumour types, by reduced expression or loss of function (Ruvolo, 2016). However, the specific mechanisms that explain its tumour suppressor function are not fully understood, probably due to the wide variety of processes in which this phosphatase is involved. In our work, the absence of PP2A-B55α/δ isoforms favoured the appearance of segregation defects in mitosis, which could be one of the mechanisms why inactivation of these tumour suppressors could contribute to cancer that is by increasing chromosome instability or chromosome aberrations. Recently, some specific mutants in *twins*, the B55 subunit in *Drosophila*, have been reported as the responsible of increased chromosome aberrations as a consequence of its function in the DNA

damage response, suggesting additional mechanisms of tumour suppression for these PP2A complexes (Merigliano et al, 2017).

In our studies, we have found that depletion of B55 affects the response to microtubule poisons. These agents are regularly used in the clinics as therapeutic agents for cancer. Their mode of action relies on perturbing microtubule dynamics, disrupting the formation of a proper and functional mitotic bipolar spindle. This circumstance is controlled by the SAC, which delays mitosis giving more time to cells to resolve errors in microtubule-kinetochore attachments (Musacchio, 2015). This mitotic delay increases the predisposition of cells to die, fact that might partially explain the therapeutic effect of the microtubule poisons in cancer. One limitation for the efficiency of these drugs is a process known as mitotic slippage, in which prolonged mitotic-arrested cells exit mitosis, in the absence of chromosome segregation, progressing through cell division but in a tetraploid state. Due to this fact, strategies to enhance the potential of these antimitotic treatments towards a fully mitotic death by preventing mitotic slippage have been suggested (Topham and Taylor, 2013, Doménech and Malumbres, 2013).

In this work, using the microtubule poison nocodazole, we show that the presence of this drug in B55-deficient cells provokes a huge chromosome scattering effect (Figure 27) that in many cases lead to death in mitosis (Figure 28), especially when both isoforms (B55α and δ) are co-depleted. This effect seems to be nocodazole-dependent, as in the presence of taxol there are no major differences in the behaviour of B55-deficient cells compared to the wt. Therefore, inhibiting PP2A-B55 could improve the efficacy of these treatments by preventing slippage. The direct application of this strategy to the clinics is limited by the difficulty to target specifically phosphatase complexes, since all current PP2A inhibitors target the catalytic activity and therefore are not selective for PP2A specific complexes (Kalev and Sablina, 2011, Kiely and Kiely, 2015).

However, this new role of PP2A-B55 could be relevant in the up-to-date treatment of certain cancers that present genetic mutations or aberrations and deregulation in gene expression of PP2A subunits or some of their regulatory partners (Seshacharyulu et al., 2013; Perotti and Neviani, 2013). It is well known that PP2A-B55 function is impaired in a huge variety of cancer, reported in some cases as an haploinsuficient tumour

suppressor (Mao et al., 2011; Cheng et al., 2011, Curtis et al., 2012; Mosca et al.,2013), increasing genetic risk. Using PP2A-B55 levels as predictors of response to microtubule poisons could contribute to the therapeutic benefit of these treatments. The knowledge of PP2A-B55 patient status and its use as biomarker of response to this type of treatments could suppose an advantage in order to increase the success of these therapies.

CONCLUSIONS/CONCLUSIONES

CONCLUSIONS

1. The phosphatase PP2A-B55α is essential for late stages of mouse embryonic development.

2. PP2A-B55δ is dispensable for mouse embryonic development and its constitutive depletion does not compromise mouse survival. Elimination of PP2A-B55δ does not cause any obvious phenotype, neither in young or adult mice.

3. Single depletion of B55α or B55δ does not affect proliferation in mouse cells. However, combined elimination of B55α and B55δ leads to prolonged mitosis with severe segregation defects and reduced proliferation.

4. B55-depletion in combination with nocodazole favours chromosome scattering during prometaphase arrest promoting an increase in multinucleation in mitotic exit or cell death in mitosis.

5. PP2A-B55 regulates the perichromosomal protein Ki-67 to maintain chromosome clustering in prometaphase during mitosis.

CONCLUSIONES

1. La fosfatasa PP2A-B55α es esencial en los últimos estadios del desarrollo embrionario de ratón.

2. PP2A-B55δ es dispensable en el desarrollo embrionario de ratón y su deleción constitutiva no compromete la supervivencia de estos animales. La eliminación de PP2A-B55δ no causa ningún fenotipo destablabe en ratones jóvenes ni en adultos.

3. La depleción individual de las isoformas B55α o B55δ no afecta la proliferación en células de ratón. Sin embargo, la depleción combinada de ambas isoformas, B55α y B55δ, provoca un retraso en la salida de mitosis acompañada de graves defectos en segregación cromosómica y reduce la proliferación.

4. La ausencia de B55 en combinación con nocodazol favorece dispersión cromosómica durante el arresto en prometafase promoviendo un incremento de multinucleación en salida de mitosis o la muerte celular en mitosis.

5. PP2A-B55 regula la proteína pericromosómica Ki-67 para mantener la estructura cromosomal en prometafase, durante mitosis.

BIBLIOGRAPHY

BIBLIOGRAPHY

Adams, D. G., Coffee, R. L., Zhang, H., Pelech, S., Strack, S. & Wadzinski, B. E. 2005. Positive regulation of Raf1-MEK1/2-ERK1/2 signaling by protein serine/threonine phosphatase 2A holoenzymes. *The Journal of Biologicla Chemistry,* 280**,** 42644-42654.

Adams, R. R., Eckley, D. M., Vagnarelli, P., Wheatley, S. P., Gerloff, D. L., Mackay, A. M., Svingen, P. A., Kaufmann, S. H. & Earnshaw, W. C. 2001. Human INCENP colocalizes with the Aurora-B/AIRK2 kinase on chromosomes and is overexpressed in tumour cells. *Chromosoma,* 110**,** 65-74.

Álvarez-Fernández, M. & Malumbres, M. 2014. Preparing a cell for nuclear envelope breakdown: Spatio-temporal control of phosphorylation during mitotic entry. *Bioessays,* 36**,** 757-765.

Álvarez-Fernández, M., Sánchez-Martínez, R., Sanz-Castillo, B., Gan, P. P., Sanz-Flores, M., Trakala, M., Ruiz-Torres, M., Lorca, T., Castro, A. & Malumbres, M. 2013. Greatwall is essential to prevent mitotic collapse after nuclear envelope breakdown in mammals. *Proc Natl Acad Sci U S A,* 110**,** 17374-9.

Barr, R. A. & Gerlegy, F. 2007. Aurora-A: the maker and breaker of spindle poles. *Journal of Cell Science,* 120**,** 2987-96.

Beca, F., Pereira, M., Cameselle-Teijeiro, J. F., Martins, D. & Schmitt, F. 2015. Altered PPP2R2A and Cyclin D1 expression defines a subgroup of aggressive luminal-like breast cancer. *BMC Cancer,* 15**,** 285.

Berdougo, E., Nachury, M. V., Jackson, P. K. & Jallepalli, P. V. 2008. The nucleolar phosphatase Cdc14B is dispensable for chromosome segregation and mitotic exit in human cells. *Cell Cycle,* 7**,** 1184-90.

Bialojan, C. & Takai, A. 1988. Inhibitory effect of a marine-sponge toxin, okadaic acid, on photein phosphatases. *Biochem. J.,* 256.

Bollen, M., Gerlich, D. W. & Lesage, B. 2009. Mitotic phosphatases: from entry guards to exit guides. *Trends Cell Biol,* 19**,** 531-41.

Booth, D. G., Beckett, A. J., Molina, O., Samejima, I., Masumoto, H., Kouprina, N., Larionov, V., Prior, I. A. & Earnshaw, W. C. 2016. 3D-CLEM Reveals that a Major Portion of Mitotic Chromosomes Is Not Chromatin. *Mol Cell,* 64**,** 790-802.

Booth, D. G., Takagi, M., Sanchez-Pulido, L., Petfalski, E., Vargiu, G., Samejima, K., Imamoto, N., Ponting, C. P., Tollervey, D., Earnshaw, W. C. & Vagnarelli, P. 2014. Ki-67 is a PP1-interacting protein that organises the mitotic chromosome periphery. *eLife,* 5.

Brennan, I. M., Peters, U., Kapoor, T. M. & Straight, A. F. 2007. Polo-Like Kinase Controls Vertebrate Spindle Elongation and Cytokinesis. *PLoS ONE,* 2**,** e409.

Brownlee, C. W., Klebba, J. E., Buster, D. W. & Rogers, G. C. 2011. The Protein Phosphatase 2A regulatory subunit Twins stabilizes Plk4 to induce centriole amplification. *J Cell Biol,* 195**,** 231-43.

Burgess, A. E. A. 2010. Loss of human Greatwall results in G2 arrest and multiple mitotic defects due to deregulation of the cyclin B-Cdc2-PP2A balance. . *Proc Natl Acad Sci U S A,* 107**,** 12564-12569.

Calin, G. A., Di Iasio, M. G., Caprini, E., Vorechovsky, I., Natali, P. G., Sozzi, G., Croce, C. M., Barbanti-Brodano, G., Russo, G. & Negrini, M. 2000. Low frequency of alterations of the alpha (PPP2R1A) and beta (PPP2R1B) isoforms of the subunit A of the serine-threonine phosphatase 2A in human neoplasms. *Oncogene,* 19**,** 1191-5.

Castilho, P. V., Williams, B. C., Mochida, S., Zhao, Y. & Goldberg, M. L. 2009. The M phase kinase Greatwall (Gwl) promotes inactivation of PP2A/B55delta, a phosphatase directed against CDK phosphosites. *Mol Biol Cell,* 29**,** 4777-89.

Cohen, R. L. & Margolis, R. L. 2016. Spinocerebellar ataxia type 12: clues to pathogenesis. *Curr Opin Neurol,* 29**,** 735-742.

Cowley, D. O., Rivera-Perez, J. A., Schliekelman, M., He, Y. J., Oliver, T. G., Lu, L., O'quinn, R., Salmon, E. D., Magnuson, T. & Van Dyke, T. 2009. Aurora-A kinase is essential for bipolar spindle formation and early development. *Mol Cell Biol,* 29**,** 1059-71.

Cristobal, I., Madoz-Gurpide, J., Manso, R., González-Alonso, P., Rojo, F. & García-Foncillas, J. 2016. Potential anti-tumor effects of FTY720 associated with PP2A activation: a brief review. *Current Medical Research and Opinio,* 32**,** 1137-1141.

Cundell, M. J., Hutter, L. H., Nunes Bastos, R., Poser, E., Holder, J., Mohammed, S., Novak, B. & Barr, F. A. 2016. A PP2A-B55 recognition signal controls substrate dephosphorylation kinetics during mitotic exit. *The Journal of Cell Biology*.

Curtis, C., Shah, S. P., Chin, S. F., Turashvili, G., Rueda, O. M., Dunning, M. J., Speed, D., Lynch, A. G., Samarajiwa, S., Yuan, Y., Graf, S., Ha, G., Haffari, G., Bashashati, A., Russell, R., Mckinney, S., Langerod, A., Green, A., Provenzano, E., Wishart, G., Pinder, S., Watson, P., Markowetz, F., Murphy, L., Ellis, I., Purushotham, A., Borresen-Dale, A. L., Brenton, J. D., Tavare, S., Caldas, C. & Aparicio, S. 2012. The genomic and transcriptomic architecture of 2,000 breast tumours reveals novel subgroups. *Nature,* 486**,** 346-52.

Cuylen, S., Blaukopf, C., Politi, A. Z., Muller-Reichert, T., Neumann, B., Poser, I., Ellenberg, J., Hyman, A. A. & Gerlich, D. W. 2016. Ki-67 acts as a biological surfactant to disperse mitotic chromosomes. *Nature,* 535**,** 308-12.

Chen, M. J., Dixon, J. E. & Manning, G. 2017. Genomics and evolution of protein phosphatase. *Science Signaling,* 10.

Cheng, Y., Liu, W., Kim, S. T., Sun, J., Lu, L., Zheng, S. L., Isaacs, W. B. & Xu, J. 2011. Evaluation of PPP2R2A as a prostate cancer susceptibility gene: a comprehensive germline and somatic study. *Cancer Genet,* 204**,** 375-81.

Doménech, E. & Malumbres, M. 2013. Mitosis-targeting therapies: a troubleshooting guide. *Curr Opin Pharmacol,* 13**,** 519-28.

Eichhorn, P. J., Creyghton, M. P. & Bernards, R. 2009. Protein phosphatase 2A regulatory subunits and cancer. *Biochim Biophys Acta,* 1795**,** 1-15.

Everett, A. D., Kamibayashi, C. & Brautigan, D. L. 2002. Transgenic expression of protein phosphatase 2A regulatory subunit B56d disrupts distal lung differentiation. *Am J Physio Lung Cell Mol Physiol,* 282**,** 1266-1271.

Fan, Y. L., Chen, L., Wang, J., Yao, Q. & Wan, J. Q. 2013. Over expression of PPP2R2C inhibits human glioma cells growth through the suppression of mTOR pathway. *FEBS Lett,* 587**,** 3892-7.

Fang, C., Li, L. & Li, J. 2016. Conditional Knockout in Mice Reveals the Critical Roles of Ppp2ca in Epidermis Development. *Int J Mol Sci,* 17.

Funabiki, H. & Wynne, D. J. 2013. Making an effective switch at the kinetochore by phosphorylation and dephosphorylation. *Chromosoma,* 122**,** 135-58.

Gerdes, J., Dallenbach, F., Lennert, K., Lemke, H. & Stein, H. 1984. Growth fractions in malignant non-Hodgkin's lymphomas (NHL) as determined in situ with the monoclonal antibody Ki-67. *Hematol Oncol,* 2**,** 365-71.

Gharbi-Ayachi, A., Labbe, J. C., Burgess, A., Vigneron, S., Strub, J. M., Brioudes, E., Van-Dorsselaer, A., Castro, A. & Lorca, T. 2010. The substrate of Greatwall kinase, Arpp19, controls mitosis by inhibiting protein phosphatase 2A. *Science,* 330**,** 1673-7.

Gillies, R. J., Verduzco, D. & Gatenby, R. A. 2012. Evolutionary dynamics of carcinogenesis and why targeted therapy does not work. *Nat Rev Cancer,* 12**,** 487-93.

Glover, D. M. 2012. The overlooked greatwall: a new perspective on mitotic control. *Open Biol,* 2**,** 120023.

Gomes, R., Karess, R. E., Ohkura, H., Glover, D. M. & Sunkerl, C. E. 1993. Abnormal anaphase resolution (aar): a locus required for progression through mitosis in *Drosophila*. *Journal of Cell Science,* 104**,** 583-593.

Goto, H., Yasui, Y., Nigg, E. A. & Inagaki, M. 2002. Aurora-B phosphorylates Histone H3 at serine28 with regard to the mitotic chromosome condensation. *Genes to Cells,* 7**,** 11-17.

Gotz, J., Probst, A., Ehler, E., Hemmings, B. & Kues, W. 1998. Delayed embryonic lethality in mice lacking protein phosphatase 2A catalytic subunit Ca. *PNAS,* 95**,** 12370-12375.

Grallert, A., Boke, E., Hagting, A., Hodgson, B., Connolly, Y., Griffiths, J. R., Smith, D. L., Pines, J. & Hagan, I. M. 2015. A PP1-PP2A phosphatase relay controls mitotic progression. *Nature,* 517**,** 94-8.

Gu, P., Qi, X., Zhou, Y., Wang, Y. & Gao, X. 2012. Generation of Ppp2Ca and Ppp2Cb conditional null alleles in mouse. *Genesis,* 50**,** 429-36.

Guillamot, M., Manchado, E., Chiesa, M., Gomez-Lopez, G., Pisano, D. G., Sacristan, M. P. & Malumbres, M. 2011. Cdc14b regulates mammalian RNA polymerase II and represses cell cycle transcription. *Sci Rep,* 1**,** 189.

Hanahan, D. & Weinberg, R. A. 2011. Hallmarks of cancer: the next generation. *Cell,* 144**,** 646-74.

Hernandez-Verdun, D. & Gautier, T. 1994. The chromosome periphery during mitosis. *Bioessays,* 16**,** 179-85.

Jayadeva, G., Kurimchak, A., Garriga, J., Sotillo, E., Davis, A. J., Haines, D. S., Mumby, M. & Grana, X. 2010. B55alpha PP2A holoenzymes modulate the phosphorylation status of the retinoblastoma-related protein p107 and its activation. *J Biol Chem,* 285**,** 29863-73.

Junttila, M. R., Puustinen, P., Niemela, M., Ahola, R., Arnold, H., Bottzauw, T., Ala-Aho, R., Nielsen, C., Ivaska, J., Taya, Y., Lu, S. L., Lin, S., Chan, E. K., Wang, X. J., Grenman, R., Kast, J., Kallunki, T., Sears, R., Kahari, V. M. & Westermarck, J. 2007. CIP2A inhibits PP2A in human malignancies. *Cell,* 130**,** 51-62.

Kalev, P. & Sablina, A. A. 2011. Protein phosphatase 2A as a potential target for anticancer therapy. *Anti-Cancer Agents in Medical Chemistry,* 11**,** 38-46.

Kametaka, A., Takagi, M., Hayakawa, T., Haraguchi, T., Hiraoka, Y. & Yoneda, Y. 2002. Interaction of the chromatin compaction-inducing domain (LR domain) of Ki-67 antigen with HP1 proteins. *Genes to Cells,* 7**,** 1231-1242.

Kiely, M. & Kiely, P. A. 2015. PP2A: The Wolf in Sheep's Clothing? *Cancers (Basel),* 7**,** 648-69.

Kumar, S. G., Gokhan, E., De Munter, S., Bollen, M., Vagnarelli, P., Peti, W. & Page, R. 2016. The Ki-67 and RepoMan mitotic phosphatases assemble via an identical, yet novel mechanism. *eLife*.

Kuo, Y. C., Huang, K. Y., Yang, C. H., Yang, Y. S., Lee, W. Y. & Chiang, C. W. 2008. Regulation of phosphorylation of Thr-308 of Akt, cell proliferation, and survival by the B55alpha regulatory subunit targeting of the protein phosphatase 2A holoenzyme to Akt. *J Biol Chem,* 283**,** 1882-92.

Kurimchak, A., Haines, D. S., Garriga, J., Wu, S., De Luca, F., Sweredoski, M. J., Deshaies, R. J., Hess, S. & Grana, X. 2013. Activation of p107 by fibroblast growth factor, which is essential for chondrocyte cell cycle exit, is mediated by the protein phosphatase 2A/B55alpha holoenzyme. *Mol Cell Biol,* 33**,** 3330-42.

Lee, K. W., Chen, W., Junn, E., Im, J. Y., Grosso, H., Sonsalla, P. K., Feng, X., Ray, N., Fernandez, J. R., Chao, Y., Masliah, E., Voronkov, M., Braithwaite, S. P., Stock, J. B. & Mouradian, M. M. 2011. Enhanced phosphatase activity attenuates alpha-synucleinopathy in a mouse model. *J Neurosci,* 31**,** 6963-71.

Lens, S. M., Voest, E. E. & Medema, R. H. 2010. Shared and separate functions of polo-like kinases and aurora kinases in cancer. *Nat Rev Cancer,* 10**,** 825-41.

Li, L., Fang, C., Xu, D., Xu, Y., Fu, H. & Li, J. 2016. Cardiomyocyte specific deletion of PP2A causes cardiac hypertrophy. *Am J Transl Res*.

Lindqvist, A., Rodriguez-Bravo, V. & Medema, R. H. 2009. The decision to enter mitosis: feedback and redundancy in the mitotic entry network. *J Cell Biol,* 185**,** 193-202.

Litter, S. C., Curran, J., Makara, M. A., Kline, C. F., Ho, H., Xu, Z., Wu, X., Polina, I., Musa, H., Meadows, A. M., Carnes, C. A., Biesiadecki, B. J., Davis, J. P., Weisleder, N., Györke, S., Wehrens, X. H., Hund, T. J. & Mohler, P. J. 2015. Protein phosphatases 2A regulatory subunit B56a limits phosphatase activity in the heart. *Science Signaling,* 8.

Lorca, T. & Castro, A. 2013. The Greatwall kinase: a new pathway in the control of the cell cycle. *Oncogene,* 32**,** 537-43.

Louis, J. V., Martens, E., Borghgraef, P., Lambrecht, C., Sents, W., Longin, S., Zwaenepoel, K., Pijnenborg, R., Landrieu, I., Lippens, G., Ledermann, B., Götz, J., Van Leuven, F., Goris, J. & Janssens, V. 2011. Mice lacking phosphatase PP2A subunit PR61/B'd (Ppp2r5d) develop spatially restricted tauopathy by deregulation of CDK5 and GSK3B. *PNAS,* 108**,** 6957-6962.

Lu, N., Liu, Y., Tang, A., Chen, L., Miao, D. & Yuan, X. 2015. Hepatocyte-specific ablation of PP2A catalytic subunit alpha attenuates liver fibrosis progression via TGF-beta1/Smad signaling. *Biomed Res Int,* 2015**,** 794862.

Majchrzak-Celinska, A., Slocinska, M., Barciszewska, A. M., Nowak, S. & Baer-Dubowska, W. 2016. Wnt pathway antagonists, SFRP1, SFRP2, SOX17, and PPP2R2B, are methylated in gliomas and SFRP1 methylation predicts shorter survival. *J Appl Genet,* 57**,** 189-97.

Malumbres, M. 2011. Physiological relevance of cell cycle kinases. *Physiol Rev,* 91**,** 973-1007.

Manchado, E., Guillamot, M., De Carcer, G., Eguren, M., Trickey, M., Garcia-Higuera, I., Moreno, S., Yamano, H., Canamero, M. & Malumbres, M. 2010. Targeting mitotic exit leads to tumor regression in vivo: Modulation by Cdk1, Mastl, and the PP2A/B55alpha,delta phosphatase. *Cancer Cell,* 18**,** 641-54.

Mao, X., Boyd, L. K., Yáñez-Muñoz, R. J., Chaplin, T., Xue, L., Lin, D., Shan, L., Berney, D. M., Young, B. D. & Lu, Y. J. 2011. Chromosome rearrangement associated inactivation of tumour suppressor genes in prostate cancer. *Am J Cancer Res,* 1**,** 604-17.

Matheson, T. D. & Kaufman, P. D. 2017. The p150N domain of chromatin assembly factor-1 regulates Ki-67 accumulation on the mitotic perichromosomal layer. *Mol Biol Cell,* 28**,** 21-29.

Mayer-Jaekel, R. E., Ohkura, H., Ferrigno, P., Andjelkovic, N., Shiomi, K., Uemura, T., Glover, D. M. & Hemmings, B. 1994. Drosophila mutants in the 55 kDa regulatory subunit of protein phosphatase 2A show strongly reduced ability to dephosphoryate substrates of p34cdc2. *Journal of Cell Science,* 107**,** 2809-2616.

Mayer-Jaekel, R. E., Ohkura, H., Gomes, R., Sunkel, C. E., Baumgartner, S., Hemmings, B. A. & Glover, D. M. 1993. The 55 kd regulatory subunit of *Drosophila* protein phosphatase 2A is required for anaphase. *Cell,* 72**,** 621-33.

Medema, R. H. & Lindqvist, A. 2011. Boosting and suppressing mitotic phosphorylation. *Trends Biochem Sci,* 36**,** 578-84.

Mochida, S., Ikeo, S., Gannon, J. & Hunt, T. 2009. Regulated activity of PP2A-B55 delta is crucial for controlling entry into and exit from mitosis in Xenopus egg extracts. *EMBO J,* 28**,** 2777-85.

Mochida, S., Maslen, S. L., Skehel, M. & Hunt, T. 2010. Greatwall phosphorylates an inhibitor of protein phosphatase 2A that is essential for mitosis. *Science,* 330**,** 1670-3.

Morgan, D. O. 2007. *The Cell Cycle: Principles of control*.

Mosca, L., Musto, P., Todoerti, K., Barbieri, M., Agnelli, L., Fabris, S., Tuana, G., Lionetti, M., Bonaparte, E., Sirchia, S. M., Grieco, V., Bianchino, G., D'auria, F., Statuto, T., Mazzoccoli, C., De Luca, L., Petrucci, M. T., Morabito, F., Offidani, M., Di Raimondo, F., Falcone, A., Caravita, T., Omede, P., Boccadoro, M., Palumbo, A. & Neri, A. 2013. Genome-wide analysis of primary plasma cell leukemia identifies recurrent imbalances associated with changes in transcriptional profiles. *Am J Hematol,* 88**,** 16-23.

Muggerud, A. A., Ronnegerg, J. A., Wärnberg, F., Botling, J., Busato, F., Jovanovic, J., Solvang, H., Bukholm, I., Borresen-Dale, A. L., Kristensen, V. N., Sorlie, T. & Tost, J. 2010. Research article Frequent aberrant DNA methylation of ABCB1, FOXC1, PPP2R2B and PTEN in ductal carcinoma in situ and early invasive breast cancer. *Breast Cancer Research,* 12.

Musacchio, A. 2015. The molecular biology of spindle assembly checkpoint signaling dynamics. *Current Biology,* 25**,** 1002-1018.

Nagasaka, K., Hossain, M. J., Roberti, M. J., Ellenberg, J. & Hirota, T. 2016. Sister chromatid resolution is an intrinsic part of chromosome organization in prophase. *Nat Cell Biol,* 18**,** 692-9.

Nam, H. J., Naylor, R. M. & Van Deursen, J. M. 2015. Centrosome dynamics as a source of chromosomal instability. *Trends Cell Biol,* 25**,** 65-73.

Nematullah, M., Hoda, M. N. & Khan, F. 2017. Protein phosphatase 2A: a double-faced phosphatase of cellular system and its role in neurodegenerative disorders. *Mol Neurobiol*.

Neviani, P. & Perrotti, D. 2014. SETting OP449 into the PP2A-activating drug family. *Clin Cancer Res,* 20**,** 2026-8.

Neviani, P., Santhanam, R., Trotta, R., Notari, M., Blaser, B. W., Liu, S., Mao, H., Chang, J. S., Galietta, A., Uttam, A., Roy, D. C., Valtieri, M., Bruner-Klisovic, R., Caligiuri, M. A., Bloomfield, C. D., Marcucci, G. & Perrotti, D. 2005. The tumor suppressor PP2A is functionally inactivated in blast crisis CML through the inhibitory activity of the BCR/ABL-regulated SET protein. *Cancer Cell,* 8**,** 355-68.

Nobumori, Y., Shouse, G. P., Wu, Y., Lee, K. J., Shen, B. & Liu, X. 2013. B56γ tumor-associated mutations provide new mechanisms for B56γ-PP2A tumor suppressor activity. *Mol Cancer Res,* 11**,** 995-1003.

Ohta, S., Bukowski-Wills, J. C., Sanchez-Pulido, L., Alves Fde, L., Wood, L., Chen, Z. A., Platani, M., Fischer, L., Hudson, D. F., Ponting, C. P., Fukagawa, T., Earnshaw, W. C. & Rappsilber, J. 2010. The protein composition of mitotic chromosomes determined using multiclassifier combinatorial proteomics. *Cell,* 142**,** 810-21.

Ohta, S., Kimura, M., Takagi, S., Toramoto, I. & Ishihama, Y. 2016. Identification of Mitosis-Specific Phosphorylation in Mitotic Chromosome-Associated Proteins. *J Proteome Res,* 15**,** 3331-41.

Ory, S., Zhou, M., Conrads, T. P., Veenstra, T. D. & Morrison, D. K. 2003. Protein Phosphatase 2A Positively Regulates Ras Signaling by Dephosphorylating KSR1 and Raf-1 on Critical 14-3-3 Binding Sites. *Current Biology,* 13**,** 1356-1364.

Pallas, D. C., Shahrik, L. K., Martin, B. L., Jaspers, S., Miller, T. B., Brautigan, D. L. & Roberts, T. M. 1990. Polyoma small and middle T antigens and SV40 small t antigen form stable complexes with protein phosphatase 2A. *Cell* 60**,** 167-76.

Pan, X., Chen, X., Tong, X., Tang, C. & Li, J. 2015. Ppp2ca knockout in mice spermatogenesis. *Reproduction,* 149**,** 385-91.

Qian, J., Lesage, B., Beullens, M., Van Eynde, A. & Bollen, M. 2011. PP1/Repo-Man Dephosphorylates Mitotic Histone H3 at T3 and Regulates Chromosomal Aurora B Targeting. *Curr Biol* 21**,** 766-773.

Queralt, E. & Uhlmann, F. 2008. Cdk-counteracting phosphatases unlock mitotic exit. *Curr Opin Cell Biol,* 20**,** 661-8.

Ruediger, R., Ruiz, J. & Walter, G. 2011. Human cancer-associated mutations in the Aalpha subunit of protein phosphatase 2A increase lung cancer incidence in Aalpha knock-in and knockout mice. *Mol Cell Biol,* 31**,** 3832-44.

Ruvolo, P. P. 2016. The broken "Off" switch in cancer signaling: PP2A as a regulator of tumorigenesis, drug resistance, and immune surveillance. *BBA Clin,* 6**,** 87-99.

Ruvolo, P. P., Qui, Y. H., Coombes, K. R., Zhang, N., Ruvolo, V. R., Borthakur, G., Konopleva, M., Andreeff, M. & Kornblau, S. M. 2011. Low expression of PP2A regulatory subunit B55alpha is associated with T308 phosphorylation of AKT and shorter complete remission duration in acute myeloid leukemia patients. *Leukemia,* 25**,** 1711-7.

Samejima, K., Samejima, I., Vagnarelli, P., Ogawa, H., Vargiu, G., Kelly, D. A., De Lima Alves, F., Kerr, A., Green, L. C., Hudson, D. F., Ohta, S., Cooke, C. A., Farr, C. J., Rappsilber, J. & Earnshaw, W. C. 2012. Mitotic chromosomes are compacted laterally by KIF4 and condensin and axially by topoisomerase IIalpha. *J Cell Biol,* 199**,** 755-70.

Samuel Rogers, R. M., D.Neil Watkins and Andrew Burgess 2015. Mechanisms regulating phosphatase specificity and the removal of individual phosphorylation sites during mitotic exit. *Bioessays,* 38**,** S24-S32.

Santamaria, D., Barriere, C., Cerqueira, A., Hunt, S., Tardy, C., Newton, K., Caceres, J. F., Dubus, P., Malumbres, M. & Barbacid, M. 2007. Cdk1 is sufficient to drive the mammalian cell cycle. *Nature,* 448**,** 811-5.

Schmidt, K., Kins, S., Schild, A., Nitsch, R. M., Hemmings, B. & Götz, J. 2002. Diversity, developmental regulation and distribution of murine PR55/B subunits of protein phosphatase 2A. *European Journal of Neuroscience,* 16**,** 2039-2048.

Schmitz, M. H., Held, M., Janssens, V., Hutchins, J. R., Hudecz, O., Ivanova, E., Goris, J., Trinkle-Mulcahy, L., Lamond, A. I., Poser, I., Hyman, A. A., Mechtler, K., Peters, J. M. & Gerlich, D. W. 2010. Live-cell imaging RNAi screen identifies PP2A-B55alpha and importin-beta1 as key mitotic exit regulators in human cells. *Nat Cell Biol,* 12**,** 886-93.

Scholzen, T., Endl, E., Wohlenberg, C., Van Der Sar, S., Cowell, I. G., Gerdes, J. & Singh, P. B. 2002. The Ki-67 protein interacts with members of the heterochromatin protein 1 (HP1) family: a potential role in the regulation of higher-order chromatin structure. *J Pathol,* 196**,** 135-44.

Seki, A., Coppinger, J. A., Jang, C., Yates, J. R. & Fang, G. 2008. Bora and the Kinase Aurora A Cooperatively Activate the Kinase Plk1 and Control Mitotic Entry. *Science,* 320.

Seong, Y., Kamijo, K., Lee, J., Fernandez, E., Kuriyama, R., Miki, T. & Lee, K. S. 2002. A spindle checkpoint arrest and a cytokinesis failure by the dominant-negative Polo-box domain in Plk1 in U2OS cells. *The Journal of Biological Chemistry,* 277**,** 32282-32293.

Seshacharyulu, P., Pandey, P., Datta, K. & Batra, S. K. 2013. Phosphatase: PP2A structural importance, regulation and its aberrant expression in cancer. *Cancer Lett,* 335**,** 9-18.

Sobecki, M., Mrouj, K., Camasses, A., Parisis, N., Nicolas, E., Llères, D., Gerbe, F., Prieto, S., Krasinska, L., David, A., Eguren, M., Birling, M., Urbach, S., Hern, S., Déjardin, J., Malumbres, M., Jay, P., Dulic, V., Lafontain, D. L. J., Feil, R. & Fisher, D. 2016. The cell proliferation antigen Ki-67 organises heterochromatin

eLife.

Song, M. H., Liu, Y., Anderson, D. E., Jahng, W. J. & O'connell, K. F. 2011. Protein phosphatase 2A-SUR-6/B55 regulates centriole duplication in C. elegans by controlling the levels of centriole assembly factors. *Dev Cell,* 20**,** 563-71.

Sontag, E., Luangpirom, A., Hladik, C., Mudrak, I., Ogris, E., Speciale, S. & White, C. L. 2004. Altered expression levels of the protein phosphatase 2A ABalphaC enzyme are associated with

Alzheimer disease pathology. *J Neuropathol Exp Neurol,* 63**,** 287-301.

Starborg, M., Gell, K., Brundell, E. & Höög, C. 1996. The murine Ki-67 cell proliferation antigen accumulates in the nucleolar and heterochromatic regions of interphase cells and at the periphery of the mitotic chromosomes in a process essential for cell cycle progression. *Journal of Cell Science,* 109**,** 143-153.

Strack, S., Chang, D., Zaucha, J. A., Colbran, R. J. & Wadzinski, B. E. 1999. Cloning and characterization of Bδ, a novel regulatory subunit of protein phosphatase 2A. *FEBS Letters,* 460**,** 462-466.

Strack, S., Zaucha, J. A., Colbran, R. J. & Wadzinski, B. E. 1998. Brain Protein Phosphatase 2A: Developmental Regulation and Distinct Cellular and Subcellular Localization by B Subunits. *The journal of comparative neurology,* 392**,** 515-527.

Sudakin, V., Chan, G. K. & Yen, T. J. 2001. Checkpoint inhibition of the APC/C in HeLa cells is mediated by a complex of BUBR1, BUB3, CDC20, and MAD2. *J Cell Biol,* 154**,** 925-36.

Takagi, M., Natsume, T., Kanemaki, M. T. & Imamoto, N. 2016. Perichromosomal protein Ki67 supports mitotic chromosome architecture. *Genes Cells,* 21**,** 1113-1124.

Takagi, M., Nishiyama, Y., Taguchi, A. & Imamoto, N. 2014. Ki67 antigen contributes to the timely accumulation of protein phosphatase 1gamma on anaphase chromosomes. *J Biol Chem,* 289**,** 22877-87.

Tan, J., Lee, P. L., Li, Z., Jiang, X., Lim, Y. C., Hooi, S. C. & Yu, Q. 2010. B55beta-associated PP2A complex controls PDK1-directed myc signaling and modulates rapamycin sensitivity in colorectal cancer. *Cancer Cell,* 18**,** 459-71.

Tang, Z., Shu, H., Qi, W., Mahmood, N. A., Mumby, M. C. & Yu, H. 2006. PP2A is required for centromeric localization of Sgo1 and proper chromosome segregation. *Dev Cell,* 10**,** 575-85.

Topham, C. H. & Taylor, S. S. 2013. Mitosis and apoptosis: how is the balance set? *Curr Opin Cell Biol,* 25**,** 780-5.

Toyoshima-Morimoto, F., Taniguchi, E., Shinya, N., Iwamatsu, A. & Nishida, E. 2001. Polo-like kinase 1 phosphorylates cyclin B1 and targets it to the nucleus during prophase. *Nature,* 410**,** 215-20.

Traut, W., Endl, E., Garagna, S., Scholzen, T., Schwinger, E., Gerdes, J. & Winking, H. 2002. Chromatin preferences of the perichromosomal layer constituent pKi-67. *Chromosome Res,* 10**,** 985-94.

Vagnarelli, P., Ribeiro, S., Sennels, L., Sanchez-Pulido, L., De Lima Alves, F., Verheyen, T., Kelly, D. A., Ponting, C. P., Rappsilber, J. & Earnshaw, W. C. 2011. Repo-Man coordinates chromosomal

reorganization with nuclear envelope reassemby during mitotic exit. *Dev Cell,* 21**,** 328-342.

Van Hooser, A. A., Yuh, P. & Heald, R. 2005. The perichromosomal layer. *Chromosoma,* 114**,** 377-88.

Varadkar, P., Daryl, D., Kraman, M., Lozier, J., Phadke, A., Nagaraju, K. & Mccright, B. 2014. The protein phosphatase 2A B56c regulatory subunit is required for heart development. *Developmental Dynamics,* 243.

Vazquez-Novelle, M. D., Esteban, V., Bueno, A. & Sacristan, M. P. 2005. Functional homology among human and fission yeast Cdc14 phosphatases. *J Biol Chem,* 280**,** 29144-50.

Vigneron, S., Brioudes, E., Burgess, A., Labbé, J. C., Lorca, T. & Castro, A. 2009. Greatwall maintains mitosis through regulation of PP2A. *EMBO J,* 28**,** 2786-93.

Voets, E. & Wolthuis, R. M. 2010. MASTL is the human orthologue of Greatwall kinase that facilitates mitotic entry, anaphase and cytokinesis. *Cell Cycle,* 9**,** 3591-601.

Wachowicz, P., Fernández-Miranda, G., Marugán, C., Escobar, B. & De Cárcer, G. 2016. Genetic depletion of Polo-like kinase 1 leads to embryonic lethality due to mitotic aberrancies. *Inside the Cell,* 1**,** 59-69.

Walter, G. & Ruediger, R. 2012. Mouse model for probing tumor suppressor activity of protein phosphatase 2A in diverse signaling pathways. *Cell Cycle,* 11**,** 451-9.

Whitfield, M. L., George, L. K., Grant, G. D. & Perou, C. M. 2006. Common markers of proliferation. *Nat Rev Cancer,* 6**,** 99-106.

Wu, J. Q., Guo, J. Y., Tang, W., Yang, C. S., Freel, C. D., Chen, C., Nairn, A. C. & Kornbluth, S. 2009. PP1-mediated dephosphorylation of phosphoproteins at mitotic exit is controlled by inhibitor-1 and PP1 phosphorylation. *Nat Cell Biol,* 11**,** 644-51.

Wurzenberger, C. & Gerlich, D. W. 2011. Phosphatases: providing safe passage through mitotic exit. *Nat Rev Mol Cell Biol,* 12**,** 469-82.

Xian, L., Hou, S., Huang, Z., Tang, A., Shi, P., Wang, Q., Song, A., Jiang, S., Lin, Z., Guo, S. & Gao, X. 2015. Liver-specific deletion of Ppp2ca enhances glucose metabolism and insulin sensitivity. *Aging,* 7.

Yu, J., Fleming, S. L., Williams, B., Williams, E. V., Li, Z., Somma, P., Rieder, C. L. & Goldberg, M. L. 2004. Greatwall kinase: a nuclear protein required for proper chromosome condensation and mitotic progression in Drosophila. *J Cell Biol,* 164**,** 487-92.

Zhang, W., Yang, J., Liu, Y., Chen, X., Yu, T., Jia, J. & Liu, C. 2009. PR55 alpha, a regulatory subunit of PP2A, specifically regulates PP2A-

mediated beta-catenin dephosphorylation. *J Biol Chem,* 284**,** 22649-56.